BEHAVIOR OF RC BEAM-COLUMN CONNECTIONS STRENGTHENED WITH EXTERNALLY BONDED FRP COMPOSITES

HAMID SINAEI

FACULTY OF ENGINEERING
UNIVERSITY OF MALAYA
KUALA LUMPUR

2018

BEHAVIOR OF RC BEAM-COLUMN CONNECTIONS STRENGTHENED WITH EXTERNALLY BONDED FRP COMPOSITES

HAMID SINAEI

THESIS SUBMITTED IN FULLFILMENT OF THE REQUIREMENTS FOR THE DEGREE OF DOCTOR OF PHILOSOPHY

FACULTY OF ENGINEERING
UNIVERSITY OF MALAYA
KUALA LUMPUR

2018

UNIVERSITY OF MALAYA

ORIGINAL LITERARY WORK DECLARATION

Name of Candidate: Hamid Sinaei

Registration/Matric No: KHA080048

Name of Degree: Doctor of Philosophy

Title of Project Paper/Research Report/Dissertation/Thesis ("this Work"):

BEHAVIOR OF RC BEAM-COLUMN CONNECTIONS STRENGTHENED WITH EXTERNALLY BONDED FRP COMPOSITES

Field of Study: Structural Engineering

I do solemnly and sincerely declare that:

(1) I am the sole author/writer of this Work;
(2) This Work is original;
(3) Any use of any work in which copyright exists was done by way of fair dealing and for permitted purposes and any excerpt or extract from, or reference to or reproduction of any copyright work has been disclosed expressly and sufficiently and the title of the Work and its authorship have been acknowledged in this Work;
(4) I do not have any actual knowledge nor do I ought reasonably to know that the making of this work constitutes an infringement of any copyright work;
(5) I hereby assign all and every rights in the copyright to this Work to the University of Malaya ("UM"), who henceforth shall be owner of the copyright in this Work and that any reproduction or use in any form or by any means whatsoever is prohibited without the written consent of UM having been first had and obtained;
(6) I am fully aware that if in the course of making this Work I have infringed any copyright whether intentionally or otherwise, I may be subject to legal action or any other action as may be determined by UM.

Candidate's Signature **Date:**

Hamid Sinaei

Subscribed and solemnly declared before,

Witness's Signature **Date:**

Name:

Designation:

BEHAVIOR OF RC BEAM-COLUMN CONNECTIONS STRENGTHENED WITH EXTERNALLY BONDED FRP COMPOSITES

ABSTRACT

The beam-column connections (BCCs) are the crucial part of RC framed structures intended to provide resistance to apply static or seismic load in plastic region. The majority of past published research has focused on the repair and retrofit of the RC framed BCCs using conventional methods like, concrete jacketing, steel jacketing, addition of external steel and fibre reinforced polymeric (CFRP) laminates. RC and steel jacketing have been the popular choices in areas with high seismicity, especially for RC columns applications. However, these processes are labor intensive and may be considered impractical in some cases as in case of interior joints with beams in two orthogonal directions. A practical way of controlling plastic hinging and implement the strong-column weak-beam concept is through the use of the CFRP retrofitting system. In order to successfully and effectively use the CFRP overlay technique, the mechanical behavior of the CFRP-RC needs to be understood and its response needs to be accurately predicted. The main focus of this research is strengthening of concrete BCC with the use of various configurations of CFRP sheet and plate, and investigates the load capacity and ductility of these connections using experimental and numerical investigations. A total of six (6) scaled-down RC exterior joints, comprising of a control specimen (non-retrofitted) and five (5) retrofitted specimens with different CFRP arrangements were tested under moderately monotonic loads. The retrofitted specimens include; BCC strengthened with two cross-shaped CFRP plates bonded at the joint (RCS2), BCC strengthened with two CFRP plates added to the top and bottom of the beam (RCS3), BCC reinforced at the top and bottom corners of the connection with L-shaped CFRP sheets (RCS4), BCC with two reinforcing CFRP plates on both sides of

the beam web (RCS5), and a BCC wrapped with CFRP layers at some parts of the column close to the connection and at the end of beam (RCS6). In addition, accurate modeling of CFRP strengthened RC BCCs was conducted using finite element method (ABAQUS) and the exact details of its performance were verified with experimental results. After validating the accuracy of the numerical method, several parametric studies were carried out for CFRP reinforced samples, with different lengths and thicknesses in order to relocate the plastic hinge away from the face of the column. Two categories of samples were used. Samples reinforced with CFRP plates on both sides of the beam web and samples reinforced with CFRP plates on the upper and lower beam flanges. Both groups of samples were reinforced with CFRP plates in the web and flanges of the beam. The experimental results showed that the configuration of the CFRP had a different effect on the joint capacity and the connection ductility coefficient. The greatest effect on increasing the ductility factor was seen in the sample where two CFRP plates were used on both sides of the beam web (RCS5 sample). For the sample with the presence of CFRP plates at the top and bottom of the beam (RCS3 sample), the ductility factor was reduced, although the load capacity of this sample increased. Except for the RCS3 sample, the rest of the samples exhibited an increase in the ductility factor due to the CFRP reinforcement. In both groups, increasing the thickness of the reinforcing CFRP plates causes the effective length of these plates' increases for the transfer of the plastic hinge. However, this increase is limited and excessive thickening may have a negative effect. The optimum effective length of the CFRP plate can be considered about twice the height of the beam from the exterior face of the column.

Keyword: Beam-Column Connection, Composite, Plastic-Hinge, Abaqus, CFRP.

KELAKUAN SAMBUNGAN RASUK-TIANG KONKRIT BERTETULANG YANG DIPERKUATKAN DENGAN KOMPOSIT FRP IKATAN LUARAN

ABSTRAK

Sambungan rasuk-tiang (BCCs) adalah bahagian penting bagi struktur kerangka RC yang bertujuan untuk memberikan rintangan kepada beban statik atau seismik di kawasan plastik. Majoriti penyelidikan yang diterbitkan sebelum ini menumpukan kepada pembaikan dan pengubahsuaian BCC kerangka RC menggunakan kaedah konvensional seperti, jaket konkrit, jaket besi, penambahan keluli luaran dan polimer bertetulang gentian (CFRP) berlapis. RC dan jaket keluli telah menjadi pilihan popular di kawasan ber seismik yang tinggi, terutamanya untuk aplikasi bagi tiang RC. Walau bagaimanapun, proses ini memerlukan kerja intensif buruh dan mungkin dianggap tidak praktikal dalam beberapa kes seperti dalam kes sambungan dalaman dengan rasuk dalam dua arah ortogonal. Satu cara praktikal untuk mengawal pengengselan plastik dan melaksanakan konsep tiang-kuat dan rasuk-lemah adalah melalui penggunaan sistem pengubahsuaian CFRP. Dalam rangka untuk berjaya menggunakan teknik CFRP tindihan atas dengan berkesan, kelakuan mekanikal CFRP-RC perlu di fahami dan tindak balasnya perlu di ramalkan dengan tepat. Fokus utama penyelidikan ini adalah untuk memperkukuhkan BCC konkrit dengan penggunaan pelbagai konfigurasi lembaran dan plat CFRP, dan menyiasat keupayaan beban dan kemuluran sambungan menggunakan kaedah eksperimen dan penyiasatan berangka. Sejumlah enam (6) sambungan luaran RC berskala-kecil, terdiri daripada satu spesimen kontrol (tidak-pengubahsuaian) dan lima (5) spesimen diubahsuai dengan pelbagai susunan CFRP telah diuji di bawah beban monotonik sederhana. Spesimen-spesimen yang diubahsuai itu termasuk; BCC yang diperkukuh dengan dua plat CFRP bentuk-silang diikat pada sambungan (RCS2), BCC yang diperkukuhkan dengan dua plat CFRP yang di tambah

pada atas dan bawah rasuk (RCS3), BCC yang diperkukuhkan di atas dan di bawah sudut sambungan dengan lembaran CFRP bentuk-L (RCS4), BCC yang diperkukuhkan dengan dua plat CFRP yang di tambah pada kedua-dua sisi web rasuk (RCS5), dan satu BCC yang dibalut dengan lapisan CFRP pada sebahagian dari tiang yang dekat dengan sambungan dan pada hujung rasuk (RCS6). Tambahan lagi, pemodelan yang tepat bagi RC BCC yang diperkuatkan oleh CFRP telah dijalankan menggunakan kaedah unsur terhingga (ABAQUS) dan butir-butir yang tepat mengenai prestasinya telah disahkan dengan keputusan dari eksperimen. Setelah mengesahkan ketepatan kaedah berangka, beberapa kajian parametrik telah dijalankan bagi sampel yang diperkukuhkan oleh CFRP, dengan panjang dan ketebalan yang berbeza dalam rangka untuk memindahkan engsel plastik jauh dari permukaan tiang. Dua kategori sampel telah digunakan. Sampel yang diperkuat dengan plat CFRP di kedua-dua belah web rasuk dan sampel yang diperkuat dengan plat CFRP pada bebibir rasuk atas dan bawah. Kedua-dua kumpulan sampel telah diperkuatkan dengan plat CFRP di web dan bebibir rasuk. Keputusan eksperimen menunjukkan, konfigurasi CFRP mempunyai kesan yang berbeza terhadap kapasiti sambungan dan pekali kemuluran sambungan. Kesan terbesar untuk meningkatkan faktor kemuluran dilihat dalam sampel di mana dua plat bertetulang digunakan pada kedua-dua belah web rasuk (sampel RCS5). Untuk sampel yang mempunyai plat CFRP di bahagian atas dan bawah rasuk (sampel RCS3), faktor kemuluran dikurangkan, walaupun kapasiti beban bagi sampel ini meningkat. Kecuali bagi sampel RCS3, sampel-sampel yang lain memperlihatkan peningkatan dalam faktor kemuluran dengan pengukuhan CFRP. Dalam kedua-dua kumpulan, meningkatkan ketebalan CFRP plat menyebabkan panjang berkesan plat ini meningkat untuk pemindahan engsel plastik. Walaubagaimanapun, peningkatan ini adalah terhad dan penebalan berlebihan mungkin mempunyai kesan negatif. Panjang berkesan optimum bagi plat CFRP boleh diambil kira-kira dua kali ganda ketinggian rasuk dari permukaan luar tiang.

Kata kunci: Sambungan Rasuk-Tiang, Komposit, Engsel-Plastik, Abaqus, CFRP.

ACKNOWLEDGEMENTS

First and foremost, I would like to thank God for giving me strength and guidance throughout my life.

I would like to express my sincere gratitude to my supervisors Prof. Dr. Mohd Zamin Bin Jumaat and Associate Prof. Dr. Zainah Binti Ibrahim for providing an opportunity to work in their group and giving me the regular guidance and support through this research.

I am grateful to the whole lab members for helping me all the times.

In addition, I am thankful to my supportive wife and parents for their encouragement and endless support through this part of my life.

TABLE OF CONTENTS

LIST OF FIGURES

LIST OF TABLES

LIST OF SYMBOLS

A_S	:	Area of steel
E_c	:	Concrete Young's modulus
E_s	:	Steel Young's modulus
T/F_s	:	Tensile or shear force in bars or connector
I	:	Second moment of area
I_{cr}	:	Second moment of area of cracked section
I_u	:	Second moment of area of uncracked section
L	:	Span of beam
M	:	Applied test bending moment
M_{beam}	:	Predicted ultimate moment capacity of beam
M_E	:	Beam end moment at limiting beam rotation
M_{ED}	:	Design beam end moment at limiting beam rotation
M_R	:	Moment resistance of beam
M_{RC}	:	Moment of resistance of connector
M_{span}	:	Predicted ultimate moment capacity at mid-span of beam
M_U	:	Test ultimate moment
P	:	Applied beam load
b	:	Breadth of section
d	:	Effective depth to rebar

f_{cu}	:	Compressive strength of concrete in beams and columns
f_y	:	Yield stress of reinforcement
h	:	Depth of section
l_e	:	Embedment length for tie steel bars
x	:	Depth to neutral axis in beam
x_c	:	Depth to neutral axis in connector
z	:	Lever arm in beam/connector
δ	:	Deformation
γ_m	:	Partial safety factor
θ	:	Rotation of beam or column
ϕ	:	Relative beam-to-column rotation
ϕ_E	:	Relative rotation at beam rotation limit

CHAPTER 1: INTRODUCTION

1.1 Background

Thus, structures built several decades ago may need strengthening and upgrading to meet current service load demands. Strengthening and retrofitting programs are more reasonable compared to demolishing and rebuilding structures in terms of service disruption, labor and material costs (Hadi & Tran, 2016); Tang et al. (2006). Strengthening may be required for both structures subjected to static loading and to repeated loading, which cause failure at load levels below the structure's static load-carrying capacity (El-Hacha & Gaafar, 2011; Nordin & Täljsten, 2006). The required strength and serviceability performance of a strengthened structure is only achievable by completely understanding the materials' behavior and strengthening techniques used(Daly & Witarnawan, 1997; McCormac & Brown, 2015; Nordin, 2005).

Several methods of strengthening RC structures containing various materials have been studied and applied in the rehabilitation field. The most recent type of material utilized for strengthening purposes in modern times is Fiber-Reinforced Polymer (FRP) composite (Aslam et al., 2015). Advantages of FRP that supersede traditional strengthening materials are said to be sufficient resistance to rust, excellent strength as compared to the self-weight, user-friendliness and neutrality to electromagnetic forces. All these benefits strongly encourage FRP use for RC structure strengthening, especially in cases where traditional steel reinforcement fails to provide the required serviceability (Aslam et al., 2015). Strengthening with FRP composites is one of the more recent retrofitting and strengthening techniques (Engindeniz et al., 2005).

Prior to 1970, the majority of RC frame buildings constructed had deficient beam-column joints due to the absence of design code requirements for transverse steel reinforcement at the joint locations. The lack of joint confinement leads to a weakened link between the column and beam, and consequently, the collapse of the entire structure. A typical building structure failure due to inadequate beam-column joint strength is shown in Figure 1.1.

Figure 1.1: Type of failure observed in pre-1970s building structures
(Turkey Earthquake 1999)

Failure modes observed and reported from past earthquakes indicate that these deficiency details result in insufficient joint shear strength and/or buckling of the column's longitudinal rebars. Another major contributor to beam-column joint failure is the so-called "strong beam/weak column" philosophy from the 1960s and 1970s. The poor performance of a building structure constructed in the early 1960s is shown in Figure 1.2.

Figure 1.2: Poor structure performance in pre-1970s construction
(Turkey Earthquake 1999)

The use of FRPs for strengthening RC structures has become increasingly popular over the last two decades due to material cost reductions, versatility and benefits as well as the ability to significantly improve member strength, fatigue life and serviceability. Among FRPs, Carbon Fiber-Reinforced Polymer (CFRP) composites are used most frequently in the construction industry because they generally contain high-performance carbon fibers placed in the resin matrix. Statistics reveal that among various FRP types, CFRP contributes to 95% of usage for deficient RC structure strengthening (Aslam et al., 2015). One of the primary reasons is that this composite can easily bond externally to RC elements.

Beam-to-column connections (BCCs) are perilous regions in RC framed structures and are intended to provide resistance to static or seismic loads in plastic regions. Ineffectively designed exterior RC BCCs usually exhibit premature brittle failure because of the greater shear stresses. The most important causes for the failure of BCCs under any unanticipated loading are: (i) the absence of transverse reinforcement in the joint, (ii) insufficient development length for the beam reinforcement, and (iii) inadequately spliced reinforcement for the column just above the joint (Mahmoud et al., 2014). It has been brought to light that externally bonded CFRP reinforcement is a practical means of increasing the static and seismic performance of badly designed RC BCCs subjected to high-magnitude shear stresses (Costas P. Antonopoulos & Triantafillou, 2003). Moreover, configuring CFRPs to strengthen RC BCCs with inadequate transverse reinforcement in the joints is a critical factor that necessitates proper understanding of the strengthening phenomenon (Abdel-Wahed et al., 2005).

In earthquake-prone regions, RC BCCs are commonly designed as ductile moment-resisting (DMR) connections to facilitate the conversion of mechanical energy into heat energy in head-to-head plastic hinges by preventing any noticeable decrease in the connections' ductility and strength. Thus, careful strengthening of RC BCCs is required for structural safety. Despite the fact that the detailing of the connection is dependent on member size, in reality the loading combinations affecting the connections are not the same as those considered in designing major frame members. Therefore, it is essential for the consideration extended in designing connection reinforcements to be of the same extent as for other members. A poor frame design enhances the chances of plastic hinge formation in the column, which would make the column fail at lower ultimate loads as well as reduce the column's energy dissipation capability that is dependent on axially applied load and reinforcement design (Thomas & Priestley, 1992). A way to mitigate this problem is to design DMR frames based on the strong-column-weak-beam design. This method of designing members allows both the connection and the column to remain in elastic stage when the lateral load intensity is higher than in normal situations. Moreover, most energy dissipation occurs within the plastic hinge formed in a beam, provided that the plastic hinge develops at a sufficient distance from the connection. This is to ensure that plasticity will not penetrate to the joint core, as this may trigger brittle failure within the core(Chutarat & Aboutaha, 2003; Thomas & Priestley, 1992)

Although the defect of inadequate transverse reinforcement in RC BCCs has been studied extensively in literature, other defects remain to be studied in detail. The current study focuses on experimental and numerical analyses of RC BCC strengthening using different CFRP composite configurations. The behavior of RC BCCs reinforced externally with innovative CFRP composite elements under static loading is primarily investigated. This involves wrapping and attaching CFRP plies around the connection area, while the influence of axial force, thickness, length and number of CFRP plies is verified. This study will determine how various CFRP configurations affect the performance of strengthened RC BCCs as connections. The validity of these innovative external reinforcement systems is verified by comparing the experimental results with nonlinear finite element modeling results. Then, by choosing appropriate CFRP plates length and thickness, it will be shown how to transfer the plastic hinges from inside the column to the beam. And the effective length will be optimized, and the limitation of the length and thickness of the plates will be checked

1.2 Problem statement

Rehabilitating and strengthening old or pre-damaged building structures and bridges comprising Reinforced Concrete (RC) present vexatious challenges for structural design engineers. It is not always to replace deficient structures due to high expenses and usage limitations(Ali et al., 2018). Beam-to-column connections (BCCs) are perilous regions in RC framed structures and are intended to provide resistance to static or seismic loads in plastic regions. Ineffectively designed exterior RC BCCs usually exhibit premature brittle failure. One of the main goals of the recent researches is relocation the plastic hinge away from the column face toward the beam in order to achieve a ‘weak beam - strong column’ failure mode can be useful. In the event of beam collapse, the forces are distributed to adjacent members and the structure can maintain its stability. However, the collapse of a column can cause the entire structure to collapse.

Several studies were therefore conducted in order to develop rehabilitation schemes for beam-column joints. Some retrofit schemes were proposed; all made use of steel sections and/or concrete jacketing in several configurations for different types of joints. Since column confinement with concrete or steel jacketing is labor-intensive and adds considerable weight to the elements, it is always desirable to use cost-effective, durable and fast techniques such as externally bonded CFRP composite laminates for the rehabilitation of existing structures. But conducting lab experiments in large numbers is very costly; so using a suitable numerical method can be useful.

1.3 Objectives of study

In order to apply the CFRP overlay technique to enhancement of structures successfully and effectively, the mechanical behavior of CFRP-RC should be understood and its response predicted accurately. The main focus of this research is to experimentally and numerically investigate the behavior of externally reinforced RC BCCs with innovative CFRP composite elements. The sub-objectives of the study are as follows:

1. To increase the load capacity and ductility of concrete beam-column connections by reinforcing with a variety of CFRP configurations.

2. To develop accurate modeling of reinforced concrete beam-column connections with CFRP using finite element software and verify the exact details of performance.

3. To determine the appropriate length and thickness of CFRP plates in order to relocate the plastic hinge away from the column face toward the beam.

1.4 Scope of work

The present study consists of three phases. The first phase involves a literature review of topics related to the performance analysis of RC BCCs, external strengthening techniques, non-conventional internal reinforcement details, and state-of-the-art modeling techniques for RC BCCs. The second phase entails developing finite element (FE) models for control, externally strengthened, and internally reinforced BCC details. The numerical results along with the literature review will form the basis of the experimental program that includes specimen sizing, load history, reinforcement details, strain, deflection and rotational sensor locations, and details of the test setup. The third phase of the study involves the development and execution of the downscale test program. Based on the downscale test results, the FE models are refined and the numerical results are compared with the experimental observations. It is anticipated that the findings of this thesis will convey alternative state-of-the-art reinforcement and strengthening practices to improve RC BCC repair. This thesis will further provide designers a choice of the most beneficial CFRP configurations that will result in higher dependability and protection as well as the capability to strengthen RC-FRP BCCs at optimum overall costs.

1.5 Research significance

Many studies have elaborated the need for a retrofit scheme for deficient beam-column joints. Design guidelines for reinforced concrete beam-column joints were first published in 1976. The American Concrete Institute (ACI-318-2008) mandates the adoption of the weak-beam-strong-column philosophy. This code requirement ensures the formation of potential plastic hinges along the beam span as well as the yield of a longitudinal beam reinforcement to prevent catastrophic brittle joint shear failure(Ascione et al., 2017).

A number of attractive CFRP composite features, such as high strength-to-weight ratio (specific strength), higher corrosion resistance and ease of application have urged researchers to use this material to strengthen deficient structures(Azarm et al., 2017). However, according to the literature, very few studies have been conducted to investigate the strengthening and ductility behavior of RC BCCs using external CFRP reinforcement. Besides, no study has investigated the effects of various CFRP configurations on the overall performance of strengthened RC BCCs. This has generated a research gap that calls for identifying the most effective CFRP parameters and sizes to achieve the highest possible strength and serviceability performance of strengthened RC BCCs. The current research will help designers choose the most appropriate design configuration for the strengthening of deficient RC BCCs subjected to static loading.

1.6 Thesis content

The current study is composed of five chapters. Chapter 1 provides an introduction and specifies the research needs, objectives, scope of work and significance of the research. Chapter 2 contains a comprehensive literature review of research works to date on the behavior of existing retrofitted and strengthened connections. This chapter also reviews several materials and techniques that researchers have used in the past along with the techniques' reliability according to cost. Following this review, the connection selected details for investigation in this study are presented. Chapter 3 comprises a detailed research methodology that describes the test setup, experimental test specimens and procedures employed in this study. It also describes the numerical analysis done using ABAQUS software for finite element modeling (FEM) of the RC joints. FEM analysis was employed to display the connection behavior, which was not clear from the experimental tests. Following test result verification, the FEA can be suggested for a wider investigation of connections in future works. The results and discussions of the experimental investigations and FEM of the connection specimens are presented in Chapter 4. The result comparison is investigated to identify the connection strength and joint ductility. Finally, the different models produced with various CFRP lengths and thicknesses along with a numerical analysis are applied to investigate the effect of reinforcement layer length and thickness on the different shapes and also the effect of column axial load on sample function. Finally, chapter 5 summarizes the study findings and offers a few recommendations for future work.

CHAPTER 2: LITERATURE REVIEW

2.1 General

Reinforced concrete (RC) is copiously utilized for the construction of structures and infrastructures throughout the world. Since the availability of its gradients is easier and its preparation and output in terms of strength and durability is well recognized, RC is being used both in the developed as well as developing countries. However, in the developing countries, due to less resources and know how about the structural behavior of RC, most of the structures are still being built by adopting home-grown techniques suggested by so called local experts. Regrettably, this non-technical construction is obviously not durable and reliable as compared to the construction performed under proper engineering methods of utilizing RC and consequently, many of the primary advantages of RC like simpler execution, savings in cost of project, higher strength and sustainability, good resistance to temperature and ease in maintenance with growing age are being lost. It is a universal fact that rehabilitation of RC structures is an optimum way to utilize the already built structure with better performance and at cheaper cost. Thus, it is necessary to understand the basics of preparation, execution, utilization and strength characteristics of RC in a systematic and recognized engineered way before performing the rehabilitation.

Nowadays, the huge amount of naturally available sources is used to prepare plain concrete or RC. According to statistics, the amount of cement, sand and mixing water used for the preparation of concrete is 1.5, 9 and 1 billion tones, respectively. Despite the usage of such a huge amount of naturally available resources, if the composition of concrete ingredients, especially the cement, is kept in ranges suggested by the design standards, the contribution of concrete in affecting the green environment is almost negligible. This can be said an additional considerable advantage of RC. However, RC structures are deteriorated due to several environmental impacts.

Structural deterioration has become a complex issue in structural engineering, since the cost of replacement of the original structure is quite high. Most of the infrastructures are usually subjected to repeated loads, which cause a structure to failure at a load level below its static capacity. Thus, these structures that have been built more than several decades may need to be strengthened and upgraded to meet the current service load demands. The deterioration severely reduces the serviceability of RC beams which is majorly dependent of perfect engineering design, appropriate choice and usage of construction materials. The factors such as greater cost and limitations in the usage impede the new construction of deficient RC beams. This leads towards the deployment of strengthening and renovation to achieve the required serviceability of such RC beams(Ali et al., 2018).

It is essential to provide a platform for understanding the behavior of relatively new materials that could be used for strengthening purposes under various available strengthening techniques. The major target of strengthening is to achieve the required durability of deficient RC beams at optimum cost. The strengthening of RC structures and bridges are major challenges facing structural engineers. This chapter review the several materials and techniques that have been used by the researchers in the past along with their reliability suggested by the different cost. It is desirable that the findings of this chapter will strengthen the conclusion of this study.

2.2 Strengthening or Retrofitting

Strengthening or Retrofitting may be defined as the step taken to re-achieve the original structural performance of deteriorated structure by application of strengthening materials under recognized strengthening techniques. It is essential to understand the difference between the repair and strengthening of the deficient structure. Repairing is a phenomena that brings fractional enhancement in the performance of a structure after deterioration. In simple words, repairing is like a cosmetic improvement. Whereas, strengthening of damaged structure provides a workable improvement in the performance of deficient structures similar to the performance of the originally built same structure. However, when it comes to the performance of the strengthened structure under seismic loading, it is always desirable that the strengthened structure should perform better as compared to the originally built structure.

A significant number of existing structures are now facing deterioration in the form of steel corrosion, concrete spalling, or excessive cracking. In addition, some of these structures are found to be designed at load carrying capacity lower than has been applied in reality. This necessitates an immediate upgrading of these structures in order to improve their performance under the actual existing loads. Since the application of strengthening techniques in RC is increasing day by day, it is mandatory to manage the response of the retrofitted structure in the case of seismic impacts in order to minimize the life and property loss in case of an earthquake (Dowrick, 2003). The real life example of strengthened RC structures is shown in Figure 2.1.

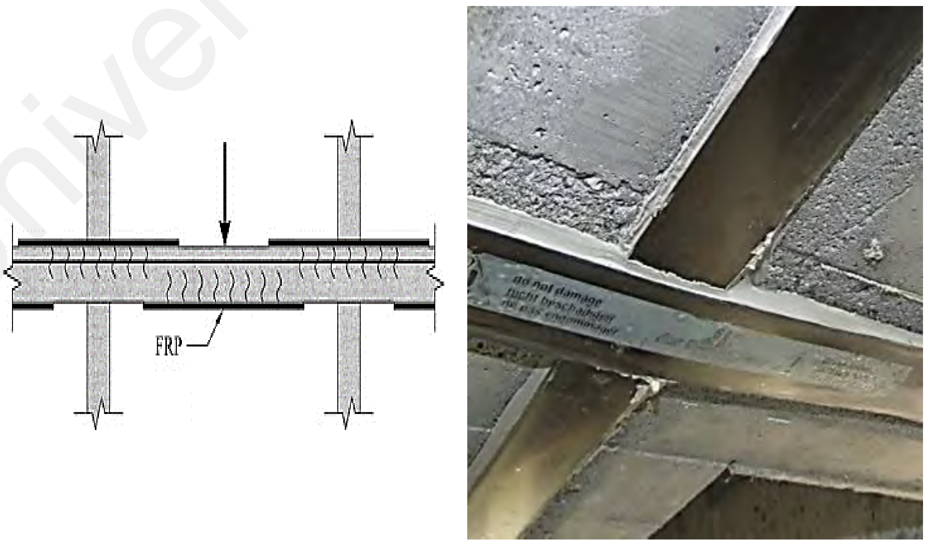

Figure 2.1: Real life strengthened structures

2.2.1 Strengthening materials

The quality of strengthening of deficient RC structures significantly depends upon the materials used for strengthening. A retrofit engineer must have an understanding of the behavior and response of such materials. This section presents a critical review of the performance of several available strengthening materials and a choice has been made to utilize the relatively appropriate material for strengthening the specimens used in this research.

2.2.1.1 Grouts

Grout is a fluid type material. The method of using grout for strengthening the structure is dependent of sufficient pressure under which grout is injected into the structural member and it is often desirable that the shrinkage in grout is of neglect able in order to fill up the gaps efficiently. Strengthening of real life structures using grouting techniques are shown in Figure 2.2. Various types of grouts used are:

- Injection grout: Most common application of injectable grout is in the retrofitting of aged masonry structures in the case of mortar degradation. It is also used for the strengthening of honey combed concrete.
- Cement sand grout: Cement sand grouts are cheapest. For injection purpose, the grout requires high water and cement contents. This results in shrinkage and cracking of grout at hardening. Suitable shrinkage compensating agents are required to minimize this. Use of cement-sand grout is very common in masonry buildings, but not very common in concrete.
- Sulfo-aluminate grout: In these grouts either shrinkage-compensating cement or anhydrous sulfo-aluminate expensive additive is used with Portland cement. The dosages of additive are recommended at 6% to 10% by weight of cement.

- Polymer grout: The most commonly used polymer resins grouts in concrete are polyester, epoxy, vinyl ester, polyurethane and acrylic. Out of these, epoxy is the most popular one. In case of underground and water seepage conditions, polyether and acrylic resins are used. Polymer grouts can be injected by pre-mixing the resins and hardener and injecting the mix through a pressure gun fitted with a nozzle. The automatic injection machine has a con of the controlled supply of resin and the hardener through two separate pipes.

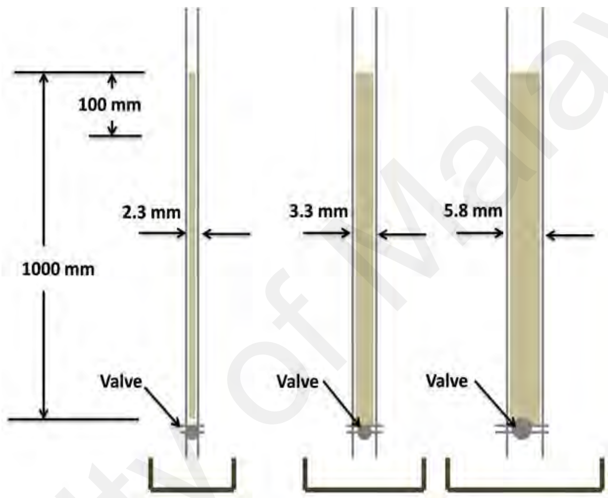

Figure 2.2: Strengthening real life structures using grouting techniques

2.2.1.2 Bonding Agents

An efficient strengthening of concrete can be achieved using bonding agents. These agents provide enhanced bond between existing concrete and new concrete and between concrete and reinforcement. Bonding agents are commonly applied using following three methods:

(a) Interface adhesives

(b) Surface interlocking

(c) Mechanical bonding

The bond between the previous and newly applied concrete as well as between the reinforcement and the newly applied concrete is provided using polymers and epoxy. When the cover of concrete is removed, the water blast and sand are used to clean the newly obtained surface of concrete and steel. When this surface becomes dry, a paint of adhesives is applied to the surface to improve the bonding and minimizing the chances of corrosion in steel. In case welding is needed in the steel that must be performed before the application of paint on the newly obtained steel-concrete surface.

2.2.1.3 Replacement and Jacketing Material

As evident from the name, these materials are used as replacement of parts of the damaged members in the structure. Among variety of the replacement or jacketing material, the steel reinforcement is also used occasionally as jacketing material. Care should be taken that the replacement materials make a non-shrinking strong bond with the existing material.

(a) ***Polymer modified concrete and mortar PMM/PMC***

Polymers are extensive fragment hydrocarbons and formed through Polymerization. Particles of polymers with negligible diameter are combined with distilled water to form polymer latexes which after drying, result in a constant film strip. Often, the powder form of these polymers, which is usually water soluble, is mixed with the dry cement aggregate. As compared to the traditionally used mortar or cement, the PMM/PMC has exhibited enhanced workability. The main advantage of PMM/PMC is its enriched bonding with existing concrete and significantly reduced permeability. The real life structures strengthened with polymer modified concrete and mortar are shown in Figure 2.3.

Figure 2.3 : Polymer modified concrete and mortar in real life structures

(b) ***Ferro cement***

Ferrocement is a multipurpose and reliable building material which is widely used in developing countries for strengthening and repairing of damaged structures (Abdullah & Takiguchi, 2000). The constant spreading and high surface area to volume ratio of its key advantages in better crack arrest mechanism due to high tensile strength. The composite material formed by a combination of steel and mortar is described as a term, 'Ferrocement'. The structural behaviour of ferrocement is highly different from traditional RC and hence, it is considered as a totally different material from RC (Al-Sulaimani & Basunbul, 1991). The thickness of ferrocement section is usually lesser than one inch and a fraction of that is used as a cover over the outermost mesh layer. Whereas, traditional RC utilizes up to one inch as a cover for the same layer. A light framework is enough for the ferrocement made reinforcement to be assembled into the desirable profile and can be poured on-site when used with a dense mortar. The structures strengthened by the ferrocement technique are shown in Figure 2.4.

Figure 2.4: Ferrocement strengthened structures

(c) ***Steel***

Steel is a well-recognized and conventional material used for the strengthening of deficient structures throughout the world. The main characteristics of steel that make it suitable for strengthening include its ductility, optimum execution cost and high strength compared to self-weight. Steel is also used in its prestressed form for strengthening (Tan & Tjandra, 2003). Using the steel-jacket retrofitting approach with recycled aggregate concrete (RAC), the initial stiffness, ultimate strength, deformation ductility and energy dissipation ability of the columns are improved significantly (He et al., 2018). A retrofitted column with recycled aggregate concrete details is shown in Figure 2.5.

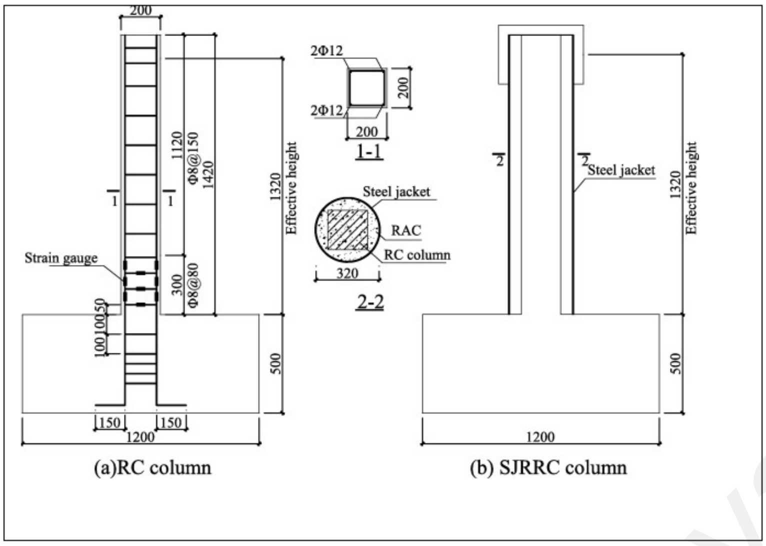

Figure 2.5: Steel-jacket retrofitting approach with recycled aggregate concrete (RAC)(He et al., 2018)

In order to achieve enhanced strength, the concrete members are bonded with external steel plates with the help of different types of epoxies. However, this whole process needs careful supervision and skilled labor work. Figure 2.6 shows another form in which steel plates can be pasted to the surface is in the form of jackets (Aslam et al., 2015).

Figure 2.6: The real life structures strengthened with steel-jacket

This process can also be achieved by grouting. The real life structures strengthened with steel plate is shown in Figure 2.7. On the other hand, prestressed steel tendons having constant material properties and increased ductility and strength are widely used as an efficient technique for retrofitting of RC beams, however, due to the reason that steel is stressed up to half of its ultimate strength, the service age of prestressed steel is reduced (Tan & Tjandra, 2003). Another disadvantage of post-tensioned prestressing is the maximize risk of corrosion due to its relatively smaller diameter. This sensitivity of such steel tendon is so high that a tiny spot of rust or a smooth layer of corrosion produce considerable decrease in the cross-section area of the post-tensioned steel (Aslam et al., 2015). A significant degradation in the mechanical properties of post-tensioned steel tendons may happens if it is left unprotected and exposed to the external environment (Nordin, 2005). Figure 2.8 showed the real life structures strengthened with prestressed steel tendons.

Being considered as a complex process due to the variable behavior of RC structure depending upon the damage and age, the retrofitting of RC structure needs a flaw less strengthening material(Elsouri & Harajli, 2015). The drawbacks of conventional steel urged the researchers to find a better and beneficial replacement strengthening material. Importantly, it is always desirable that the performance of the strengthened structure should be same as the original structure. Providing a solution of the problems exhibited by conventional steel used for strengthening, studies revealed that if used instead of conventional steel, FRPs can improve strength and first rate creep of strengthened structures (Nordin, 2005).

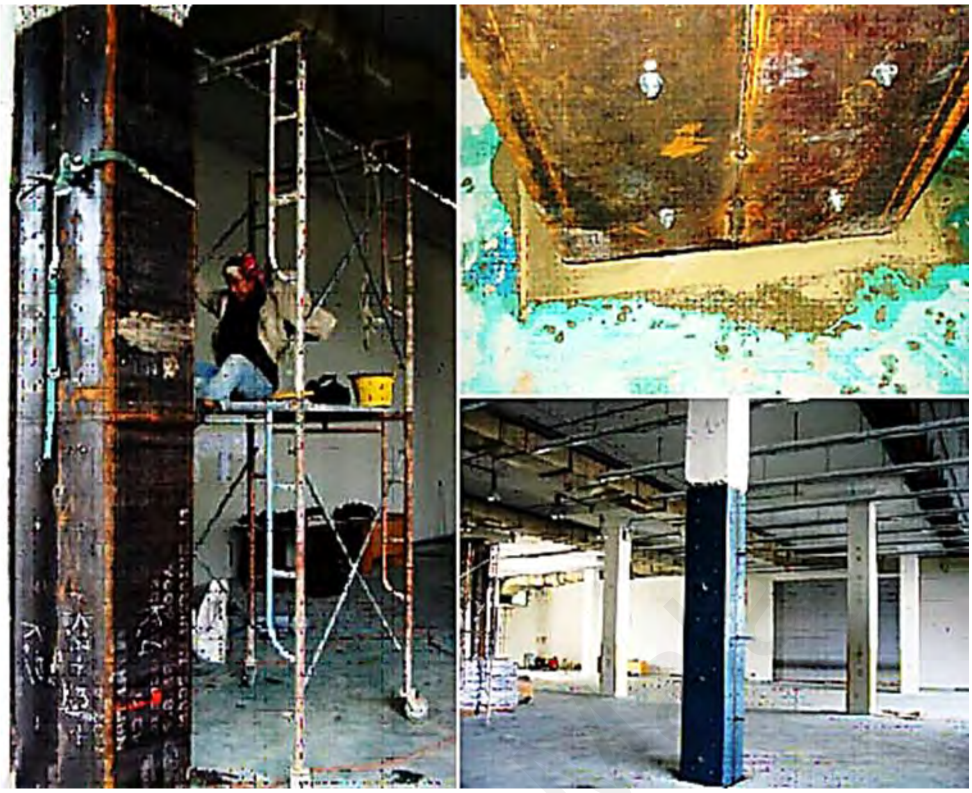

Figure 2.7: The real life structures strengthened with steel plate

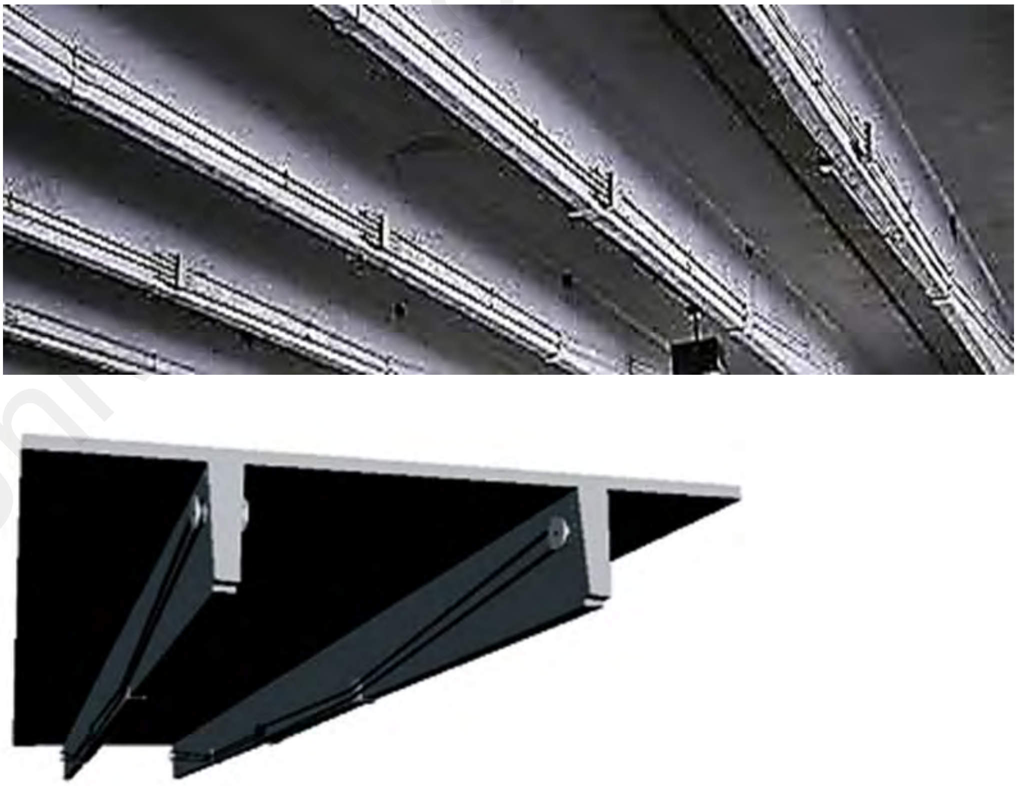

Figure 2.8: The real life structures strengthened with prestressed steel tendons

(d) ***Fiber reinforced polymers (FRP)***

FRP is a newly established material for strengthening of RC and masonry structure. It has been found to be an effective replacement of steel plates for strengthening of columns by exterior wrapping. The main advantage of FRP is its high strength to weight ratio and high corrosion resistance (Feroldi & Russo, 2016). FRP plates are two to ten times stronger than steel plates, while their weight is just 20% of that of steel (Garden & Hollaway, 1998). The real life structures strengthened with carbon fiber reinforced polymers are shown in Figure 2.9.

Figure 2.9: The real life structures strengthened with carbon fiber reinforced polymers

With the passage of time, it was brought to light by the literature and practical examples that the weak points of steel as a strengthening material are its nominal resistance to hostile environmental effects, high sensitivity to corrosion and reduced service life in case of prestressing. Consequently, the FRPs, both in normal as well as in prestressed forms, were recognized as more reliable strengthening material and initially utilized in infrastructures. Furthermore, when the size of the components which are desired to be strengthened and ease in on-site handling are the factors needed extra consideration, FRPs are more suitable as compared to the conventional steel (Garden & Hollaway, 1998). When prestressed, the suitability of FRPs increases for retrofitting purposes. Recently, the use of prestressed FRPs as reinforcement, both as internal and external, is highly increased in RC members. To control seismic effects efficiently, FRPs provide increased energy dissipation and enhanced fatigue resistance. Another important advantage is the increased serviceability life as compared to the prestressed steel tendons which helps in overcoming the aging problems of the strengthened structures. Furthermore, the alterations required due to change in the purpose of use of the strengthened structure and upgrading to resist seismic effects can be easily achieved if FRPs are used for strengthening the structural members (Badawi & Soudki, 2009; Laura De Lorenzis et al., 2000). Figures 2.10 and 2.11 show the applications of prestressed FRP bars and laminates for strengthening RC beams.

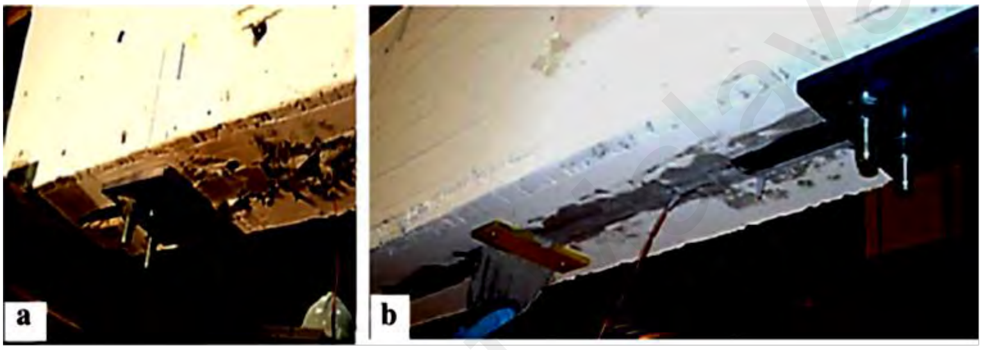

Figure 2.10: Application of prestressed CFRP bars for strengthening RC beams

Figure 2.11: Real life picture of externally prestressed CFRP laminates bonded strengthened structure

Literature review revealed that the strength and serviceability capabilities of FRPs as strengthening material are far better than steel (Badawi & Soudki, 2009; L De Lorenzis & Teng, 2007; Nordin, 2005). These properties of FRPs increase when prestressed, as compared to their steel counterpart (Association, 2002; Triantafillou et al., 1992). A comparison is illustrated in Tables 2.1 and 2.2. Having the strain capacity in limitations, an indication of premature debonding failure at earlier stages and decreased deflection in members also differentiate FRPs from other strengthening materials (Busel & Lockwood, 2000).

Table 2-1: Uniaxial tensile properties of prestressing tendons (ACI-318-2008)

Properties	Steel tendon	7 wire steel tendon	AFRP Tendon	GFRP Tendon	CFRP Tendon
Tensile Strength (MPa)	**1400- 1900**	**1725 Grad 1 1860 Grade 2**	**1200 - 2100**	**1400 - 1700**	**1650 - 2400**
Density (ib/ft^3)	**490**	**N.A**	**75-90**	**75-130**	**90-100**

Table 2-2: Uniaxial tensile properties of prestressing tendons (Association, 2002)

Mechanical Properties	Prestressing Steel	AFRP Tendon	GFRP Tendon	CFRP Tendon
Nominal Yield stress (MPa)	1034 – 1396	N/A	N/A	N/A
Tensile Strength (MPa)	1379 – 1862	1200 – 2068	1379 – 1724	1650 – 2410
Elastic Modulus (GPa)	186 – 200	50 – 74	48 – 62	152 – 165
Density (kg/m^3)	7900	1250 – 1400	1250–2400	1500 – 1600

FRPs are available in several different sub-types including CFRP, GFRP and AFRP (Carbon fibre reinforced polymers, Glass fibre reinforced polymers and Aramid fibre reinforced polymers respectively). When an enhanced seismic protection, greater service life, ease in execution and on-site handling and a shield against hostile environmental impacts is desired, AFRP performs very well with low labor cost (Deng & Xiao, 2011). There are some unavoidable disadvantages of AFRPs also exist. For instance, the acid and alkaline materials are poorly resisted by AFRPs (Kurihashi et al., 2011). However, along with other qualities same as AFRPs, this problem has been efficiently overcome by CFRPs (Deng & Xiao, 2011).

The structural behaviour of GFRPs as strengthening material is not well-recognized by the literature. One study has recognized the GFRP as a strong material with increased strength to strengthen RC beams (Kurihashi et al., 2011). GFRP has a modulus of elasticity closer to concrete but it has lower elasticity and ductility as compared to steel, AFRP and CFRP, which minimizes the usage of GFRP in the strengthening of RC structures. The stress-strain behaviour of prestressed materials (tendons) is shown in Figure 2.12.

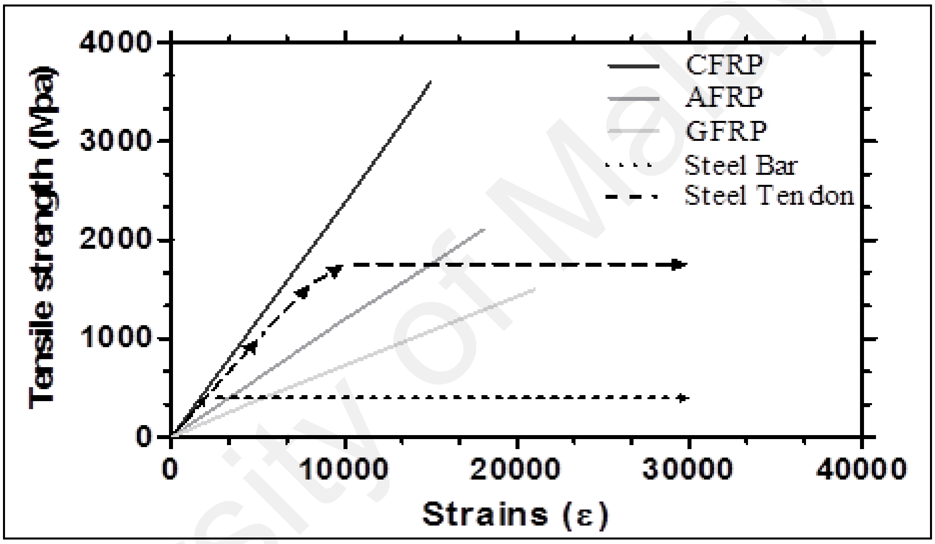

Figure 2.12: Stress-strain behaviour of prestressed materials (tendons)

2.3 FRP Composition and Types

FRPs are composite materials made up of two or more materials but having efficient structural behaviour as compared to its ingredients in their individual capacity (Badawi & Soudki, 2009). The properties of the FRP materials are mainly determined by the choice of fibres and their volume fraction. In civil engineering applications, three types of fibres are commonly used namely, Aramid (AFRP), Glass (GFRP), and Carbon (CFRP). They generally have a higher ultimate strength than that of the conventional reinforcing steel, and exhibit linear-elastic behaviour until they fail by rupture (sudden failure). The components of the composite materials are shown in Figure 2.13. One constituent is called the fibre phase and the other in which the fibres are embedded is called the matrix or resin phase.

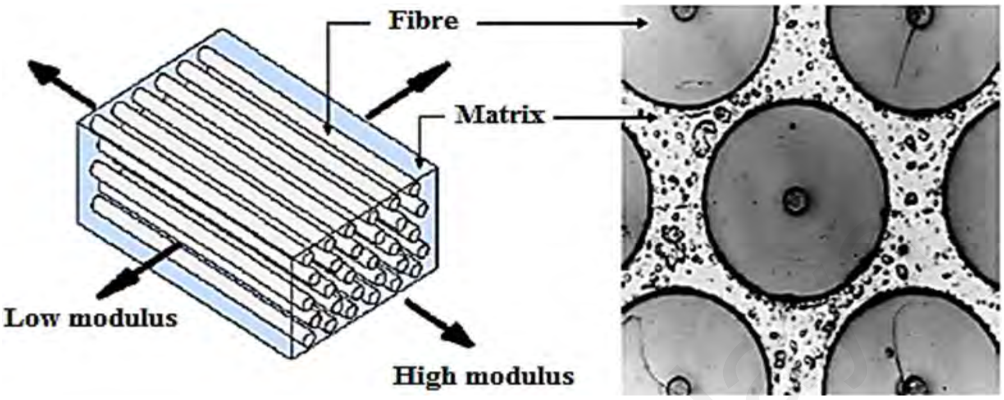

Figure 2.13: Components of composite materials (Badawi & Soudki, 2009)

2.3.1 Fibres

Mostly, three types of fibres are used in civil engineering applications: aramid, glass and carbon. Aramid fibre is used to confront great value of stresses and dynamic impacts. It provides excellent flexibility and high strength. Glass fibres provide excellent insulation properties and high ductility. Carbon fibres have high strength-to-weight ratio, high modulus-to-weight ratio, high fatigue strength, and low coefficient of thermal expansion. It has superior strength compared to others (Aramid and glass) as shown on Table 2.3 (Badawi & Soudki, 2009; Laura De Lorenzis et al., 2000).

In most cases, cost plays a very important role in the decision making process. Aramid fibres are the most expensive, carbon in the second place, and glass in the third place (Badawi & Soudki, 2009). However, it is noted that the volume of FRP required having the same effect as the reinforcing steel is usually lower which compromises its relatively high cost.

The selection of the fibres depends on the specific need. Fibres function as load carrying components in the FRP composites and provide a tensile strength, that basically depends on three factors: the type of fibres (carbon, glass, and aramid), the amount of fibres (volume fraction), and the orientation of the fibres. The mechanical properties of different FRPs as per ISIS Canada are shown in Table 2.3 (Laura De Lorenzis et al., 2000).

Table 2-3: Mechanical properties of different FRP's (Laura De Lorenzis et al., 2000)

Materials	Modulus of Elasticity (GPa)	Ultimate Elongation (%)
CFRP	200-800	0.4-2.5
GFRP	70-87	2-5.6
AFRP	74-179	1.9-4.6

2.3.2 Resins or Matrix

An efficient FRP engineering structural composite system provides the required strength and serviceability properties and also maintains its in-service physical and mechanical functionalities(Kadhim et al., 2012). Consequently, the most important properties of the matrix, in addition to binding the fibres, are its physical and in-service characteristics. Resins are classified into two main categories; thermoplastic and thermoset resins. Thermoplastic resins are characterized by their ability to soften and harden as a function of temperature increase or decrease. Thermoset resins are insoluble and infusible materials when subjected to curing by the application of heat or by chemical means (Badawi & Soudki, 2009). The latter type of resins is used mainly for civil engineering applications since it is less likely to be affected by the external in-service environment. It is important to emphasize that the matrix should have a higher strain to fracture than the fibres (Figure 2.14). If not, the matrix will crack before the fibres fail resulting in un-protected fibres. Two main types of matrix, polyester and epoxy, are used.

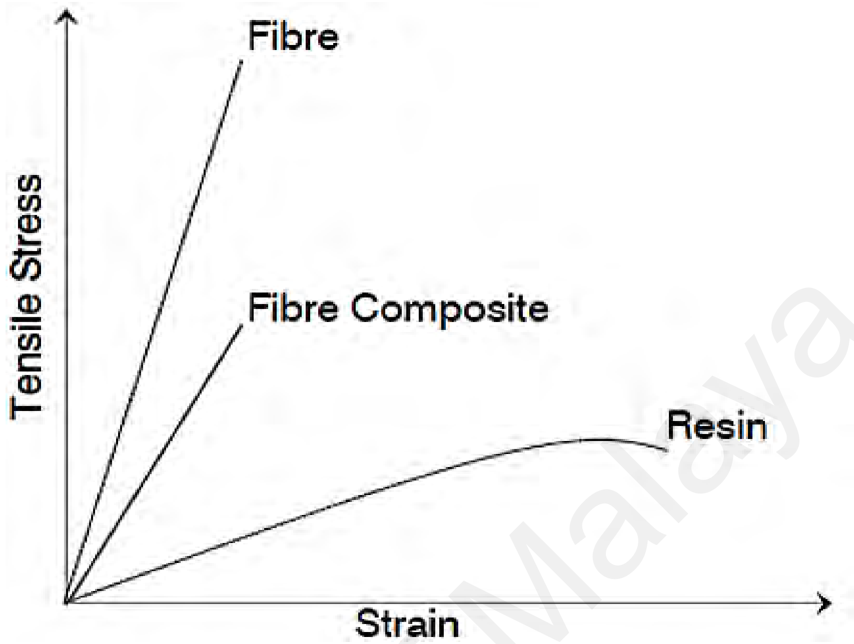

Figure 2.14: Tensile stress-strain relationships for the composite FRP and its components (Woo et al., 2013)

Their mechanical properties are given in Table 2.4.

Table 2-4: Mechanical properties of matrices (Woo et al., 2013)

Material	Tensile Strength (MPa)	Tensile Modulus (GPa)	Density (kg/m^3)	Ultimate strain (%)
Polyester	20-100	2.1-4.1	1000-1450	1-6.5
Epoxy	55-130	2.5-4.1	1100-1300	1.5-9

2.4 Strengthening of RC Structures

Over the last few decades, traffic loads on infrastructures such as bridges is increasing day by day and more frequent. It is expected that if this tendency will be continued than it will create a bigger problem in the serviceability of the structures and the structural behaviour will also be affected and the structures were being overloaded (Ozbakkaloglu & Fanggi, 2015). Impact loads due to accidents and increasing traffic creates cyclic loadings can damage bridges leading to a deficiency in structural capacity that may not be able to carry the existing service load. Moreover, sometimes, mistakes or construction errors may result in an inadequate load carrying capacity in the structure. For example in the USA, approximately 30% of the bridges (600,000 bridges) are deficient in load carrying capacity and require strengthening (Mukherjee & Rai, 2009; Woo et al., 2008; Xue et al., 2010). The process of strengthening RC structures can be shown in Figure 2.15.

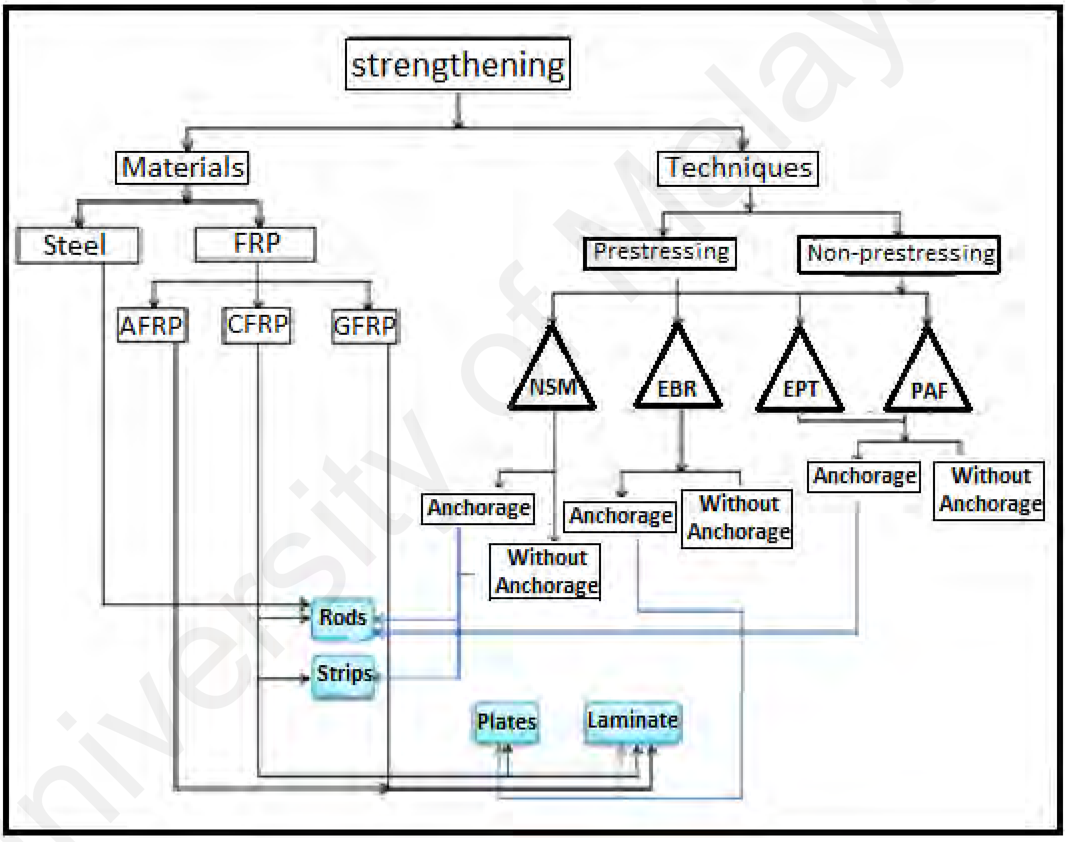

Figure 2.15: Strengthening Process (Aslam et al., 2015)

To overcome these deficiencies in the structural performance, and to maintain these infrastructures under service, structural upgrading is needed. Using FRP materials to strengthen RC structures is one of the methods used lately, and it can be applied as externally bonded or near surface mounted with non-prestressed or prestressed FRP reinforcement. Codes and guidelines are available and address the design and specifications for using FRP to strengthen RC structures (Woo et al., 2013; Yu et al., 2003).

2.5 RC Beam-Column Connection

In high-rise or multi-story moment resisting RC frames, beam-column connections (BCCs) are precarious regions and their response is usually inelastic when subjected to various types of high magnitude loadings (Thomas & Priestley, 1992). Moreover, in the case of seismic loading, where the column and beam moments transferred to contrary directions, the BCCs experience high magnitude of horizontal and vertical shear forces and becomes more critical (Chutarat & Aboutaha, 2003) Being a joining element, it is essential that care should be taken to minimize the risk of brittle failure of BCC. Thus, the design of RC BCCs must comply that the decrease in connection strength should be restricted till the ductility and design capacities of connected beams become equal (Costas P. Antonopoulos & Triantafillou, 2003). The key function of a BCC should be to enable the connected members to utilize their ultimate moment capacity (Gergely et al., 2000). Moreover, BCCs must be capable of sufficient strength and stiffness in order to counter the internal forces generated by the connected structural members.

The RC BCCs are the most susceptible structural component and most often, the failure of a structure initiates with the failure of BCCs (Engindeniz et al., 2005; Thomas & Priestley, 1992). Many examples of such phenomenon can be extracted from the effects of contemporary earthquakes. Inadequate designing of BCCs acts as “weak links” in RC frames. The reasons of failure of BCCs occur most commonly may be broadly classified as:

- Inadequate shear strength.
- Poor anchorage or bonding and
- Deficient flexural strength or ductility.

The two major failure modes for the failure at joints are: (a) joint shear failure and (b) end anchorage failure as shown in Figure 2.16.

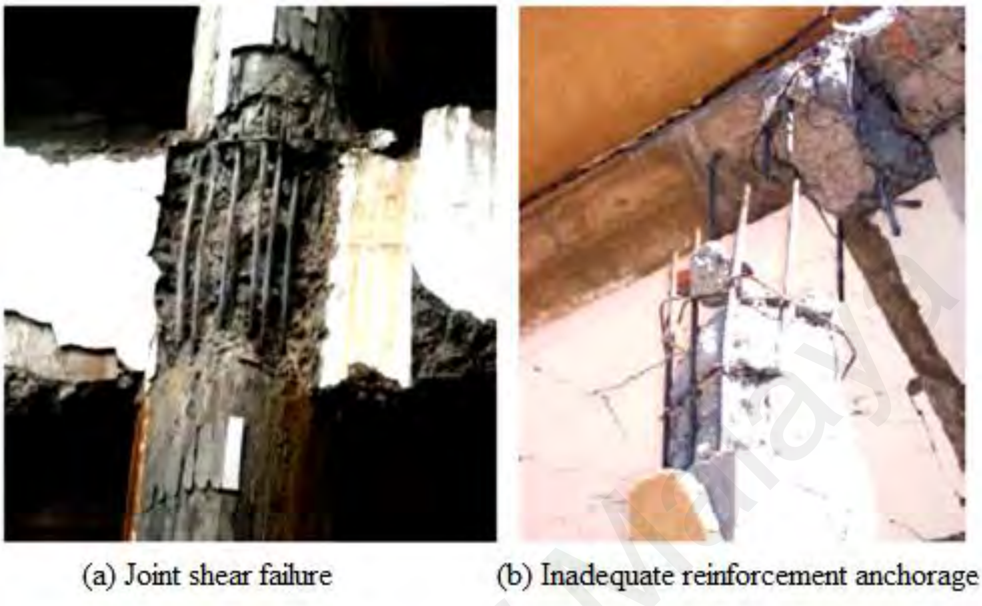

Figure 2.16: Major failure modes for a RC beam-column joint

The structural analysis of RC moment resisting frame (MRF) is generally based on the assumption of BCCs as rigid connections (Standard, 1893, 1993; Uma, 2003). Instead of careful consideration on the detailing of BCC, the consideration is given to design efficient anchorage system for the longitudinal reinforcement in connected beam. This assumption is only acceptable when the structure is subjected to the static loading only(Hasaballa et al., 2009). Literature reports that this assumption was failed in some of the recent earthquakes and the failure of structure was initiated with the failure of BCCs (Arya, 1981; Bakis et al., 2002; Standard, 1893). As illustrated in Figure 2.17. Literature suggests that the insufficient transverse reinforcement and anchorage capacity in RC BCCs are the major type of discrepancies in their structural design (Liu, 2006). This revealed that even slight negligence in the design of RC BCCs may tends towards the collapse of the whole structure, despite the fact that other structural members are designed perfectly (Ehsani & Wight, 1985). The recent design codes suggest that in order to ensure the enhanced shear strength subsequent to the BCC cracking, a shear reinforcement must be provided(PARME, 1976; Standards, 1993). Details of an exterior beam-column connection are presented in figure 2.18.

Figure 2.17: Typical beam-column joint failures (1999 Turkey earthquake)

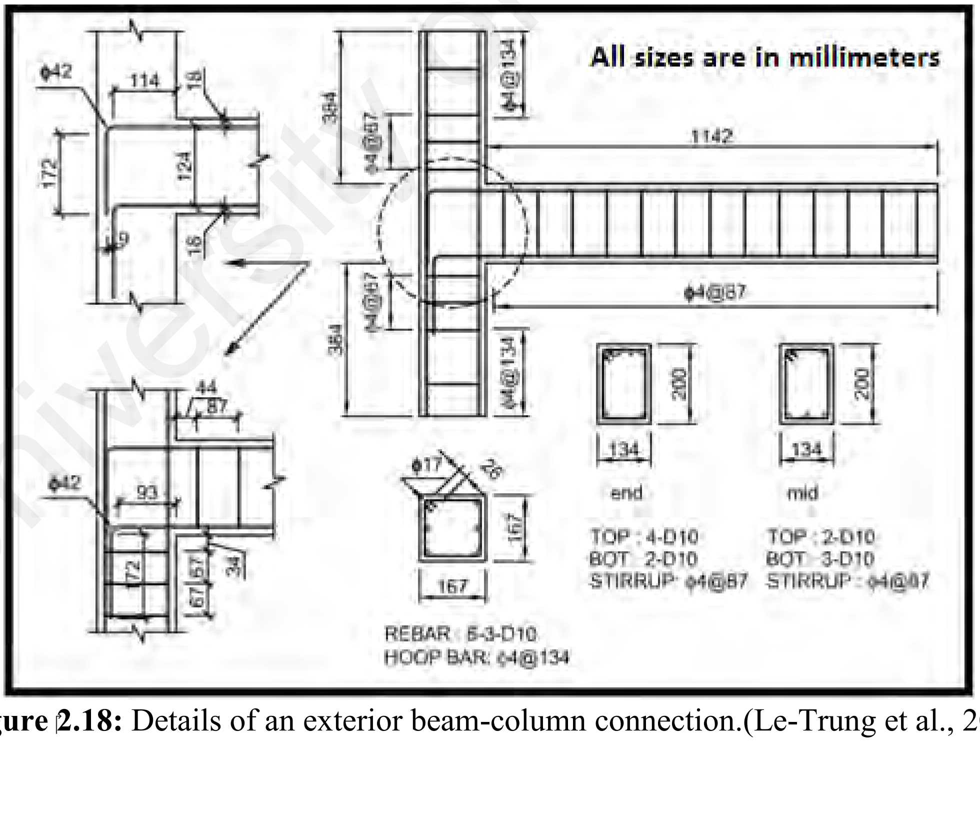

Figure 2.18: Details of an exterior beam-column connection.(Le-Trung et al., 2011)

2.5.1 Types of BCCs in Moment Resisting Frames (MRFs)

The BCCs used in MRFs are broadly classified into three types according to their location inside the frame. These types are: (i) Interior connection (ii) Exterior connection (iii) Corner connection (Figure 2.19).

- An interior connection is said to be a connection making the intersection of four beams connected to the vertical faces of a column.
- An exterior connection is said to be a connection making the intersection between one beam connected to the vertical face of the column and two more beams connected perpendicularly into the connection.
- A corner connection is said to be a connection with a beam each frames into two adjacent vertical faces of a column.

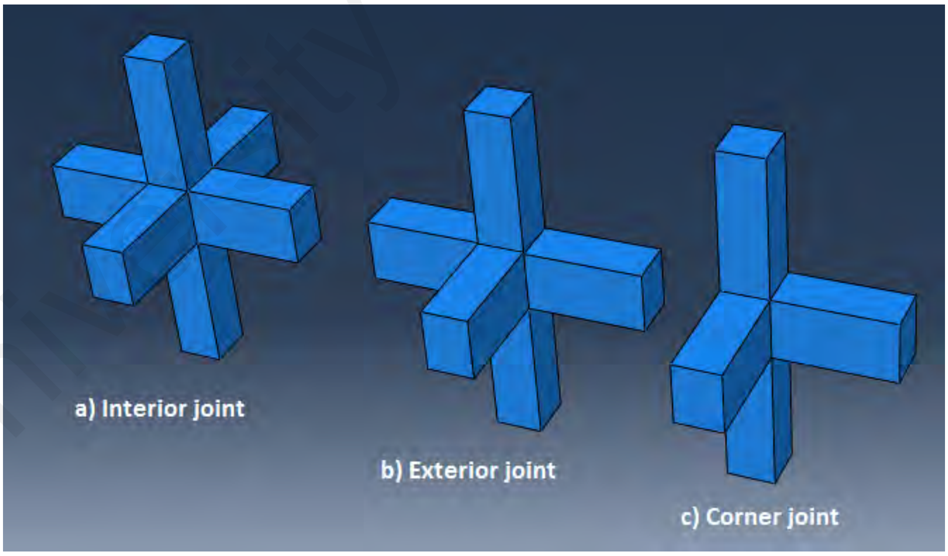

Figure 2.19: Types of joints in a frame (Pampanin et al., 2002)

2.5.2 Forces acting on Beam-Column Joint

The key factors that controls the effects of applied forces are the configuration of connection and the type of acting load. The stresses generated by the applied forces and the resultant crack propagations on all the three types of connections in RC MRFs described above were studied (Uma, 2003). The distribution of forces due to live load on interior connection are illustrated in Figure 2.20(a). It can be seen that the stresses from the end of beams and the axial load on column is transmitted by the connection. The effects of equilibrating seismic forces on the beams and column result in the development of a transverse combination of tensile and compressive forces, as shown in Figure 2.20(b). Cracks develop perpendicular to the tension diagonal A-Bin the joint and at the faces of the joint where the beams frame into the joint. The struts are presented using dashes whereas the ties are illustrated with solid lines. Due to the lack of sufficient resistance to tensile forces in the concrete, transverse reinforcements are provided in such a way that they cross the plane of failure to resist the diagonal tensile forces.

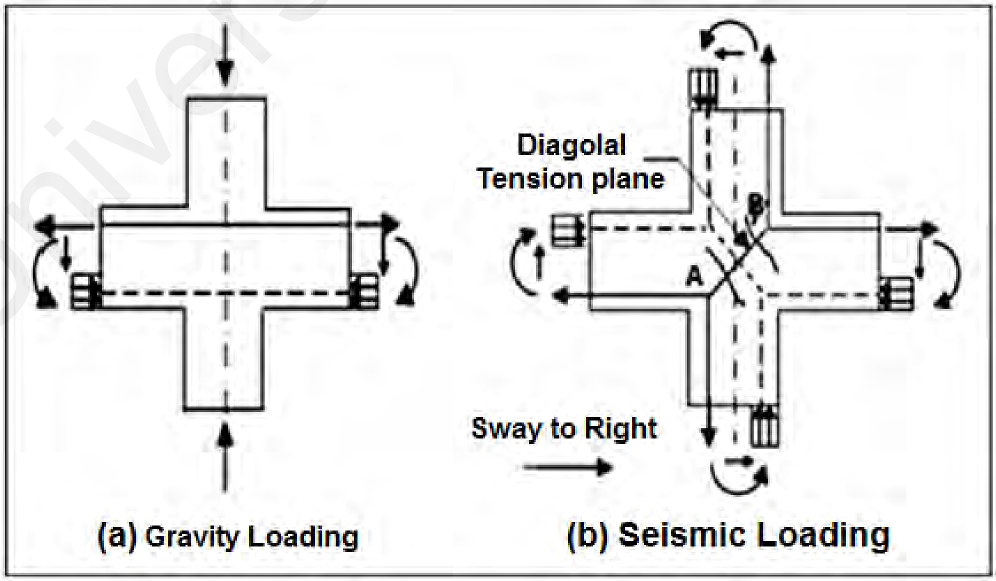

Figure 2.20: Interior joint (Uma, 2003)

Figure 2.21(a) shows a typical pattern of forces acting on an exterior connection. The propagation of transverse cracks are stimulated by the shear force in the connection that substantiated the provision of design standards to provide the shear reinforcement which enhances the structural efficiency of the connection(Bo Li et al., 2015). Figure 2.21(b) and Figure 2.21(c) represent a few of the detailing arrangement of exterior connections. Figure 2.21(b) shows that the bars bent away from the joint core result in efficiencies of 25-40 % while those passing through and anchored in the joint core show 85- 100% efficiency, provided that the concrete core is confined within the connection using stirrups.

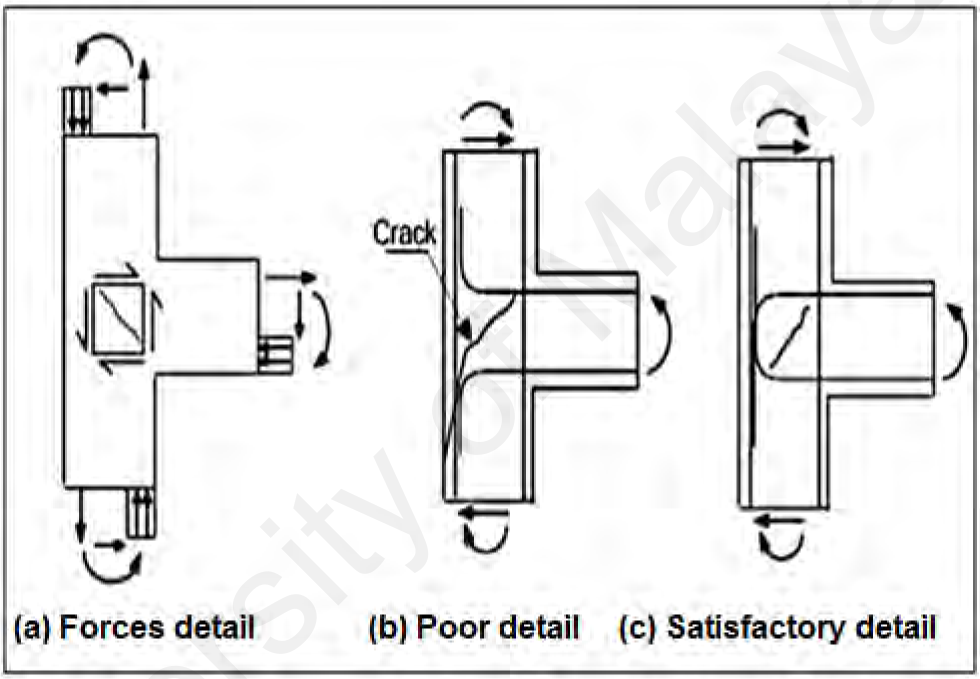

Figure 2.21: Exterior Joint (Uma, 2003)

the performance of exterior RC BCCs strengthened with FRP under cyclic load was examined(Gupta, 2012). In this experiment, both confined and unconfined external RC BCCs under cyclic excitation were examined and the same specimen after the test were retrofitted with FRP sheets in the damage area to restore their strength. Four RC T-joints having variable detailing; two were unconfined and the other two confined(Standard, 1993, 2000) . The cyclic load has been applied using Quasi-static testing technique.

Figure 2.22(c) illustrates that the distribution of forces according to the loading direction can be considered similar in both the corner and exterior connections. In case the generated moments urge to open or close the wall type corner, the corner connections are sub-categorized as knee joints or L-joints. The resultant stress propagation and the generation of consequent cracks are illustrated in Figure 2.22.

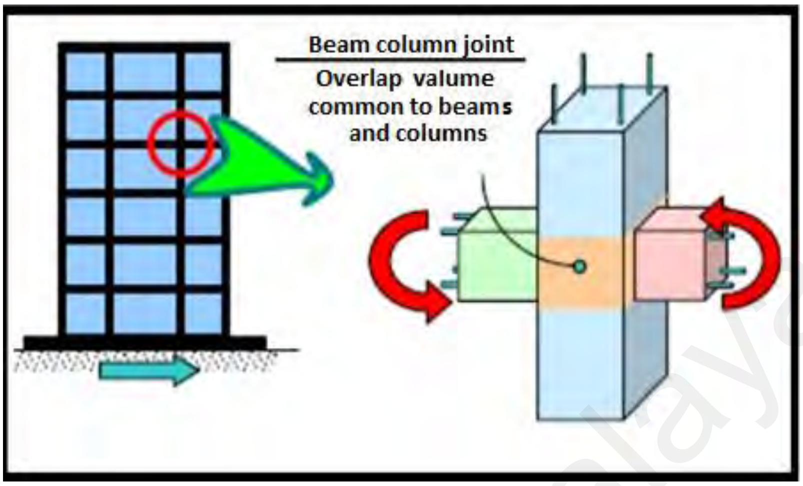

Figure 2.22: Corner Joints (Uma, 2003)

2.5.3 Earthquake Behavior of Joints

When subjected to seismic loads, the beams connected to a column through the joint experience the moments in the direction same as the direction of loading, being either clockwise or anti-clockwise. This phenomenon is shown in Figure 2.23.

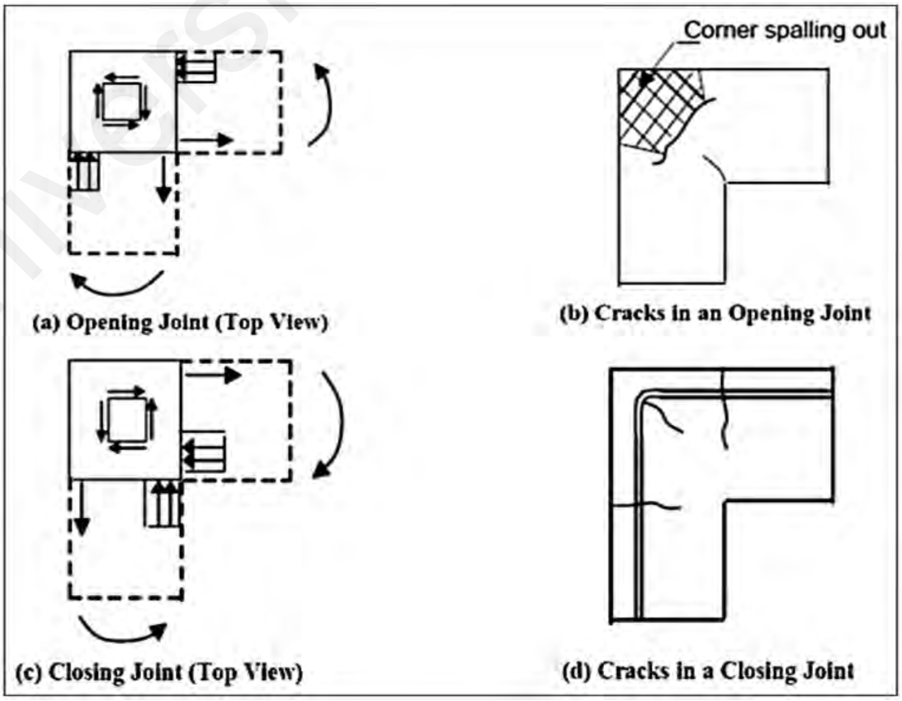

Figure 2.23: Beam-Column Joints are critical parts of a building (Ravi & Arulraj, 2010)

The seismic moments compel the top and bottom bars to be pulled in the directions opposite to each other as presented in Figure 2.24 (a). In order to efficiently balance these forces, the strength of steel and concrete existing in the RC connection plays vital role. It should be noted that the inadequacy either in the strength of the concrete or the width of the column weakens the concrete-steel bond. This leads to the slippage of steel bars into the connection which reduces the load-carrying capacity of the beams (Ravi & Arulraj, 2010). Further, under the action of the above pull-push forces at top and bottom ends, joints undergo geometric distortion; one diagonal length of the joint elongates and the other compresses as shown in Figure 2.24(b). If the column cross-sectional size is insufficient, the concrete in the joint develops diagonal cracks. these result in irreparable damage in joints under strong seismic shaking (Ravi & Arulraj, 2010).

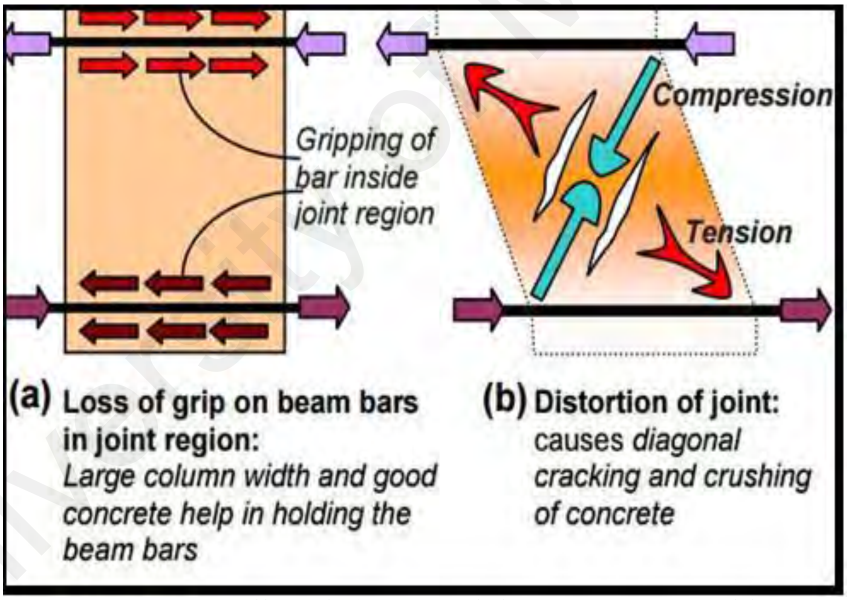

Figure 2.24: Pull-push forces on joints cause two problems

2.5.4 Bond requirements in the Beam-Column Joint

2.5.4.1 Interior joint

The forces acting in steel bars placed inside the interior BCC changes their behavior from tensile to compressive which initiates a pull and push outcome. This phenomenon requires sufficient bond strength and rebars length inside the connection. The development length should be sufficient enough to accommodate the change of tensile force into compression. An insufficient development length increases the risk of bar slippage if the limited bond stress exceeds its limits (N. Subramanian, Rao, D.S.P; , 2003). The distribution of bond along the longitudinal bars is shown in Figure 2.25.

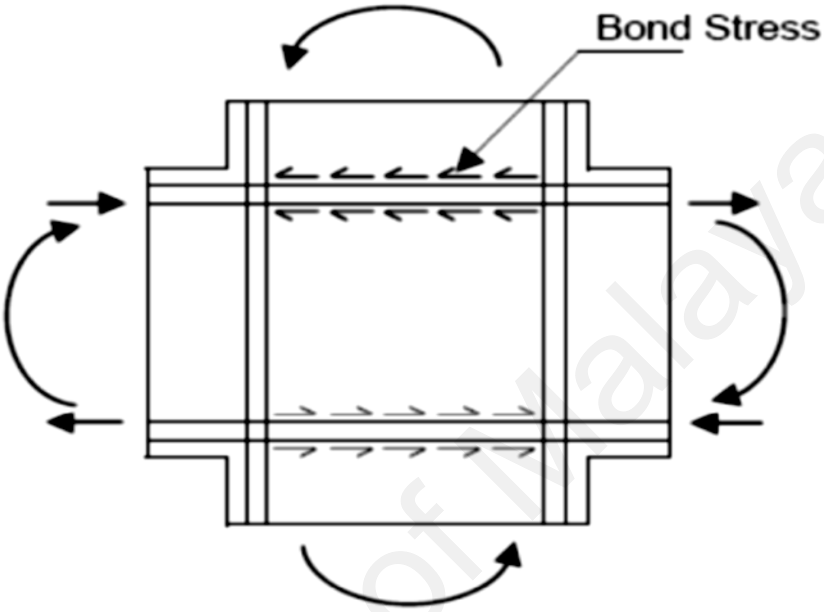

Figure 2.25: Bond stress in interior joint (N. Subramanian, Rao, D.S.P; , 2003)

The development length of longitudinal bars passing through the interior connection is determined by the depth of the column. Literature has revealed that a development length greater than 28 bar diameters results in a negligible bond degradation for variable stress magnitudes inside the connection, for instance, if 20 mm nominal bar size is to be used, the member depth to be provided is 560 mm (N. Subramanian, Rao, D.S.P; , 2003).

2.5.4.2 Exterior Joint

The exterior connection terminates the longitudinal reinforcement of beams connected to the column and restricts its length. If the termination is processed straight away, a progressive deterioration of bond occurs and the bar may be pulled out of the connection which completely reduces the flexural strength. This type of failure is dangerous and hence, proper anchorage using hooks of the beam longitudinal reinforcement bars in the joint core is essential with sufficient horizontal development length and a tail extension as shown in Figure 2.26. Because of the likelihood of yield penetration into the joint core, the development length is to be considered effective from the critical section beyond the zone of yield penetration. Thus, the size of the member should accommodate the development length considering the possibility of yield penetration (N. Subramanian, Rao, D.S.P; , 2003).

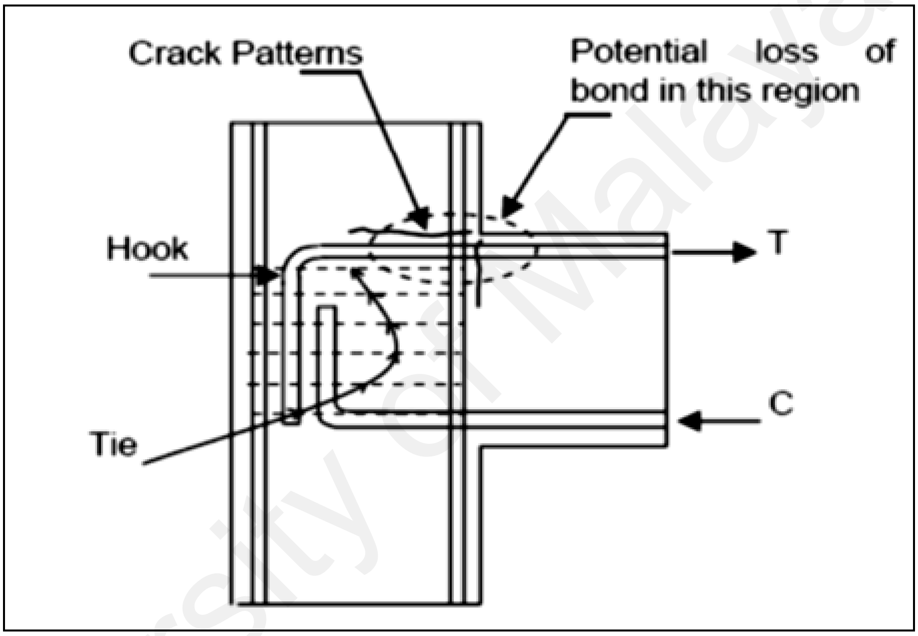

Figure 2.26: Hook in an Exterior Joint (Subramanian et al., 2003)

2.5.4.3 Corner Joint

A thorough literature review revealed that there are no noticeable differences in the requirement of steel-concrete bond for exterior BCCs and corner (or Knee type) BCCs(Le-Trung et al., 2010; Pampanin et al., 2002; N. Subramanian & Rao, 2003). The additional care which should be in taken in the design of reinforcement of corner joints is the consideration to restrict the diagonal shear cracks (N. Subramanian, Rao, D.S.P; , 2003).

2.6 Experimental Studies on Deficient Beam-Column Joints

Several experimental studies on gravity load designed (GLD) beam-column joints are available in the literature. The term GLD refers to beam-column joints or frames having acceptable performance in terms of vertical load carrying capacity. These studies aimed at investigating joint shear and bond slip deformations, joint shear capacity, and degradation of joint strength and stiffness due to cyclic load application. Hanson & Conner, (1967) published the first series of tests conducted on beam-column joints. They tested seven exterior beam-column sub assemblages in order to investigate the reinforcing details that would ensure ductility of the joint under cyclic loading(Hanson & Conner, 1967). The major test parameters were column size, load, joint reinforcement ratio and confinement by out of plane beams. They concluded that properly designed and detailed beam-column joints can resist moderate earthquakes without damage and severe earthquakes without substantial loss of strength. They also indicated that joints without transverse beams require ties to provide adequate confinement and shear resistance.

A beam-column joint under seismic actions was studied (Paulay et al., 1978). An experimental study was conducted on reinforced concrete joints with continuous positive bottom beam reinforcement in the joint region and with no joint shear reinforcement (Pessiki et al., 1990). Reversed cyclic loading tests on deficient specimens showed extensive shear cracking in joints at failure and the damage was confined to the joint panel region. The deficient specimens showed rapid stiffness and strength degradation, resulting in an increase of drift. For specimens with joint shear reinforcement, cracks within the joint panel were distributed and an increase in the joint ability to maintain load carrying capacity at larger drifts was noted. However, the peak load was not significantly changed. This is in agreement with the findings of the other researchers (Ascione et al., 2017; Ghobarah & Said, 2001, 2002).

The compression response of cracked reinforced concrete was studied (Vecchio & Collins, 1993). The seismic performance of both interior and exterior beam-column joints with substandard reinforcing details have been studied (Hakuto et al., 2000). In their study, a curve describing the relationship between displacement ductility factor and joint shear strength ratio was presented.

Beres et al.,(1992) indicated that the ACI-ASCE 352R equations underestimated the component of shear capacity provided by concrete in reinforced concrete joints (Beres et al., 1992; Beres et al., 1996). Since this was the only available formula for calculating the concrete contribution to joint shear strength, they underlined the lack of analytical tools for calculating basic information on the joint capacity. A technical report on seismic evaluation and rehabilitation of concrete buildings have been written (White & Mosalam, 1997). A study on RC beam- column joints under uniaxial and biaxial loading have been conducted (Kurose, 1988). The seismic performance of existing RC beam-column joints was investigated (Walker, 2001) .

A realistic repair and retrofit scheme using carbon fibre-reinforced polymer (CFRP) sheets to improve the ductility of the deficient joints, while providing continuity of the flexural strengthening through the joint was proposed (Pohoryles et al., 2015).

The effect of the joint shear reinforcement ratio on the shear strength of beam-column joints was experimentally investigated (Fujii & Morita, 1991). They indicated that at a joint shear strain of about 0.5%, the degradation of shear rigidity was accelerated under subsequent load reversals. The ultimate shear strength was achieved at a shear strain of 1.5% and 2.8% for exterior and interior joint specimens, respectively. An experimental study was performed on beam-column joint specimens with a ratio of joint shear stress at yielding of beams to joint shear strength of less than 0.50 (Kaku & Asakusa, 1991). It was noticed that the majority of the tested specimens failed due to joint shear after the reversed loading cycle following the yielding of the beams. For these specimens, the joint shear deformations increased rapidly after a joint shear strain of about 0.80%.

2.6.1 Beam-Column Joints Repair Using Conventional Materials

After paramount structural damage caused by several earthquakes, designers started to realize the importance of beam-column joints for structural integrity of moment resisting frames. This created a need to rehabilitate existing substandard structures. Several studies were therefore conducted in order to develop rehabilitation schemes for beam-column joints. Some retrofit schemes were proposed, all made use of steel sections and/or concrete jacketing in several configurations for different types of joints (Beres et al., 1992; Estrada, 1990; Jirsa, 1993; Migliacci et al., 1983).

An experimental study was conducted on one interior and one exterior specimen using bolting and epoxy bond external plates and angles to column face (Corazao & Durrani, 1989). The exterior and interior strength of the retrofitted beam-column joint were increased by 18% and 21%, respectively. These techniques have shown to be effective in restoring the joint capacity with substandard details and reinforcement. A new strengthening technique for exterior joint was proposed with a corrugated steel jacket around the column (Ghobarah et al., 1997). They used two steel plates bolted to the beam and joint to prevent pull-out of the beam bottom bars. The strengthened system provided an increase of 38% in strength and 180% in energy dissipation.

2.6.2 Beam-Column Joints Repair Using Epoxy Injection

A repair scheme was investigated for moderately damaged joints (Said & Nehdi, 2004). Epoxy pressure injection was found effective in restoring the strength and energy dissipation characteristics of beam-column joints. Also, the pressure injection of epoxy mortar was used through a grid of holes to repair beam-column joints (Filiatrault et al., 1995). The technique was shown to be effective in restoring the joint's capacity after moderate earthquake damage, especially for substandard specimens. Other studies on beam-column joints repair using epoxy injection were also conducted (French & Moehle, 1991; Karayannis et al., 1998; Liu et al., 2008; Tsonos, 2002).

2.6.3 Beam-Column Joints Repair Using Composite Materials

With the introduction of advanced FRP composite materials to the field of concrete structures, new possibilities for beam-column joint repair and rehabilitation became available. FRP materials provide remarkable advantages including high durability, the ability of controlling enhancements in strength and stiffness separately through the control of fibre direction, high strength to weight ratio, flexibility of use in different structural shapes, etc. In contrast, FRP materials have some disadvantages such as vulnerability to delamination, brittle failure; substantial strength could be lost when FRP laminates are wrapped around corners, fire damage, etc. Several studies were conducted to investigate the use of FRP in the rehabilitation of RC frame joints (Ehsani & Wight, 1985; A. Mosallam, 2000; C. Pantelides et al., 2001; Prota et al., 2001).

Tests were performed built on previous success for the repair of bridge bents (C. Pantelides et al., 2001). Their repair scheme, which used CFRP, was successful in enhancing the performance of deficient joints. To prevent de-bonding of CFRP laminates and provide confinement for the column hinging area, the CFRP laminates were extended to the column above and below the joint. This lap area of the joint may be reduced using mechanical anchors, and a fully wrapped beam could also have enhanced the performance, but this was not investigated in their study

(Priestley et al., 1996). The sub-assemblages' performance was assessed via axial load monitoring throughout the test. However, other researchers suggest that the axial load should be re-instated after each load cycle, since in the event of an earthquake the deterioration of the load carrying capacity of the sub-assemblage may not be associated with a reduction in the applied load.

A research study have been done on rehabilitation of RC structures using fibre reinforced polymer (FRP) composites (Zureick & Kahn, 2001). the performance of non-seismically designed RC beam-column joints strengthened by various schemes were studied subjected to seismic loads (Rao et al., 2008). A comprehensive report on application of FRP composites in construction is presented (Ei-Mikawi & Mosallam, 1996).

It was reported that the modelling complex concrete column-beam connection with hybrid fibre reinforced plastic (FRP) reinforcement properly requires understanding of the behaviour of such component and supporting from some experimental data for model updating and refinement (Bing Li & Chua, 2009). This paper, through a comprehensive experimental work, investigates the behaviour of reinforced concrete frame specimens designed to represent the column-beam connections in plane frames. As a follow-up to the previous reported work, it focuses on details of experimental analyses, in particular, a comprehensive strain analysis. Results of the analysis show that designed hybrid FRP reinforcement greatly improve the stiffness and load carrying capacity of its concrete counterpart. It also delays the crack initiation at the joint through confinement due to FRP reinforcement.

An experimental research was conducted on 18 exterior 2/3 scale joints strengthened with different configurations of carbon strips, FRP carbon and E-glass laminate (Costas P. Antonopoulos & Triantafillou, 2003). The study parameters considered the area fraction and distribution of FRP, column axial load, internal joint reinforcement, and initial damage for carbon FRP versus E-glass FRP laminates as well as for FRP laminates versus strips. All the specimens were designed to fail in joint shear before and after strengthening in order to evaluate the contribution of the FRP to the joint shear capacity. The test results were dominated by partial or full debonding of composites. An increase in the axial load from 4% to 10% of its axial capacity showed enhancement in the strength from 65% to 85% and the energy dissipation from 50% to 70% as well as increase in the stiffness reached to around 100%. The analytical prediction of shear strength found to be in good agreement with the experimental results. The description of the specimens and strengthening alternatives are given in Figure 2.27.

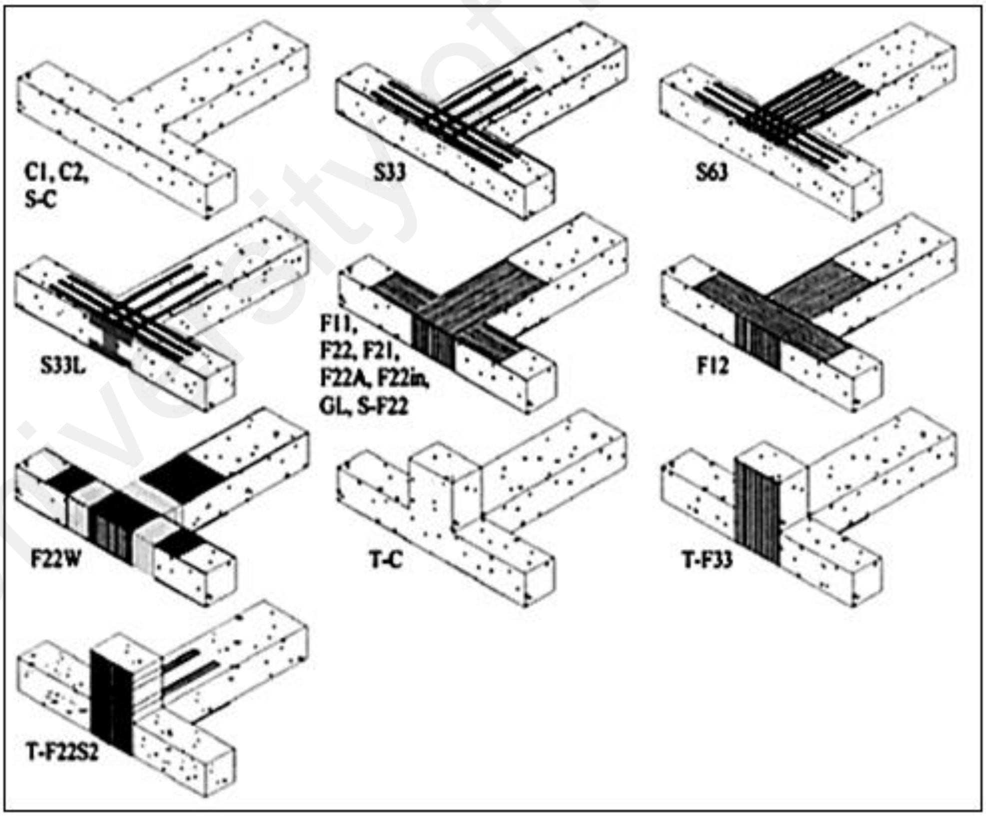

Figure 2.27: Description of specimens and strengthening alternatives
(Costas P. Antonopoulos & Triantafillou, 2003)

The strengthening of both workable and deficient RC BCCs using steel plates (control specimen), CFRPs and GFRPs were performed (Mukherjee & Joshi, 2005). The 'Ductile specimen' consisted of efficiently designed steel reinforcement and perfect detailing at critical sections. The 'Non-ductile specimen' had poor bond lengths of the beam reinforcements at BCCs. It was observed that for ductile specimens the load at yield was considerably higher in the FRP reinforced specimens than the control specimen. A comparison of load-displacement figures exhibited that initially the CFRP strengthened specimen recovered its original strength and finally, the ultimate load capacity was increased by 55%. The initial stiffness of CFRP strengthened specimen was increased by 48%. The behaviour of hybrid (Steel-GFRP) reinforced concrete frames was investigated under reversed cyclic loading (Nehdi & Said, 2005). Figures 2.28 and 2.29 showed the strengthening Type A and Type B with CFRP/GFRP Sheets.

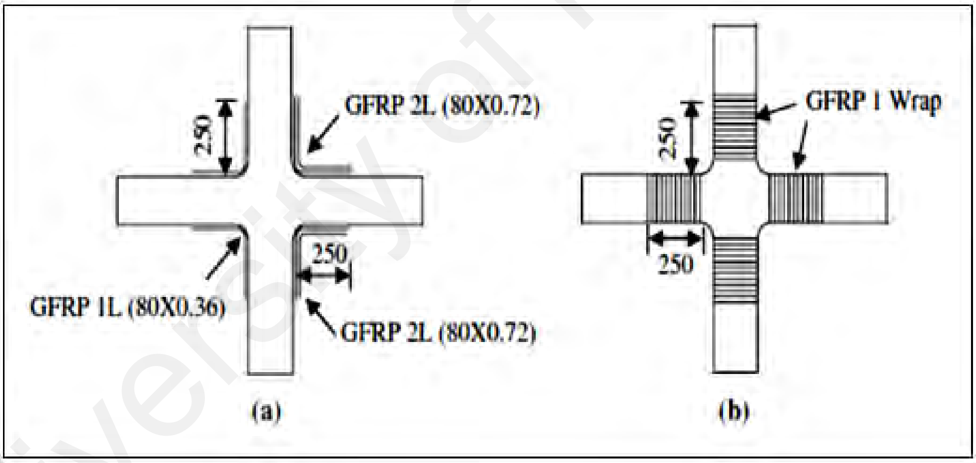

Figure 2.28: Strengthening Type A with CFRP Sheets (Nehdi & Said, 2005)

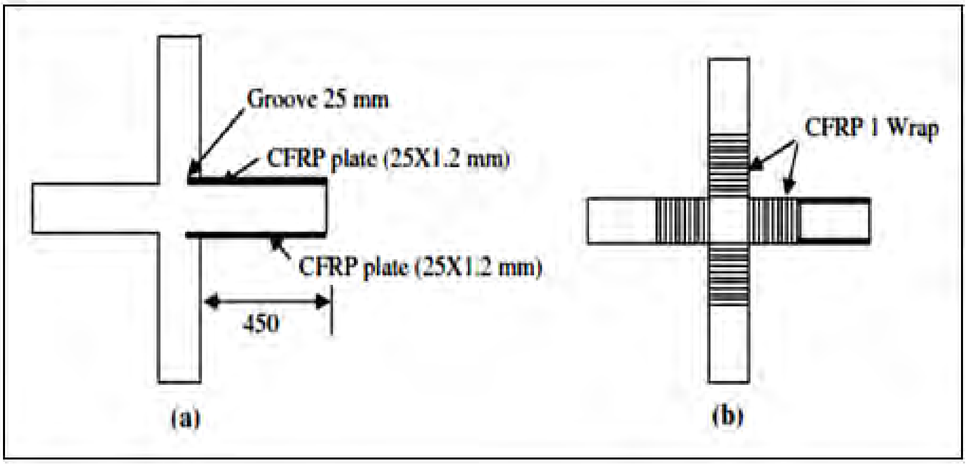

Figure 2.29: Strengthening Type B (Nehdi & Said, 2005)

Ghobarah & Said, (2002) performed retrofitting of several RC BCCs using FRPs. The BCCs were constructed as non-ductile connections according to the pre-seismic design of joints available in design codes. The major failure mode of control specimen was shear failure. Various fibre-wrap rehabilitation schemes were applied successfully to the joint panel with the objective of upgrading the shear strength of the joint. Several repair schemes using FRP composite fibres were developed to enhance the structure ductility and joint shear strength (Ghobarah & El-Amoury, 2005). The research work showed that confinement of the joint panel has improved the structure ductility and moment capacity of the repaired joint(Javanmardi & Maheri, 2017). The strengthening of different beam-column joints are shown in Figures 2.30and 2.31.

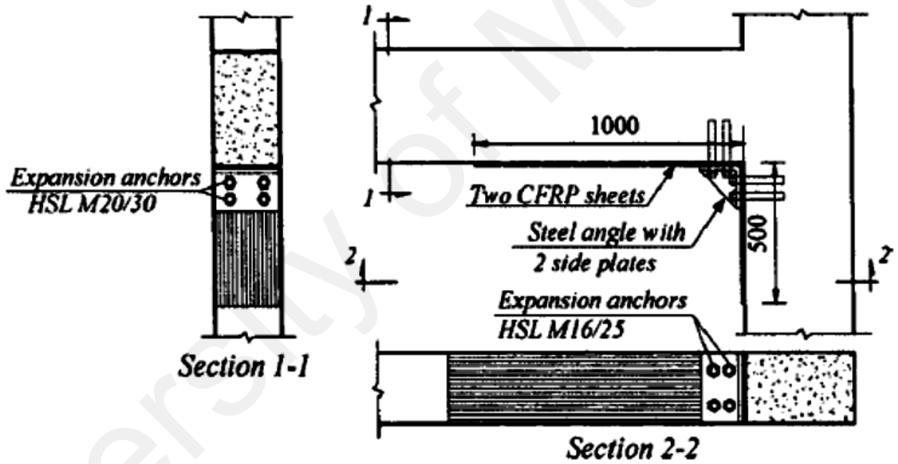

Figure 2.30: Strengthening of different beam-column joints (Ghobarah & El-Amoury, 2005)

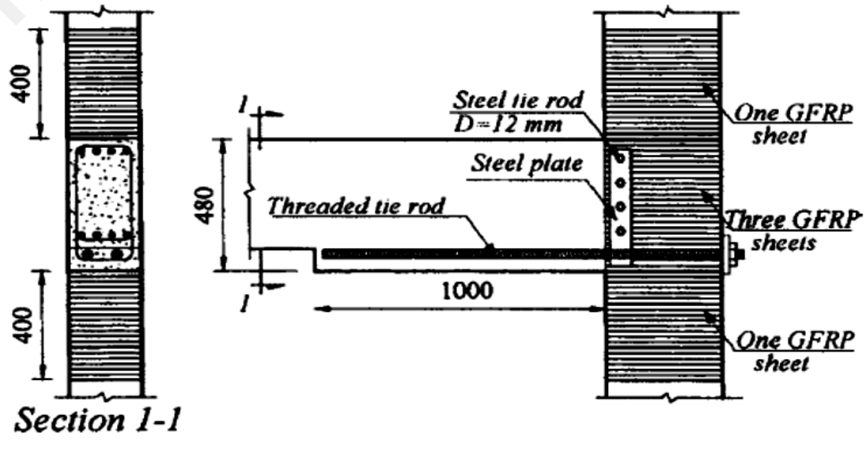

Figure 2.31: Strengthening of different beam-column joints (Ghobarah & El-Amoury, 2005)

An experimental work on one-way exterior joint using CFRP composite laminates was conducted (Clyde & Pantelides, 2002). The results of this research showed that retrofitting with CFRP composites has shifted the joint shear failure in the control specimens to the beam-column interface. The rehabilitated specimen had an increase in joint shear strength, maximum drift, and energy dissipation capacity by 5%, 78% and 200%, respectively.

Several beam-column joint retrofit schemes were investigated using combinations of near surface mounted (NSM) rebars along the beam and column and FRP laminates wrapping around the joint area (Prota et al., 2002; Prota et al., 2000; Prota et al., 2001). Their tests resulted in column, joint or combined column-joint failures, whereas ideally a beam failure should be achieved. This was likely due to the high capacity of the beam, which imposed high shear demand on the joint. For a flexural capacity ratio, it would probably be beneficial to use strength enhancing techniques for the column (e.g. RC jacketing which would include the joint as well). The preparation and strengthening setup of beam-column joints is shown in Figure 2.32.

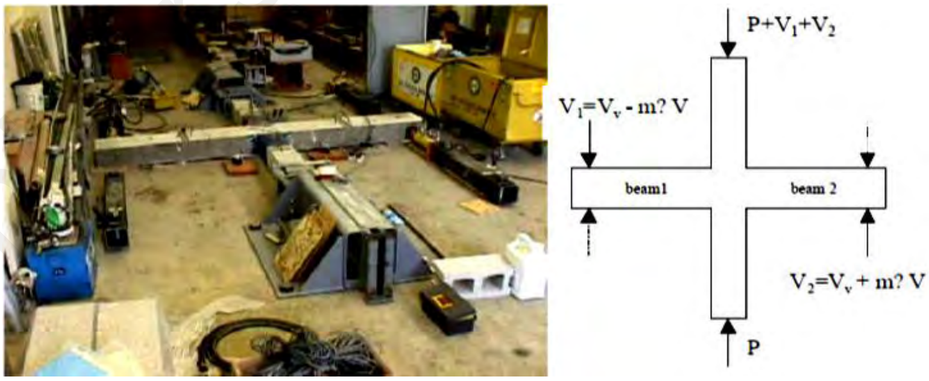

Figure 2.32: Preparation and strengthening setup of beam-column joints (Prota et al., 2002; Prota et al., 2000; Prota et al., 2001)

Antonopoulos & Triantafillou, (2002) evaluated the effects of several parameters such as the efficiency of FRP strips versus sheets, mechanical anchors, and types of fibres on the performance of rehabilitated joints. Significant enhancements in performance were reported, yet all joints failed in a brittle shear mode and did not lead to a desired beam flexural hinging.

A beam-column joint rehabilitation scheme involving jacketing the column above and below the joint with CFRP laminates was studied (Ehsani & Wight, 1985). The proposed technique was able to enhance the overall performance of the rehabilitated specimens compared to that of control specimens. Another group of tests were performed to repair shear deficient joints used specimens (A. Mosallam, 2000). The results of these tests need to be validated using fully representative beam- column joint specimens in order to demonstrate the potential benefits of the proposed repair schemes.

A study on using of FRP fabric for strengthening of reinforced concrete beam-column joints was conducted (D'Ayala et al., 2003). A research study have been done on retrofitted RC exterior beam-column joints with CFRP under cyclic loads (S. Mahini et al., 2005). The lateral load response of high performance fibre reinforced concrete beam-column joints was studied (Shannag et al., 2005).

CFRPs were used for the strengthening of damaged exterior and interior RC BCCs, respectively, subjected to repeated loading without shear reinforcement. The study was aimed to enhance the shear strength and ductility of the joints. Response histories of the specimen before and after repair were then compared (Al-Salloum & Almusallam, 2007). The results were compared through hysteretic loops, load displacement envelops, ductility and stiffness degradation. The comparison shows that CFRP sheets improve shear resistance and ductility of the joint substantially.

An experiment was conducted on strengthening of the deficient exterior RC BCCs using CFRP for seismic loading (Gencoglu & Mobasher, 2007). CFRP fabrics were laid out on the tension face of column and beam and then both column and beam were wrapped fabric. The test results of the strengthened beam-column joints were compared with the test results of both RC exterior beam-column joint built in accordance with the requirements of (Aci-318-2008) and RC exterior beam-column joint disregarded the transverse requirements at (Aci-318-2008) in terms of load carrying capacity, total energy amounts, and ductility. Examination of the specimens after testing indicated that the strengthening method shifted the localization hinge of the specimen to the beam and the mode of failure of beam-column joints could be directly affected.

The damaged RC BCCs strengthened with conventional steel tendons and FRPs was compared (Ganesan et al., 2007). It was concluded that the load carrying capacity of the joints increased with the increasing fibre content.

A study was conducted to compare the performance of a substandard beam-column joint with and without initial bond between beam longitudinal bars and concrete in the joint core (Supaviriyakit & Pimanmas, 2008). They concluded that the horizontal joint shear is the same regardless of the bond condition (Tsonos, 2008). the effect of CFRP jackets on retrofitting beam-column sub assemblages was studied (Tsonos, 2008).

A research study on full-scale RC corner beam-column-slab joints was conducted before and after retrofit with CFRP composites (Engindeniz et al., 2008). The external bonding of a CFRP system has increased the joint shear strength, column confinement, and beam positive moment capacity. The research work has concluded that retrofitting the joint using the scheme developed in their study can achieve ductile beam hinge mechanism and rigid joint behaviour up to inter-story drift ratio of 2.4%. There was improvement in joint shear strength for both pre- and post-earthquake retrofit. The loss of beam positive moment capacity caused by discontinuity of the bottom rebar were mitigated by bonding CFRP strips on the beam outside faces at the beam bottom level provided that the strips were anchored by beam U-wrapping. A research program was conducted for seismic rehabilitation of RC frame interior beam-column joints with externally applied CFRP composite laminates (C. P. Pantelides et al., 2008). The purpose of the rehabilitation was to change the failure mechanism from brittle to ductile as well as to increase the ultimate moment capacity. Two types (type I and type II) of joints were tested in this research. The deficient joint has no hoops confinement inside the joint and beam bottom steel bars without enough development length embedment to dissipate energy through seismic moment reversals. Two CFRP layers were placed at an angle of ±60º from the horizontal in the joint in addition to two layers of CFRP U shape laminates at the critical regions of the beams. The presented test results had shown a shear force capacity 1.5 times the control specimens. Type I and Type II rehabilitated specimen reached a maximum drift ratio of 2.2 and 2.7 times that of Type I and Type II control specimens respectively. The dissipated energy of the rehabilitated specimens was 1.2 (Type II) to 2.3 (Type I) times that of the control specimens.

A research was conducted on structural upgrading of RC column-tie beam assembly using FRP composites (A. S. Mosallam, 2008). Experimental results showed a potential success of the two composite systems used in the study in enhancing the strength, stiffness and the ductility of the column-tie beam assembly. In comparing the strengthened with the control specimens, the strengths of the retrofitted specimens were 152% and 154% for carbon/epoxy and E-glass/epoxy composite systems, respectively. The specimen repaired by using glass fibre composites is shown in Figure 2.33.

Figure 2.33: Specimen repaired with glass fibre composite (A. S. Mosallam, 2008)

CFRPs was used to improve the shear capacity, lateral strength and ductility of exterior RC BCCs (Le-Trung et al., 2010). In total, eight RC BCCs were tested. The specimens were included of a non-seismic specimen, a seismic specimen and six retrofitted specimens with different configurations of CFRP sheets including T-shape, L-shape, X-shape and strip combinations. The X-shaped configuration of wrapping, the strips on the column and two layers of the CFRP sheets resulted in a better performance in terms of ductility and strength.

Hasaballa et al., (2009) studied the feasibility of using the GFRP bars as a longitudinal and transverse reinforcement for reinforced concrete frames subjected to high seismic loads. The experimental results showed that the joint drift capacity can reach more than 3.0% safely without any considerable damage; also GFRP bars were capable of resisting tension-compression cycles with no strength degradation.

The experimental work was presented on behaviour of reinforced concrete beam-column joints retrofitted with GFRP-AFRP Hybrid Wrapping (Ravi & Arulraj, 2010). Two failed beam-column joint specimens, designed as per code IS

456:2000 were retrofitted with GFRP-AFRP/AFRP-GFRP hybrid fibre sheets wrapping to strengthen the specimens. The performance of the retrofitted beam-column joints was compared with the control beam-column joint specimens. A significant enhancement in the structural performance of GFRP-AFRP strengthened connections was observed as compared to the control specimen. In control specimen the failure was in the column portion of the joint but in the case of the wrapped specimens, the failure was in the beam portion only and the column was intact and therefore preventing progressive collapse of the structure under seismic loads (Ravi & Arulraj, 2010).

The effect of cocktail fibre reinforced concrete (1.5% of steel fibre and 0 to 0.6% polypropylene fibre) was examined to increase the Seismic Performance of Beam-Column Joints using M20 concrete (Perumal & Thanukumari, 2010). Six one fourth scale (to suit the loading and testing facilities) specimens were designed as per IS 456:2000 and one designed as per IS 1893 (Part 1): 2002 and detailed as per IS 13920-1993. The five specimens were similar to the first one but various combinations of cocktail fibre concrete in the joint region. Out of five fibre specimens four specimens were cast by using (constant 1.5% of steel fibre and 0 to 0.6% polypropylene fibres). The fifth fibre specimen was cast by using 1.5 % of polypropylene fibre only. The properties of ultimate strength, ductility, energy dissipation capacity and joint stiffness were compared. The increase in polypropylene fibre decreased the ultimate load carrying capacity. The energy absorption capacity increased by 87% by adding only steel fibre and 205% by adding cocktail with combination of 1.5% steel fibre and 0.2% polypropylene fibre. The specimen with 1.5% of steel fibre and 0.6% polypropylene fibre had the maximum ductility factor. The excess polypropylene fibre increases the ductility. The rate of degradation of stiffness decreases in the case of specimens additionally reinforced with fibres (Perumal & Thanukumari, 2010). The fibre strengthened beam-column joint is shown in Figure 2.34.

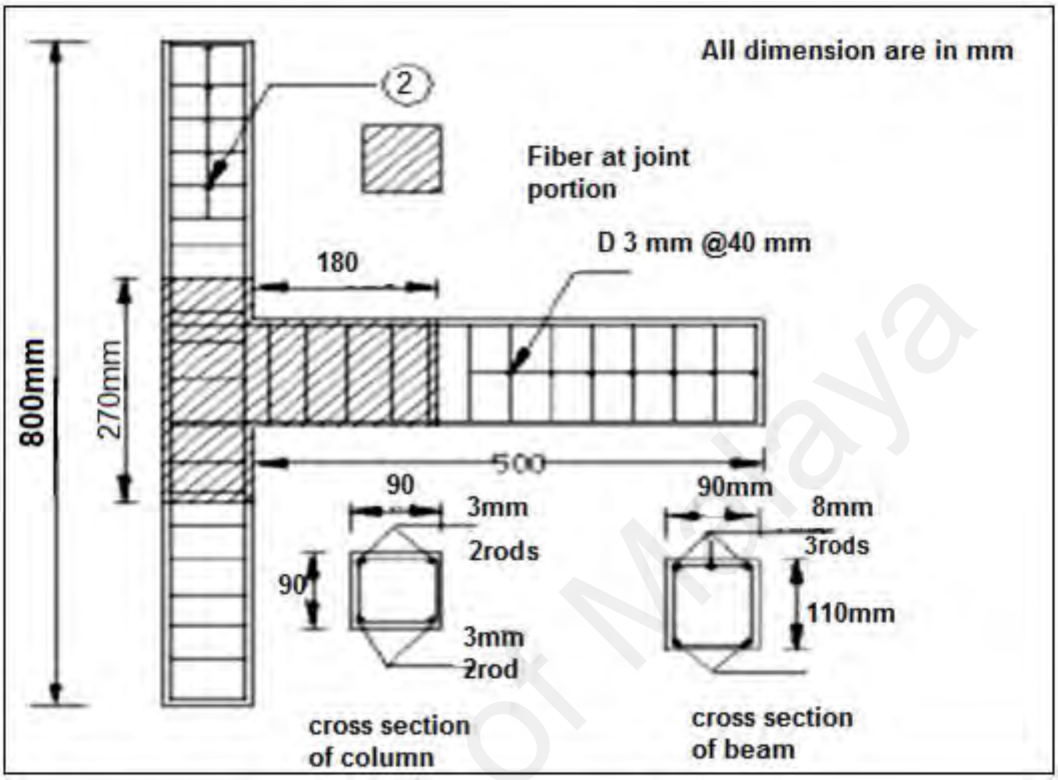

Figure 2.34: Fibre strengthened beam-column joint (Perumal & Thanukumari, 2010)

Energy dissipation was examined with emphasize on the ductility and size effect for plain and RC BCCs strengthened with and without FRPs . The load carrying capacity of the retrofitted specimen increased in comparison to control specimen. The ultimate load carrying capacity for all the specimens increased due to retrofitting and it was similar for column weak in shear specimens. Also the gain in energy dissipation due to retrofitting was 33.08% at failure stage for beam weak in shear large specimen. The gain in energy dissipation due to retrofitting was 85.7% at failure stage for beam weak in shear medium specimen and the same is 97.7% for small specimen. Energy dissipation for all the specimens increased due to retrofitting and it was similar for column weak in shear specimens also. In this paper it was observed that energy dissipation and ultimate load carrying capacity due to retrofitting increases as the specimen size decreases. Both energy dissipation and ultimate load carrying capacity followed the principle of size effect for both control and retrofitted specimens. Energy dissipation per unit volume also increased as the specimen size decreased (Choudhury, 2010; Choudhury et al., 2010).

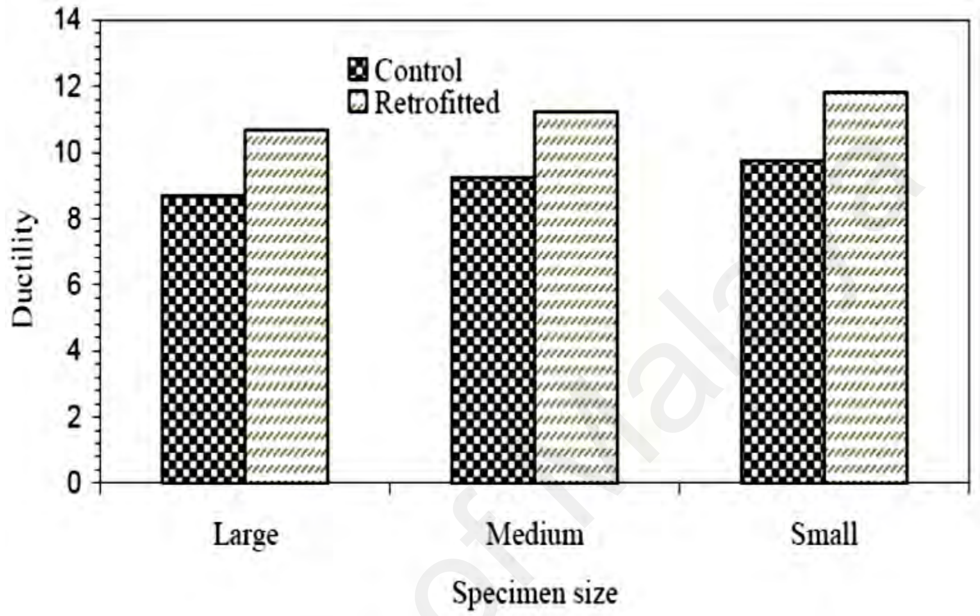

Figure 2.35: Displacement ductility of beam weak in shear specimens (Choudhury, 2010; Choudhury et al., 2010)

The experimental work(Choudhury, 2010) was presented for evaluation of Exterior RC Beam Column Joint strengthened with FRP under cyclic load (Gupta, 2012). Four RC T-joints with different detailing; two unconfined (according to IS: 456-2000) and the other two confined (according to IS: 13920-1993) were tested. Comparison of strength and ductility of undamaged and retrofitted specimen was done. Also the behaviour of confined specimen was compared with the unconfined one. The unconfined model was repaired and retrofitted with GFRP wrapping in critical damaged region around joint, it restrained the strength up to 68 % and the maximum load attained was 36.4 KN at 20.5 mm displacement. It was observed that GFRP wrapping retrofitting of RC beam column joint was effective with restoring its lateral load carrying capacity up to a significant amount and increasing its ductility. The GFRP wrapping acts as an anchor sheet at the time of earthquake as it does not allow the concrete to spall from the joints (Gupta, 2012).

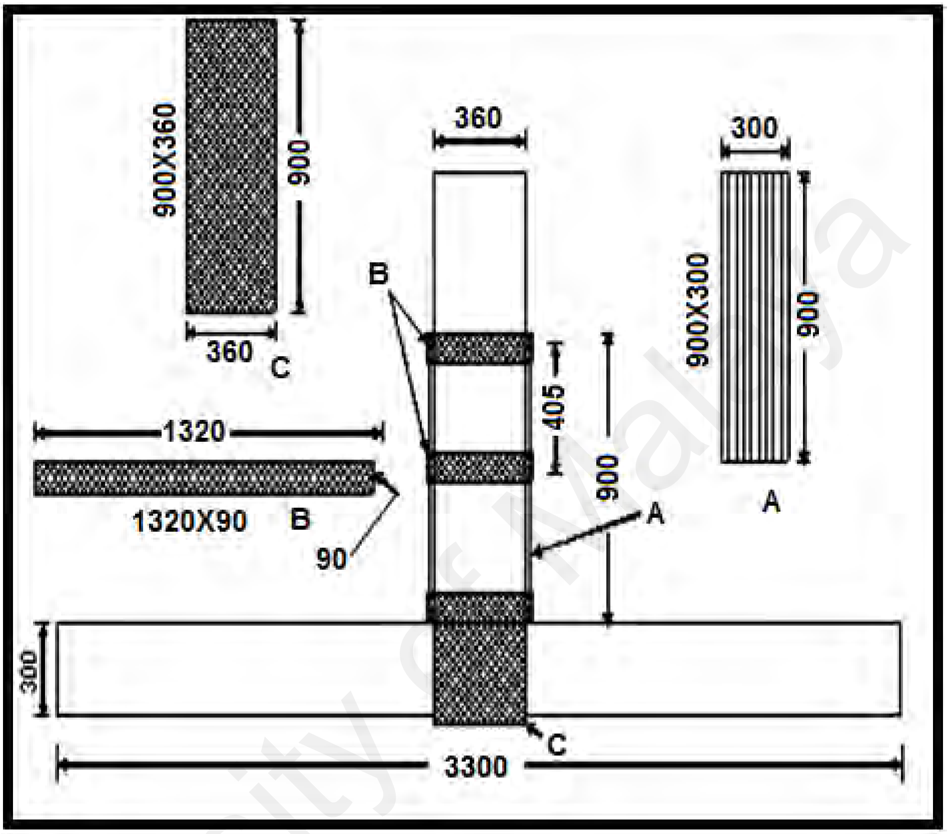

Figure 2.36: Full scaled strengthened beam-column joint (Gupta, 2012)

2.6.4 Importance of Finite Element Modelling

In the modern era, the increasing use of computer technologies has given rise to some powerful tools that are effectively used to achieve precise results of engineering problems. One of those tools is the Finite Element (FE) modelling which can predict the complex behaviour of retrofitted structures in a simple way. The response of strengthened RC BCCs is usually highly non-linear especially in the inelastic regions. FEM is useful to achieve the crack propagation associated with the observed load-displacement for various loading conditions (Hegger et al., 2004).

2.6.4.1 Analytical and numerical studies on beam-column joints

Many analytical and numerical research studies were developed to predict the behaviour of strengthened RC BCCs (Bonacci & Pantazopoulou, 1993; Hwang & Lee, 1999, 2002; Kim & LaFave, 2007; Lakshmi et al., 2008; Lowes et al., 2005; Mitra & Lowes, 2007; Mostofinejad & Talaeitaba, 2006; Pannirselvam et al., 2008; Parvin & Granata, 2000; Silva, 2008)

Parvin & Granata, (2000) analytically investigated the use of FRP in joint rehabilitation. The ANSYS finite element software was used to model rehabilitated joints and the potential of the proposed techniques was demonstrated numerically.

Antonopoulos & Triantafillou, (2002) presented an analytical model of RC BCCs strengthened with externally bonded FRP composite suggested (Pantazopoulou & Bonacci, 1993). Six stages of the BCC response at different states of stress and strain were numerically evaluated and solved until concrete crushing or FRP laminates failure caused by either fracture or de-bonding occurred(Costas P Antonopoulos & Triantafillou, 2002). Hegger et al, (2004)validated the experimental testing of FRP strengthened exterior and interior RC BCCs using FE software ATENA and a close agreement was achieved between the two types of connections (Hegger et al., 2004).

Mahini et al., (2008) studied the capability of nonlinear quasi-static FEM in simulating the hysteretic behaviour of CFRP-retrofitted exterior RC BCCs using ANSYS. The FE models were developed using a modified Hognestead model for concrete and anisotropic multi-linear model for modelling the stress-strain relations in reinforcing bars while anisotropic plasticity is considered for the FRP composite. The results obtained from the FE analysis were compared with the experimental data of two RC BCCs tested before and after retrofitting and a close agreement was achieved. FEM generated load-deflection graphs showed resemblance with experimental results up to the linear stage only, as concrete's strain softening cannot be modelled by ANSYS. The FEM model is shown in Figure 2.37.

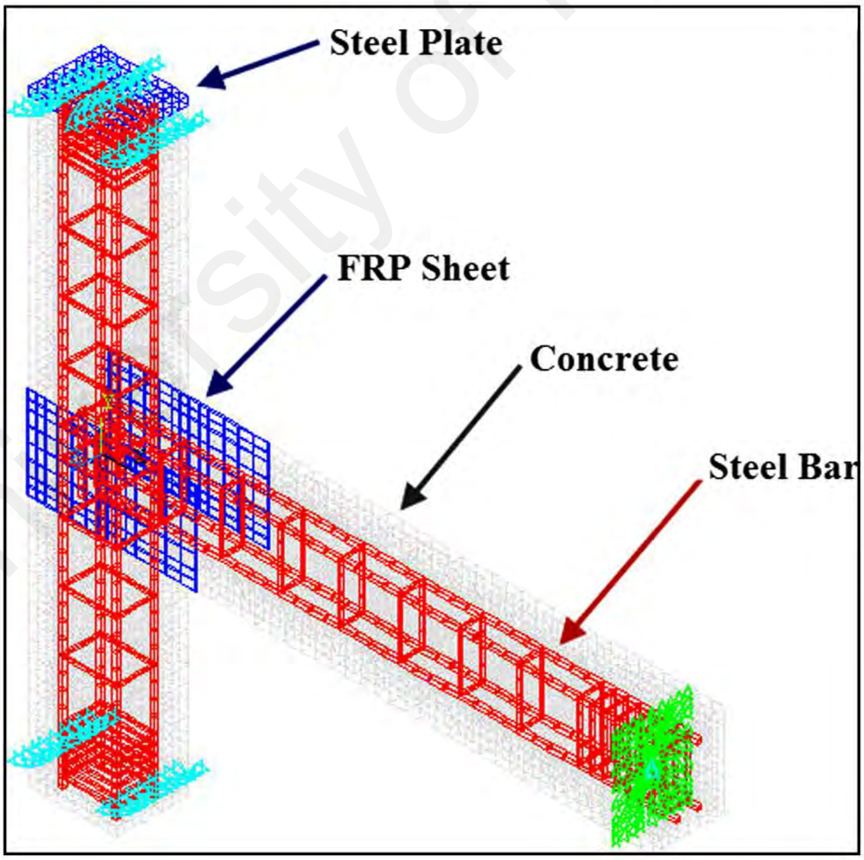

Figure 2.37: Finite Element Modelling of beam-column joint (SS Mahini et al., 2008)

Danesh et al., (2008) investigated the accuracy and efficiency of GFRP composites to strengthen the two-way corner RC BCC. A finite element model for both of the control and rehabilitated specimen were developed to validate the experimental test results. The experimental tests show the rehabilitated specimen AR1 exhibited greater ultimate load about 54% than control specimen A1. The research showed the efficiency of the suggested strengthening GFRP techniques to increase the stiffness and shear strength of the joint, reducing story drift, increasing ultimate carrying capacity and changing the shear failure mode to a relatively ductile mode. The damaged concrete zones with experimental and FEM analysis is shown in Figure 2.38.

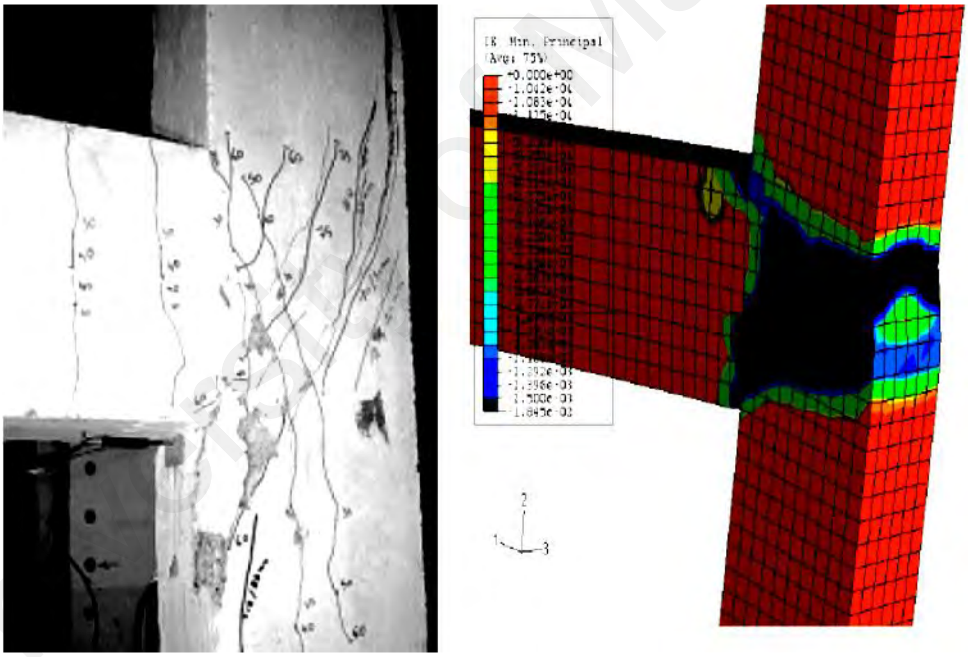

Figure 2.38: Damaged concrete zones with experimental and FEM analysis (Danesh et al., 2008)

Pannirselvam et al., (2008) numerically validated the experimental results of three different steel ratios used with two different GFRP types and two different thicknesses in each type of GFRP to strengthen RC BCCs. Rajarma et al., (2010) studied the structural behaviour of interior RC BCCs, numerically. The RC BCC was modelled to a scale of $1/5^{th}$ from the prototype and the model has been subjected to cyclic loading to find its behaviour during earthquake and close agreement was achieved between experimental and numerical results. The experimental and FEM models showing the crack patterns is showing in Figure 2.39.

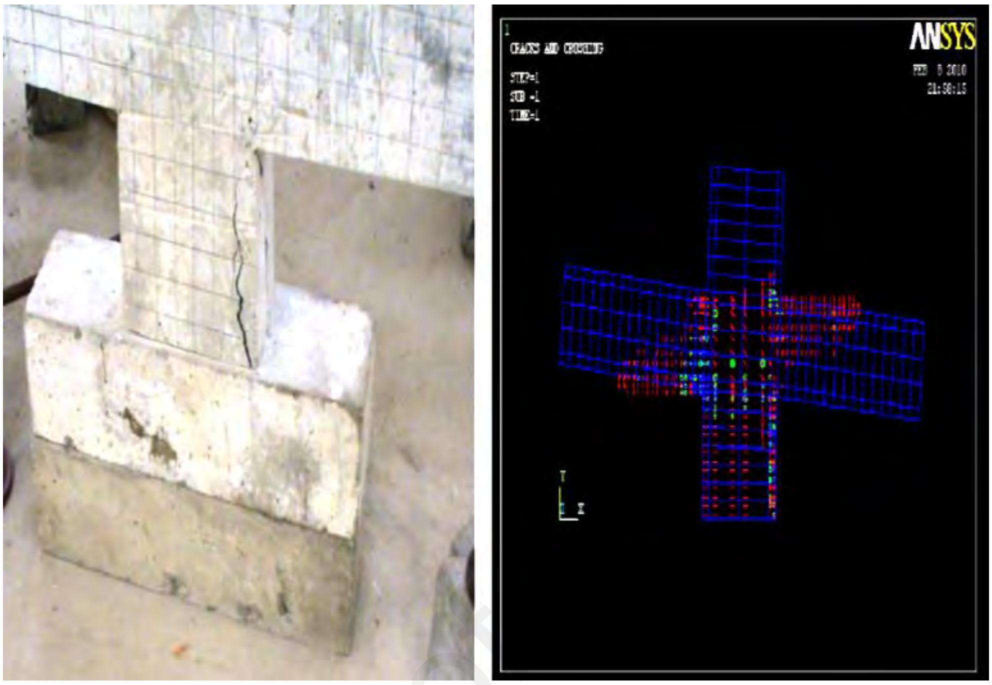

Figure 2.39: The experimental and FEM models showing the crack patterns (Rajaram et al., 2010)

Patil & Manekari, (2013) modelled the exterior RC BCC subjected to monotonic load. The FE model was developed using the geometrical lines and joining nodes. The joint was fully restrained at the column ends. The study concluded that with the gradual increase in load, a proportional increase in the displacement and stress magnitude also happens. The FEM modelling of corner beam-column joints on ANSYS is shown in Figure 2.40.

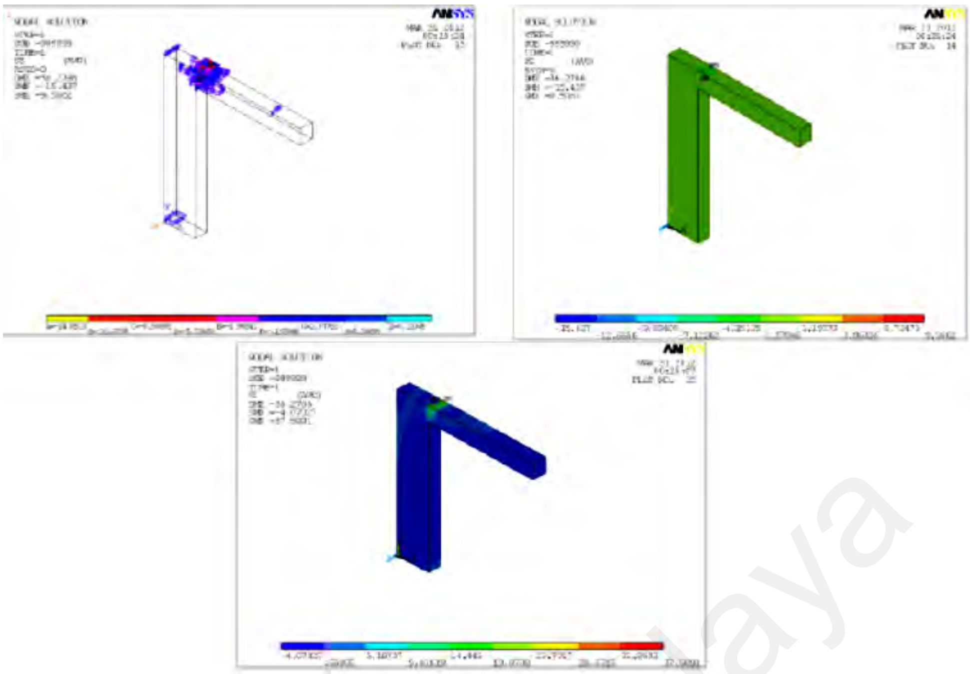

Figure 2.40: The FEM modelling of corner beam-column joints (Patil & Manekari, 2013)

2.7 Summary

- The RC BCCs are the most susceptible structural component

Most often, the failure of a structure initiates with the failure of BCCs, and even slight negligence in the design of RC BCCs may tends towards the collapse of the whole structure.

Several experimental studies on gravity load designed (GLD) beam-column joints are available in the literature. Some studies aimed at investigating joint shear and bond slip deformations, joint shear capacity, and degradation of joint strength and stiffness due to cyclic load application. They concluded that properly designed and detailed beam-column joints can resist moderate earthquakes without damage and severe earthquakes without substantial loss of strength. They also indicated that joints without transverse beams require ties to provide adequate confinement and shear resistance. Impact loads due to accidents and increasing traffic creates cyclic loadings can damage bridges leading to a deficiency in structural capacity that may not be able to carry the existing service load. Moreover, sometimes, mistakes or construction errors may result in an inadequate load carrying capacity in the structure.

- This created a need to rehabilitate existing substandard structures.
- Several studies were therefore conducted in order to develop rehabilitation schemes for beam-column joints.

Some retrofit schemes were proposed, made use of steel sections and/or concrete jacketing in several configurations for different types of joints. Some researchers indicated Epoxy pressure injection was found effective in restoring the strength and energy dissipation characteristics of beam-column joints.

- Several repair schemes using FRP composite fibres were developed to enhance the structure ductility and joint shear strength.

Results of the investigations showed that designed hybrid FRP reinforcement greatly improved the stiffness and load carrying capacity of its concrete counterpart. Also, the crack initiation at the joint was delayed through confinement due to FRP reinforcement. The effects of several parameters such as the efficiency of FRP strips versus sheets, mechanical anchors, and types of fibres on the performance of rehabilitated joints were evaluated. Significant enhancements in performance were reported, yet most joints failed in a brittle shear mode and did not lead to a desired beam flexural hinging.

The experimental testing of such connections, especially when FRP is used for strengthening, is expensive and not easy to repeat. A feasible solution is the use of well-recognized method of the Finite Element (FE) modelling, which is capable of modelling the strengthened structures efficiently and to predict the non-linear behaviour of RC BCCs.

- There are only few studies available in the literature that were conducted to investigate the strengthening of RC BCCs using external CFRP reinforcement which they have investigated the effects of various configuration of CFRPs on overall performance of strengthened RC BCCs in both experimental and numerical methods.
- This has generated a research gap to find out the most effective parameter and size of CFRP composites to achieve highest possible strength and serviceability performance of strengthened RC BCCs.
- As well as the use of a finite element software application to evaluate the impact of CFRP reinforcement dimensions on relocation the plastic hinge away from the column face toward the beam in order to achieve a 'weak beam - strong column' failure mode can be useful.

Because a large number of samples reinforced with different CFRP reinforcement dimensions can be analyzed at the lowest cost. This review is performed in order to extract the information about the strengthening of deficient RC BCCs using CFRP as an appropriate retrofitting material. The findings of this review has helped in the experimental testing phase as well as in the numerical modelling of RC BCCs strengthened in this study. The current research will help designers to choose the most appropriate design configuration for the strengthening of deficient RC BCCs subjected to static loading.

CHAPTER 3: METHODOLOGY

3.1 Introduction

This research project comprises two main parts, namely experimental testing and numerical analysis. Six T-shaped connection specimens as exterior joints were prepared for the experimental test. The first section in this chapter describes the specimen fabrication, the test setup and the experimental test program instrumentation. The second part presents the detailed Finite Element Analysis (FEA) carried out on the connections. Experimental testing is very costly and time-consuming. Hence, accurate finite element modeling of the connections is very important for more extensive verification of the test parameters and also to achieve certain results that could not otherwise be observed through experimental testing. This objective can be achieved through accurate modeling by considering parameters like nonlinearity, material geometries (i.e. concrete crushing and cracking, contact interaction) and suitable elements for modeling the interaction between steel and concrete.

3.2 Experimental Program

An experimental program was conducted to evaluate the performance and behavior of beam-column joints retrofitted with advanced CFRP composite laminates. The specimens were tested by applying both gravity and lateral loads on a subassembly of exterior reinforced concrete (RC) beam-column joints. The subassembly shown in Fig. 3.1 represents a typical exterior beam-column joint found in an RC frame building isolated between two stories and two bays at the moment inflection point under lateral loading.

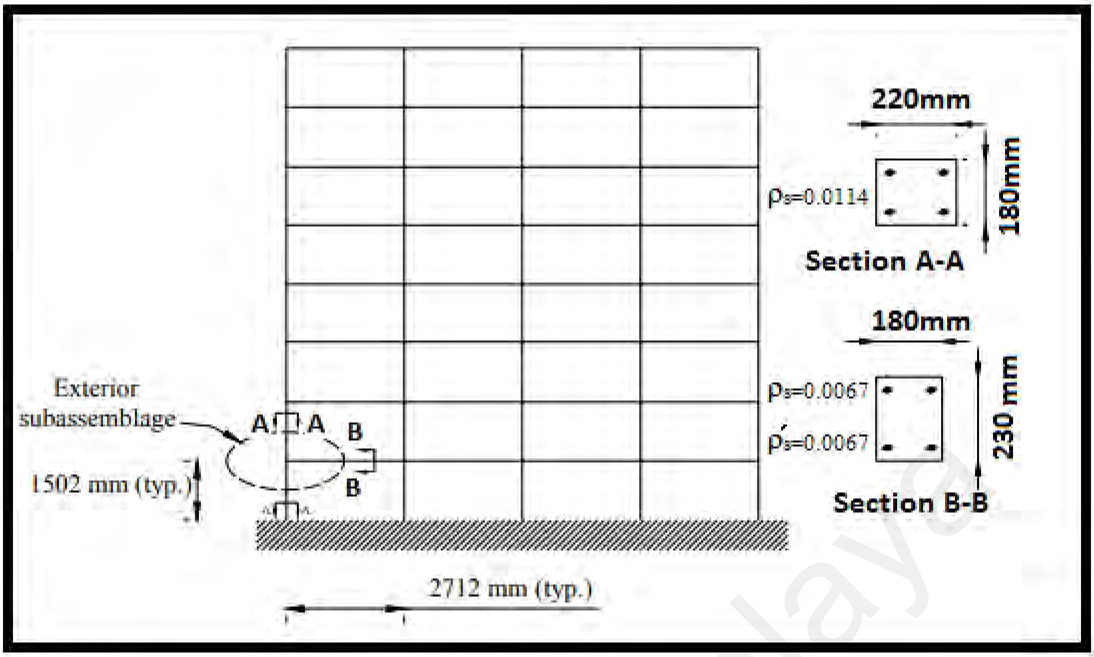

Figure 3.1: Typical exterior beam-column joint

This isolated subassembly represents an external joint in a scaled-down reinforced concrete building. Mahini et al. (2005) performed tests on such subassemblies using a testing rig. The prototype structure was a typical eight-story residential RC building, with details similar to non-ductile RC frames (ACI, 2014). A scaled-down frame was proportioned and detailed according to the Buckingham theorem requirements (Misic et al., 2010). The scaled-down joints were extended to the column mid-height and beam mid-span corresponding to the inflection points of the bending moment diagram under lateral loads.

The moment distribution in frames subjected to lateral loads caused inflection points at approximately the midpoint of the beam and the columns. A typical deflected frame shape under lateral loads is presented in Fig. 3.2.

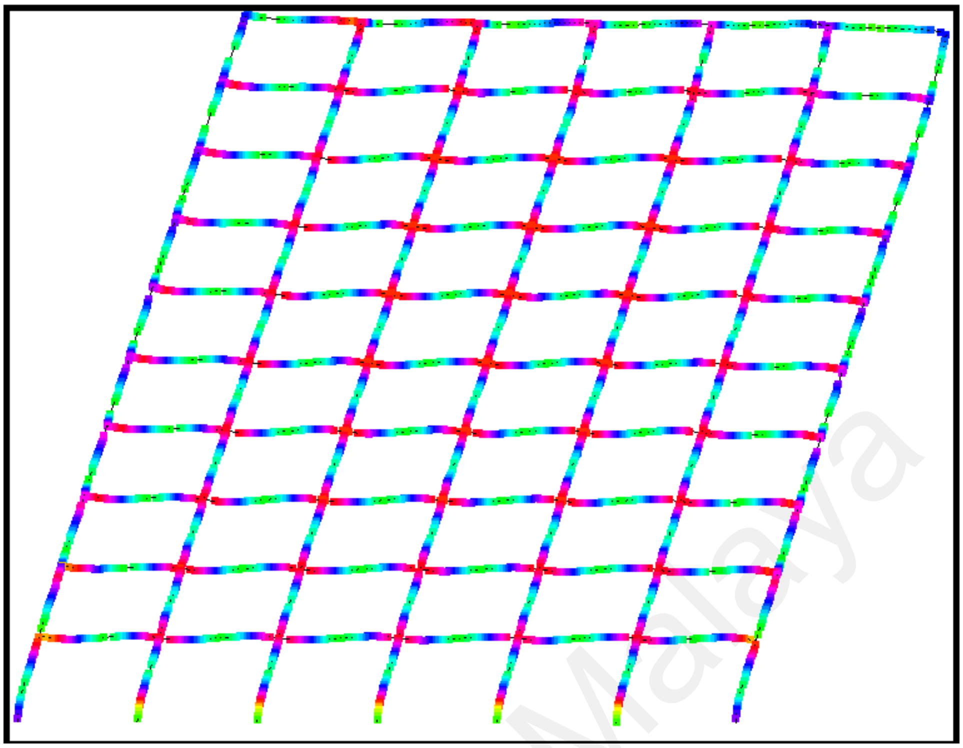
Figure 3.2: Typical deflected frame shape under lateral loads

As shown in this figure, the inflection points in the columns and beams were subjected to lateral deformation. In moment resisting frames under lateral loads, the columns and beams are subjected to shear force at the inflection points. Fig. 3.3(a) shows a typical deflected interior joint from the deformed frame. The joint was subjected to horizontal shear force at the inflection points of the columns, and consequently, it was restrained by the translational movement at the inflection point of the beams. The inter-story drift for this system is calculated with Eq. 3.1.

$$Drift = \frac{\left(\frac{\Delta c}{2}+\frac{\Delta c}{2}\right)}{H} = \frac{\Delta c}{H} \qquad (3.1)$$

Where Δc/2 is the horizontal displacement at each column end and H is the distance between the column ends. In the experimental test program, based on the available equipment and test setup, the deformed joint considered is seen in Fig. 3.3(b). Vertical shear force was applied at the beam end, while the inflection points at the column top and bottom were fixed for translational movement. This system simulates the members' shear at the inflection points of the corresponding frame members. Eq. 3.2 presents the relationship for inter-story drift in this system.

$$Drift = \frac{\left(\frac{\Delta b}{2}+\frac{\Delta b}{2}\right)}{L} = \frac{\Delta b}{L} \qquad (3.2)$$

Where Δb is the vertical displacement at each beam end and L is the horizontal distance between beam ends. Eq. 3.1 and 3.2 can also be used for exterior joints.

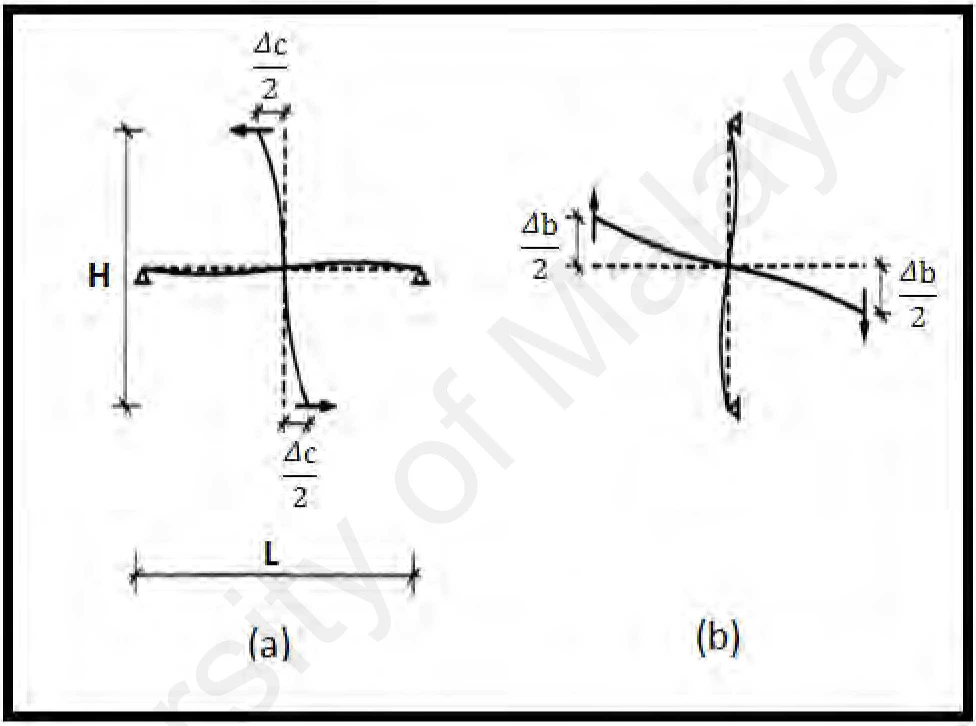

a): Idealized interior joint, b): Test specimen

Figure 3.3: Deflected interior joint

The T-shape was selected as the geometry for exterior joint specimens in the experimental test. Six exterior reinforced concrete beam-column joint specimens, including a control specimen (non-retrofitted) and five retrofitted specimens with altered CFRP arrangements were developed. The specimens selected were down-scaled from the moment resisting frame. Fig. 3.4 displays a typical test specimen used in the experimental test. The T-shaped specimens were subjected to one load on the beam end and reaction force on the column ends to represent the exterior joint's deformed shape. The specimens were subjected to lateral loading in two steps. First, an axial load representing the gravity load of the upper story was applied to the column top. Second, one load was applied to the beam end continuously until specimen failure occurred.

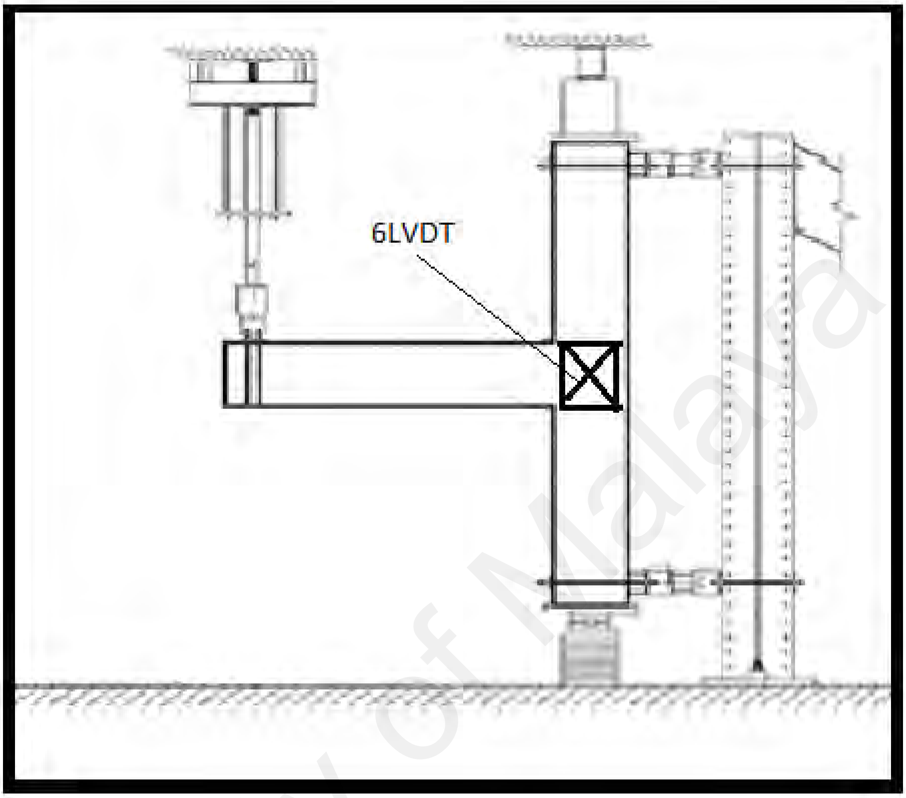

Figure 3.4: Exterior beam-column joint subassembly

The purpose of the experimental program was to evaluate the performance of exterior beam-column joints subjected to axial and lateral loads before and after strengthening with various types of external bonded CFRP composite laminates.

3.2.1 Specimen Design and Geometry

The test specimens were six 1:2.2 scale models of the prototype. All joints consisted of 180 mm wide and 230 mm deep beams with 220 mm x 180 mm columns. The reinforcement consisted of R6 (D = 6 mm) ties with f_y of 400 MPa and N12 (D = 12 mm) main bars with f_y of 500 MPa and yield strain of 0.003 mm/mm. The carbon fiber reinforced plastic (CFRP) sheets utilized in all experiments were unidirectional with ultimate stress of 3500 MPa, ultimate strain of 0.017 mm/mm and constant modulus of

210 GPa. The concrete had compressive strengths of 40.1, 40.3, 41.5, 41.3, 39.2 and 39.3 MPa in the plain (RCS1) and retrofitted specimens (RCS2, RCS3, RCS4, RCS5 and RCS6), respectively.

Summary of specimens geometry was shown in table 3.1

Table 3-1: The summery of specimens geometry

Specimen	Column section	Beam section	Longitudinal rebar	Transvers rebar	Location of CFRP	CFRP configuration
RCS1	220X180 mm	230x180 mm	4 N12	R6.5	-	-
RCS2	220X180 mm	230x180 mm	4 N12	R6.5	Both sides of joint	4PL350X100 mm Two cross shape
RCS3	220X180 mm	230x180 mm	4 N12	R6.5	Top and bottom of the beam	2PL350X100 mm
RCS4	220X180 mm	230x180 mm	4 N12	R6.5	Top and bottom corner of connection	Two L shape sheet 350X350X180mm
RCS5	220X180 mm	230x180 mm	4 N12	R6.5	Both sides of beam web	2PL600X100 mm
RCS6	220X180 mm	230x180 mm	4 N12	R6.5	A part of column and beam end	Wrapping

Both sides of the column as well as the back of the beam were wrapped with CFRP. The CFRP plate ends were also wrapped in order to provide CFRP anchorage. It should be mentioned that in a real structure, this can be achieved using a bolted CFRP system as reported by Oehlers is covered by Australian standard guidelines at present. All the specimens were subjected to axial loading and the corresponding ratio was about 20% of the column capacity (0.20Agfc), which is a practical range in real frame buildings (Hui & Irawan, 2001; Hwang & Lee, 1999, 2002; Mahini & Rounagh, 2007). The specimens' geometries and CFRP configurations are shown in Figures 3.5 to 3.10.

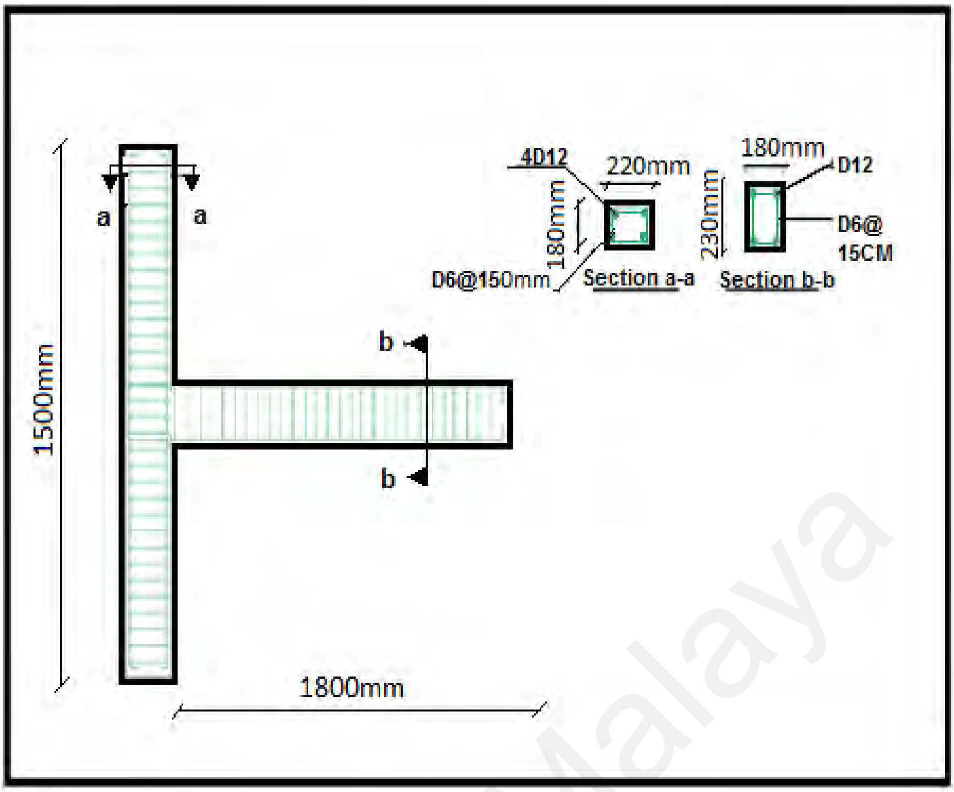

Figure 3.5: Details and geometry of control specimen

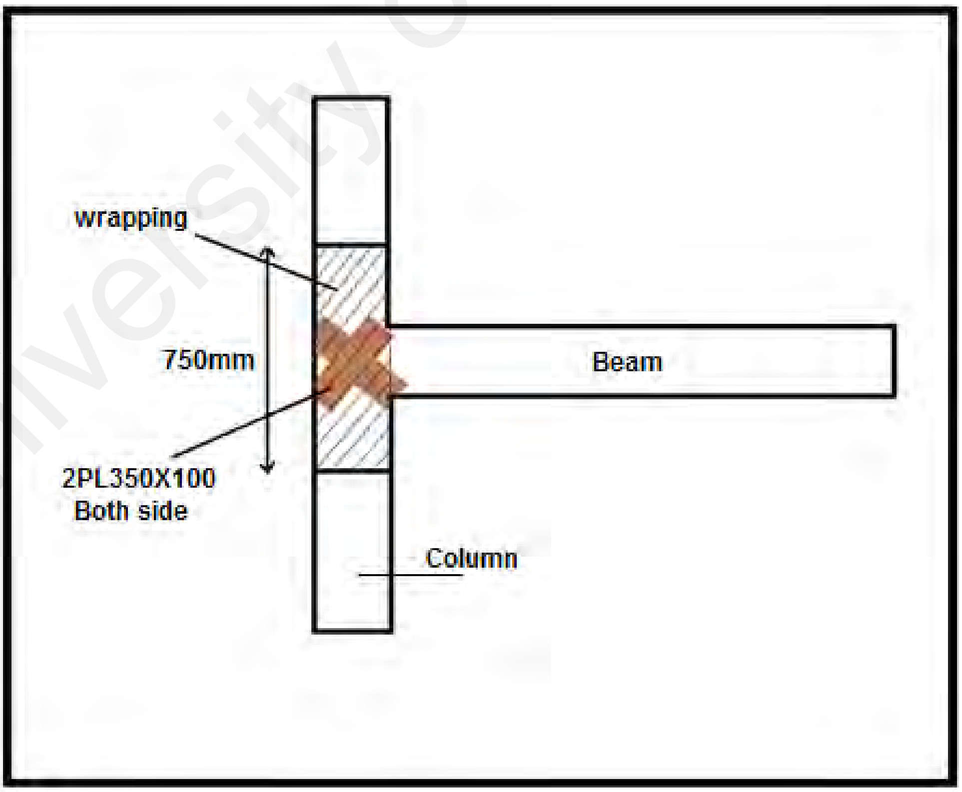

Figure 3.6: CFRP configuration of specimen RCS2

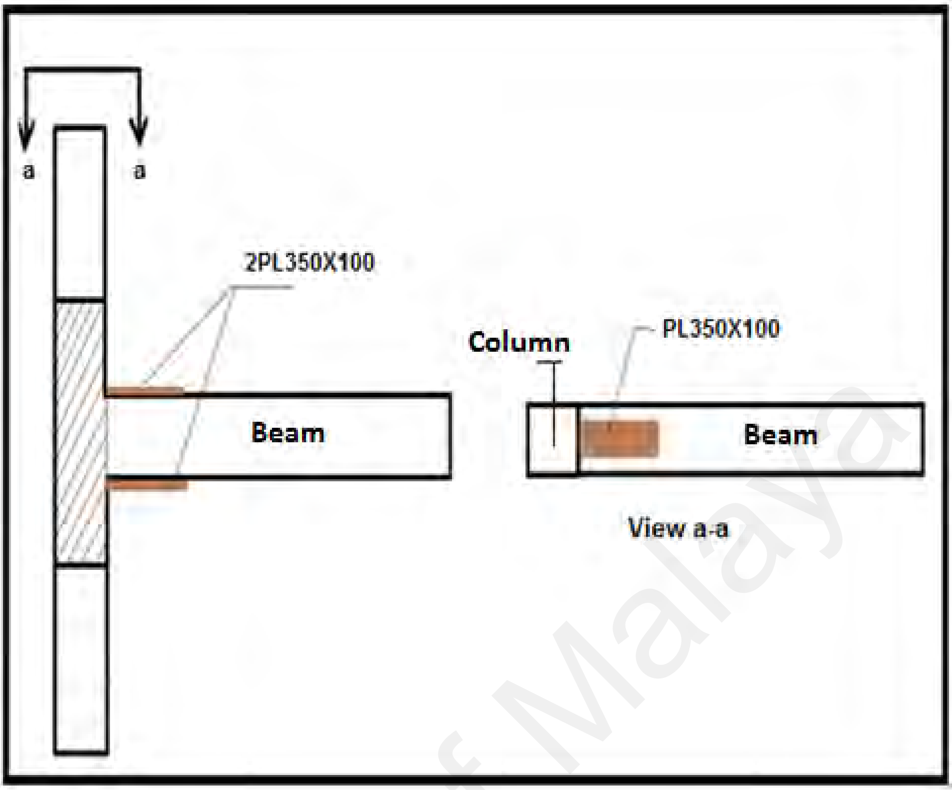

Figure 3.7: CFRP configuration of specimen RCS3

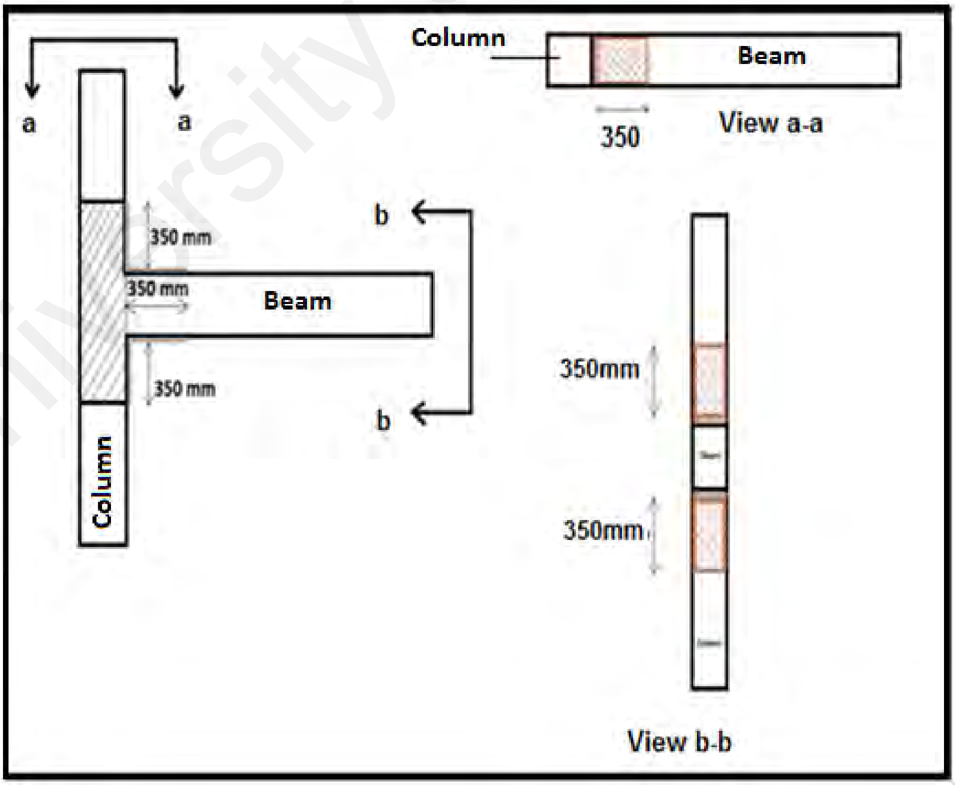

Figure 3.8: CFRP configuration of specimen RCS4

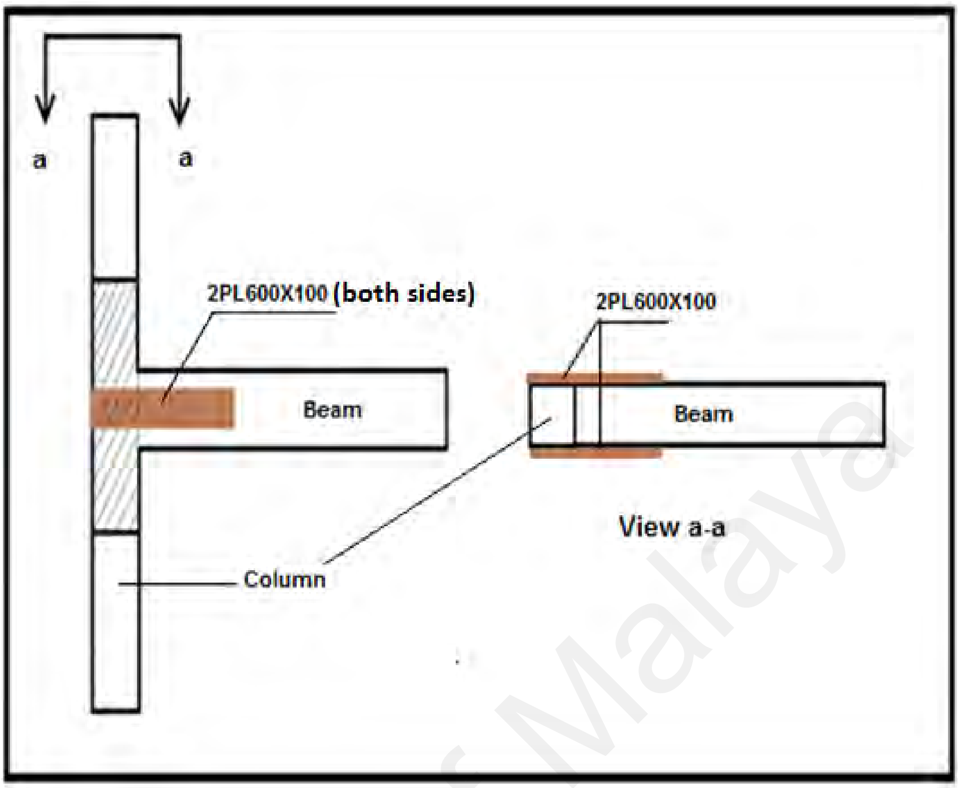

Figure 3.9: CFRP configuration of specimen RCS5

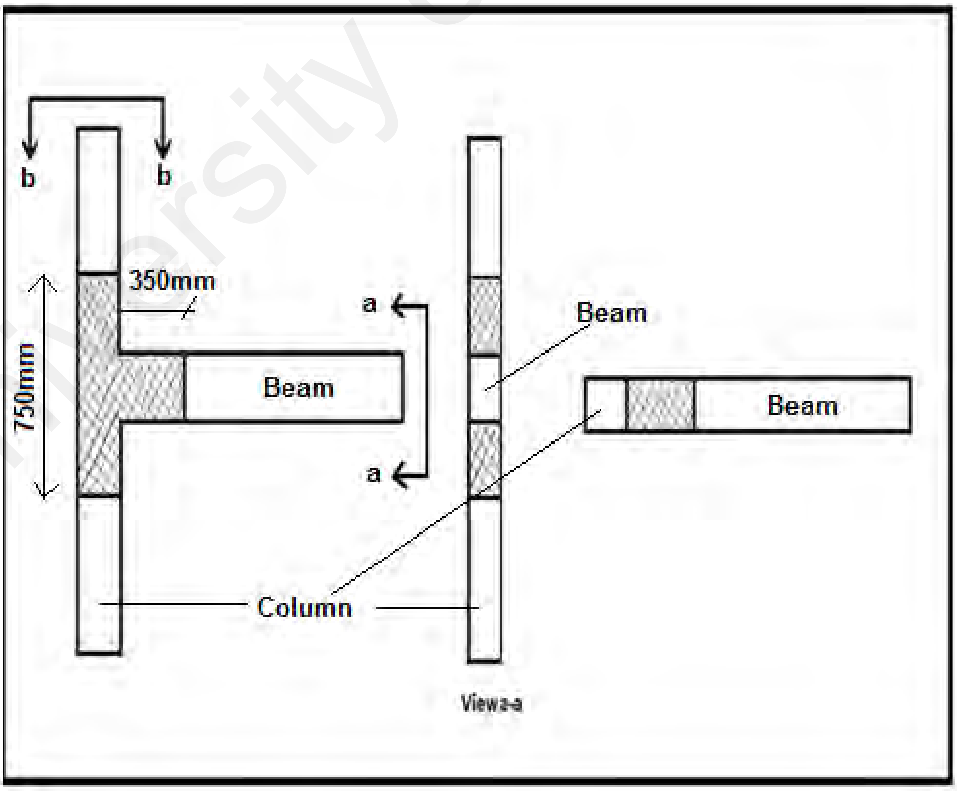

Figure 3.10: CFRP configuration of specimen RCS6

3.2.2 Construction of specimens

The specimens were fabricated at the University of Malaya Structural Engineering Laboratory. For ease of construction, the specimens were made and cased in a flat position, as shown in Fig. 3.11.

Figure 3.11: Specimen ready for concrete casting

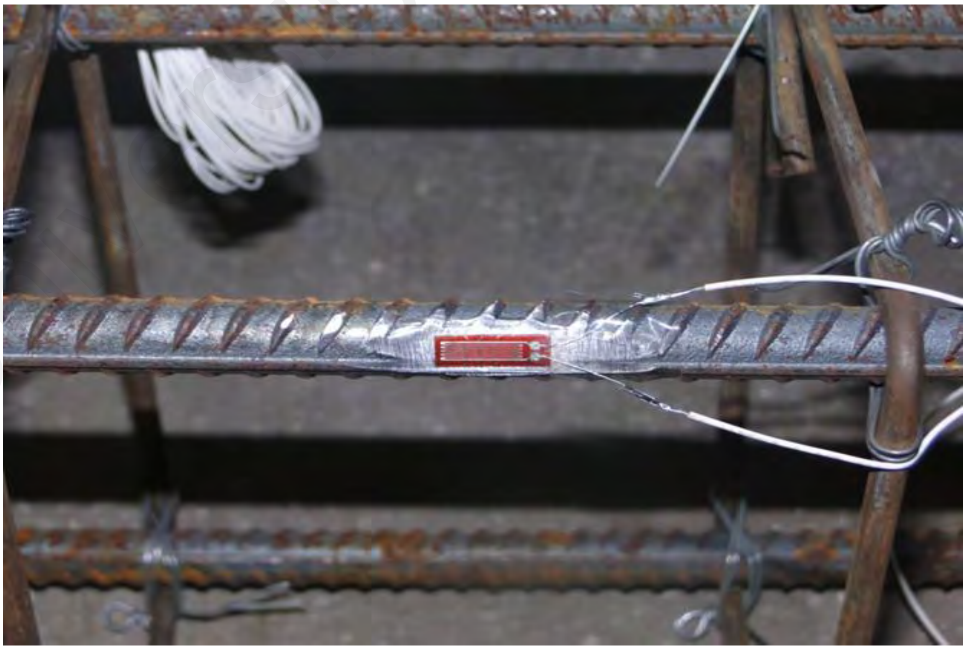

Figure 3.12: Strain gauge installation

After assembling the reinforcement rebar and installing the strain gauges (10mm in length), the concrete was cased with 80 mm slump and compacted as indicated in Fig.

3.12 to 3.14. Concrete cylinders (150X300mm) were taken from the cast concrete batch (Fig. 3.14) to test the concrete's compressive strength. The specimens were left to cure for 28 days in a controlled environment. Prior to the tests, the specimens were lifted using a crane and transferred to The Construction Industry Development (CIDB) laboratory by truck.

Figure 3.13: Concrete slump measurement

Figure 3.14: Concrete cylinders for testing the material properties

Figure 3.15: Concrete specimen casting

Figure 3.16: Installation of CFRP plate on specimen RCS2

Figure 3.17: Installation of CFRP plate on specimen RCS3

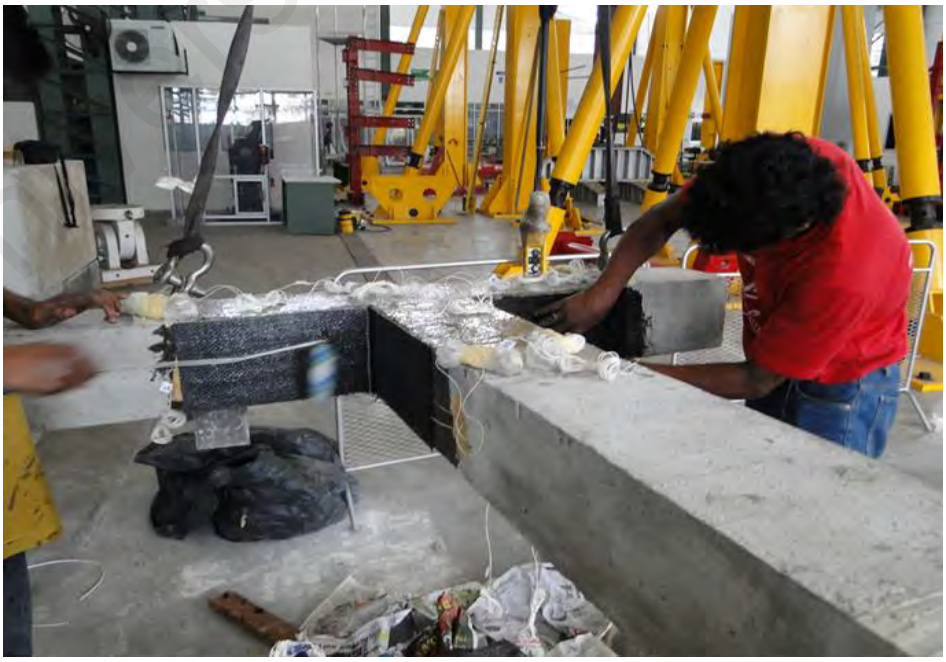

Figure 3.18: Installation of CFRP sheet on specimen RCS4

Figure 3.19: Installation of CFRP plate on specimen RCS5

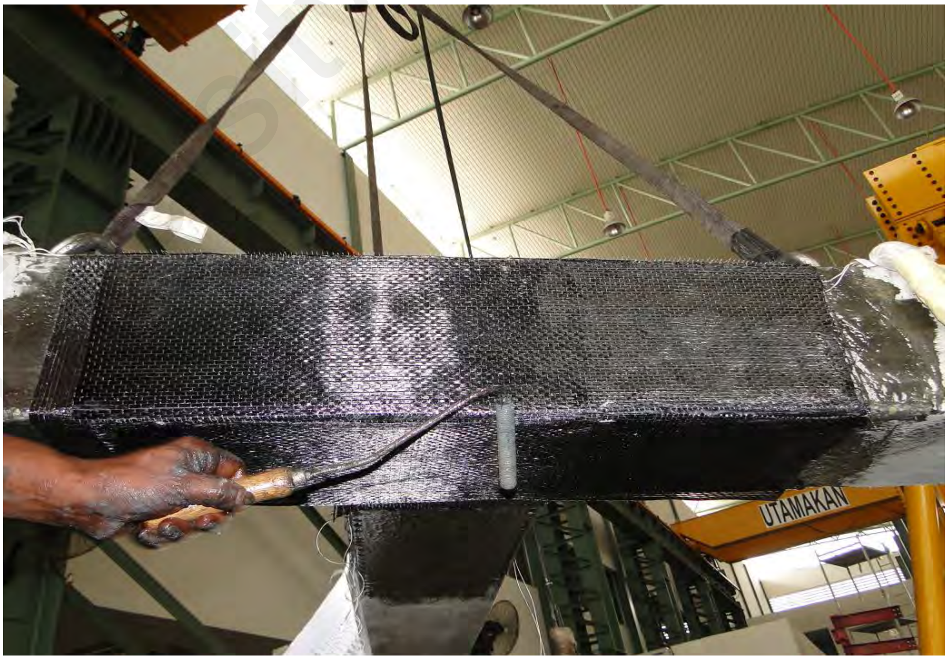

Figure 3.20: CFRP wrapping of specimen RCS6

3.2.3 Material Properties

3.2.3.1 Concrete

The six specimens evaluated in this study were cast in three groups due to laboratory space limitations. The average compressive strengths of concrete in the first, second and third groups after 28 days and on the day of the test are presented in Table 3.1.

Table 3-2: Concrete Properties

Average Compressive Strength (Day of Test) (MPa)	Average Compressive Strength (28 Days) (MPa)	Specimens
40.2	38.9	First Group (RCS1&RCS2)
41.4	40.2	Second Group (RCS3&RCS4)
39.3	38.1	Third Group (RCS5&RCS6)

The variation in compressive strength among these groups was considered acceptable since the difference was less than 5% on test day.

Concrete mix proportions of the prepared samples is according to Table 3.3.

Table 3-3: Concrete mix proportions of samples

Material	Cement (Kg/m^3)	Water (Kg/m3)	Aggregates (Kg/m3)	
			Coarse	fine
Quantities	440	210	1150	600

3.2.3.2 Steel reinforcement

All reinforcement rebars used in this research study were grade A615. The reinforcement tensile properties were tested according to ASTM A370. The mechanical properties of the reinforcement steel are presented in Table 3.2.

Table 3-4: Mechanical Properties of Reinforcement Steel

Ultimate Stress MPa	Yield Stress MPa	
600	400	#6 Rebar
700	500	#12 Rebar

3.2.3.3 FRP Composite Laminate

The composite laminates evaluated in this study were tested according to ASTM D-3039-08 to determine their mechanical properties. The carbon fiber reinforced plastic (CFRP) sheets used in all experiments were unidirectional with ultimate stress of 3500 MPa, ultimate strain of 0.017 mm/mm and constant modulus of 210 GPa.

3.2.4 Test Setup

Schematic views of the main test setup are shown in Fig. 3.21 and 3.22. Schematics of the applied loads and reaction frame for the column horizontal forces are shown in Fig. 3.23 to 3.27. The specimens were placed in the setup such that the column longitudinal axis was vertical and the beam longitudinal axis was horizontal. A rigid steel column cap was used for the top and bottom of the column to distribute the applied axial load over the concrete uniformly. Each column end was fit inside the cap using a steel plate of appropriate thickness to prevent movement between the cap and the column end. Fig. 3.28 to 3.30 illustrate the column cap installation. To produce the pinned connection for the column ends, a steel roller was welded to the caps. The column caps were supported in the loading plane using high-strength threaded rods, which were attached to the strong support from one side and connected to the caps by special swivels on the other side. The swivels allowed the specimens to rotate fully on the plane of loading. The threaded rods were pre-loaded during specimen installation to prevent lateral movement of the specimens. The column caps were also supported by a strong frame, which was restrained to the solid floor by lateral threaded rods. Special bearings connected the caps to the frame. This frame prevented out-of-plan lateral displacement of the column and also restrained the 2000kN actuator. Fig. 3.31 to 3.33 illustrate the lateral reaction system and load applied on the threaded rods. The beam was restrained in the lateral direction to prevent lateral tensional buckling. Fig. 3.34 presents photos of the lateral beam support system. All specimens underwent two loading steps. In step one, the column was loaded with a constant axial load applied by a 2,000 kN hydraulic actuator to determine the upper floors' reaction.

The axial load value was kept constant during the rest of the test. In step two, one vertical load was applied at the beam end to simulate the deformed shape of a similar connection in a building subjected to lateral loads. The beam load was applied using a 500kN actuator. Displacement control was used to apply monotonic deflection in small increments until the specimens failed.

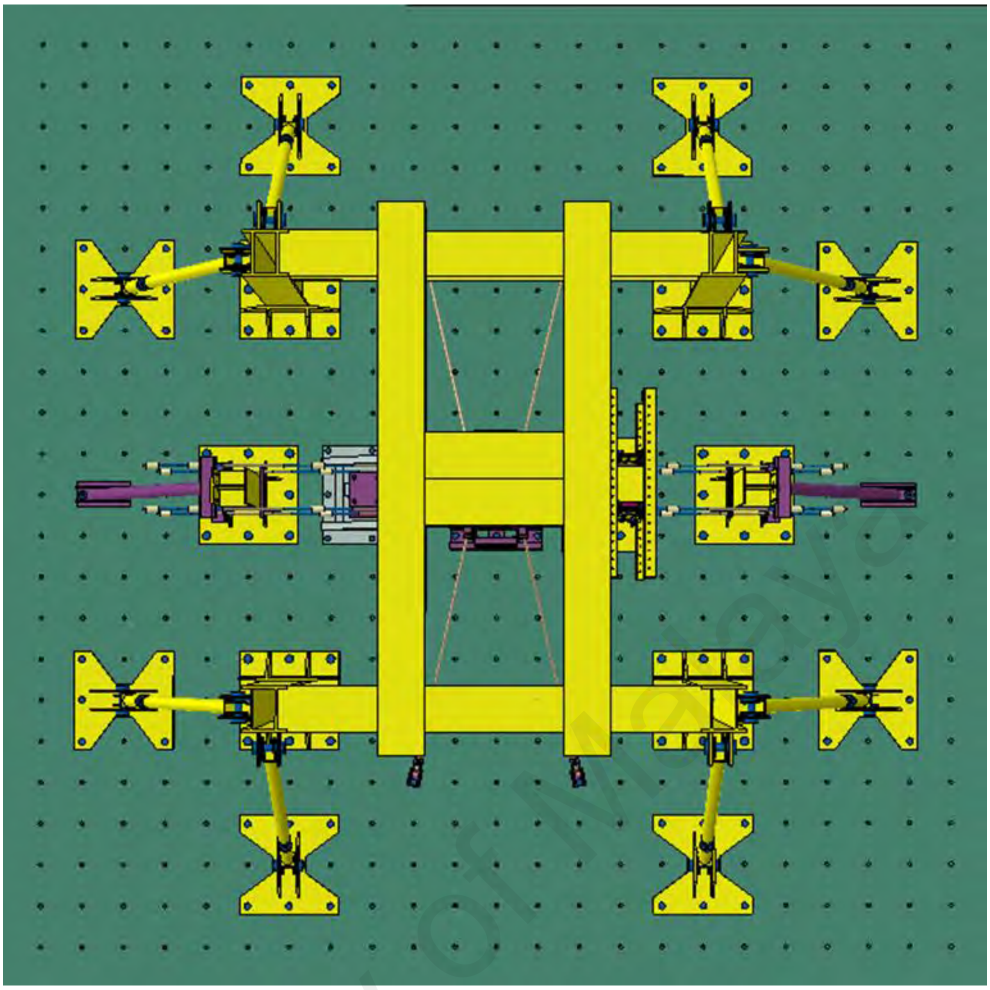

Figure 3.21: Schematic test setup plan

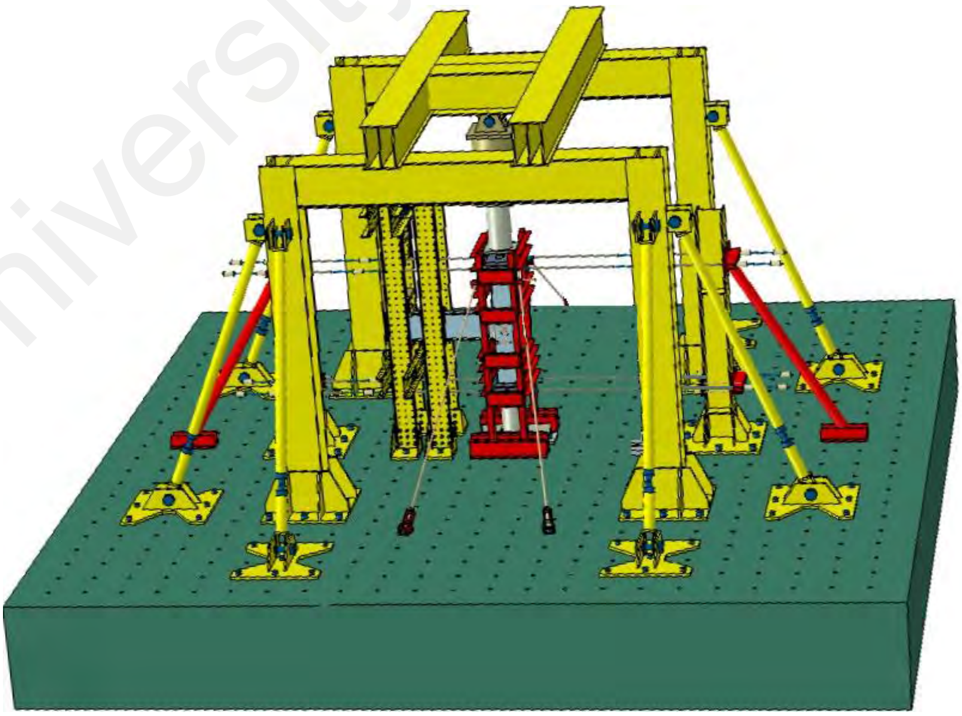

Figure 3.22: Schematic view of test setup

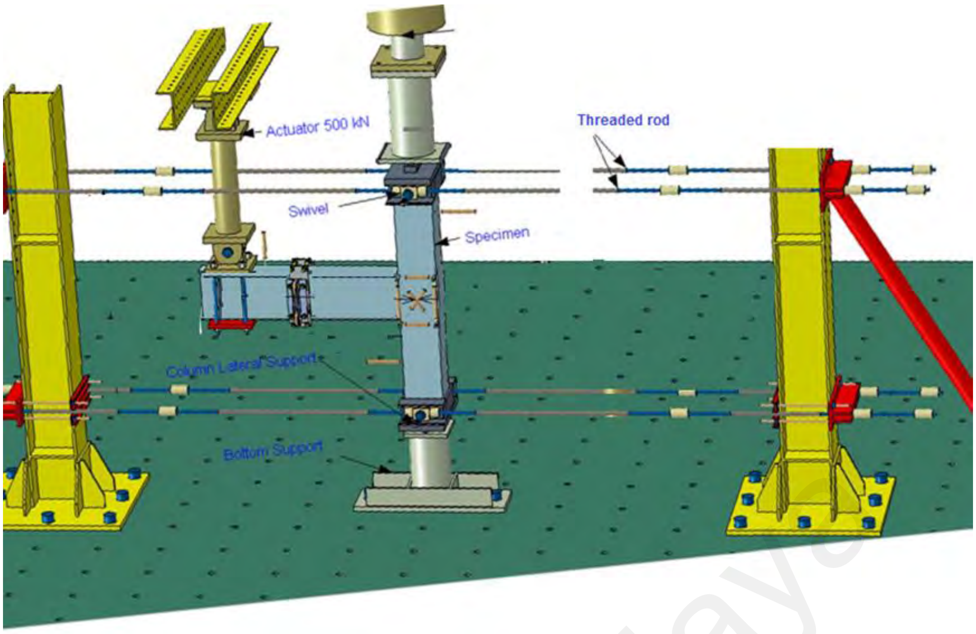

Figure 3.23: Schematic view of the loading and lateral column systems

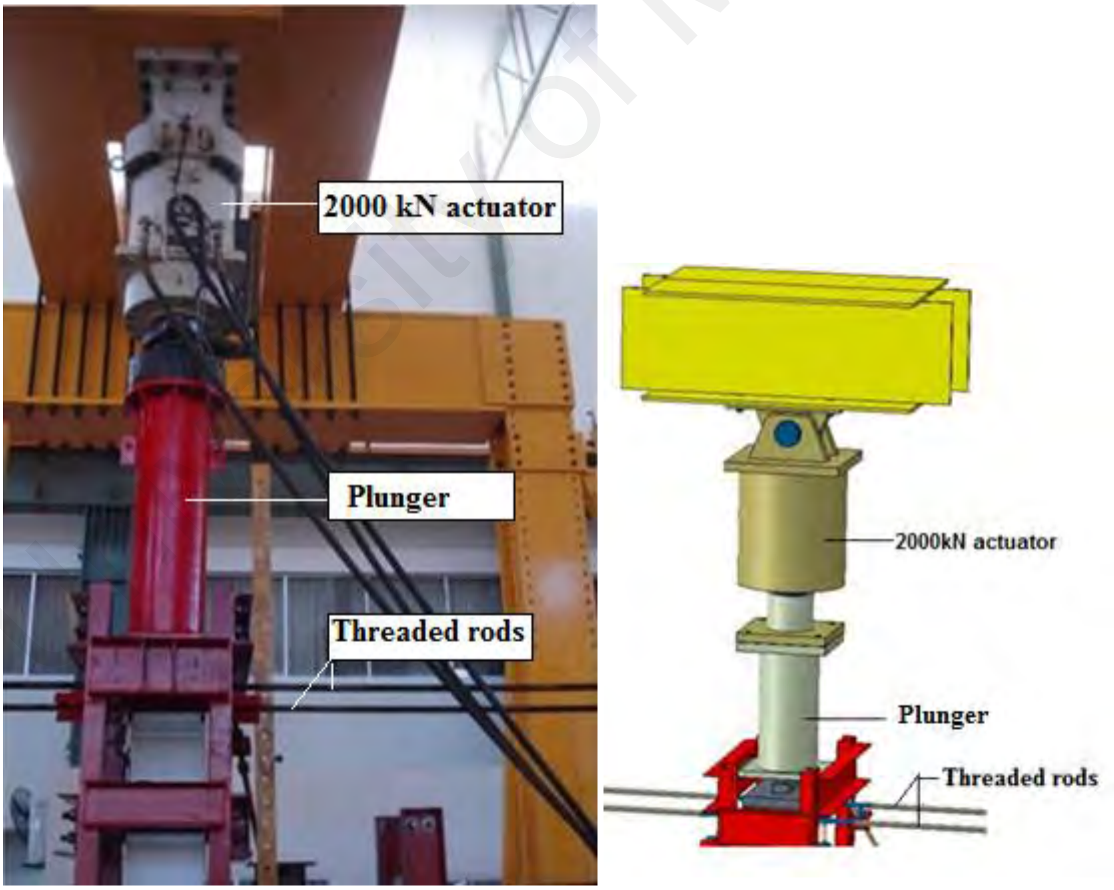

Figure 3.24: Schematic view and photograph of the 2000kN actuator on the column

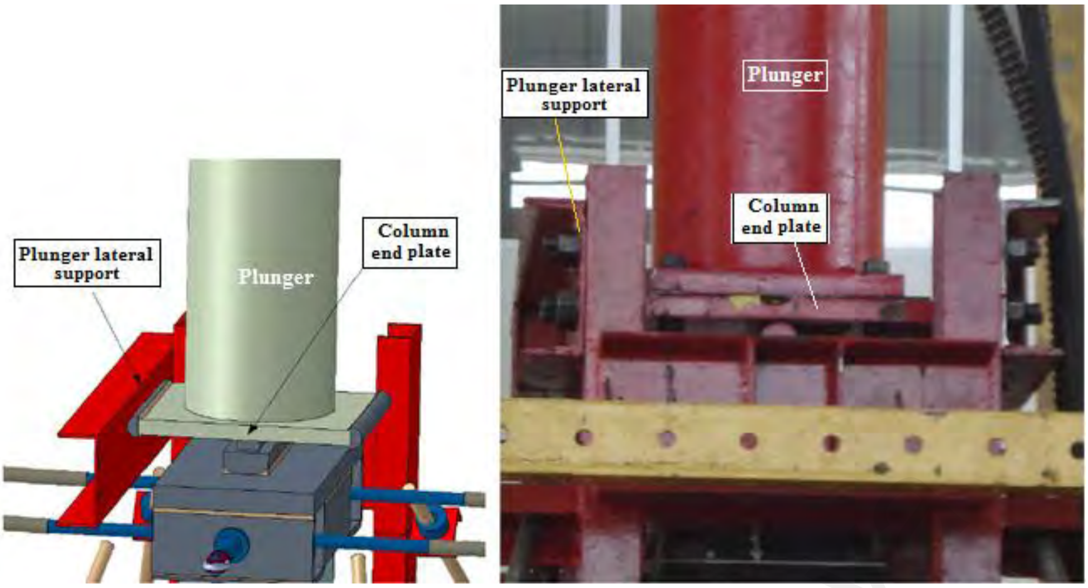

Figure 3.25: Position of 2000kN actuator on the column cap

Figure 3.26: Position of 500kN actuator

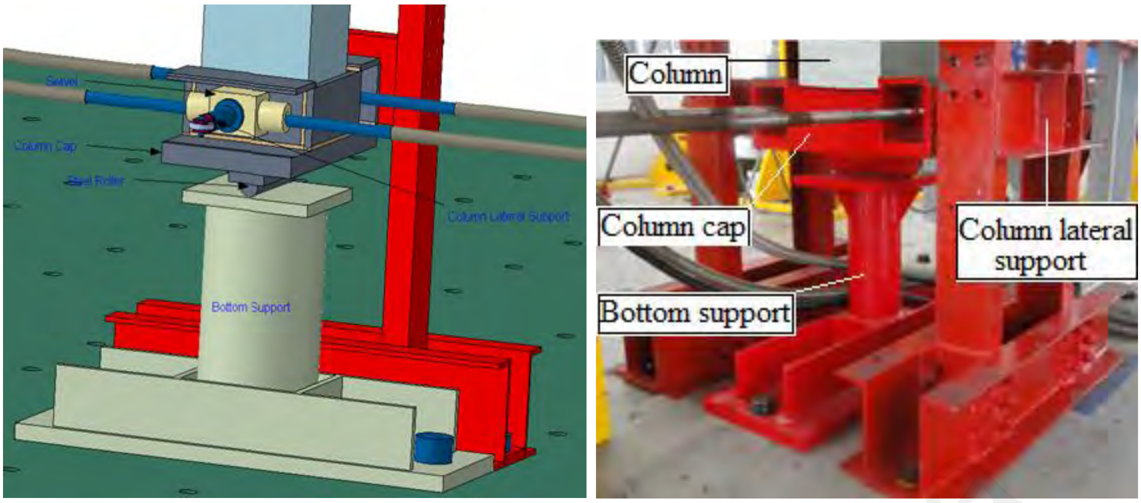

Figure 3.27: Position of bottom support

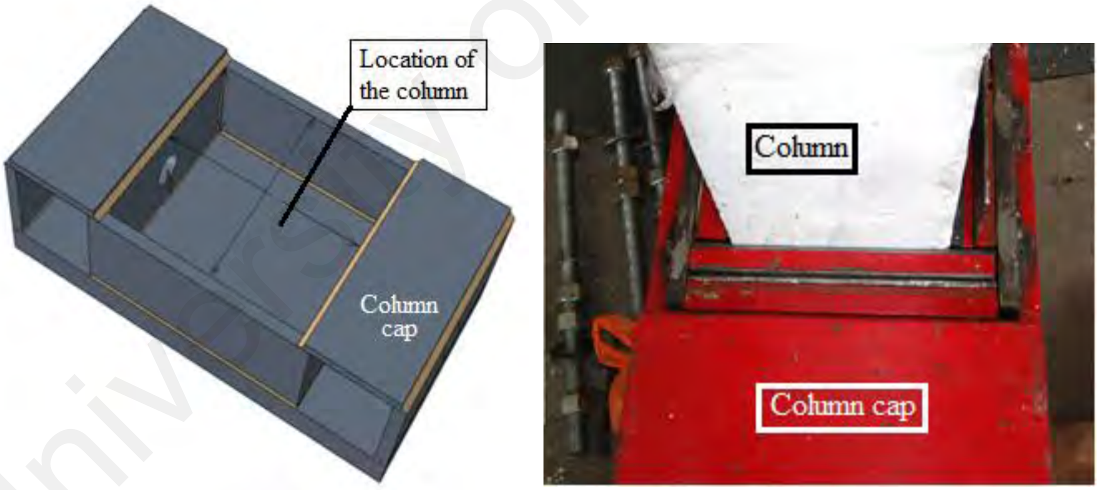

Figure 3.28: Position of column cap

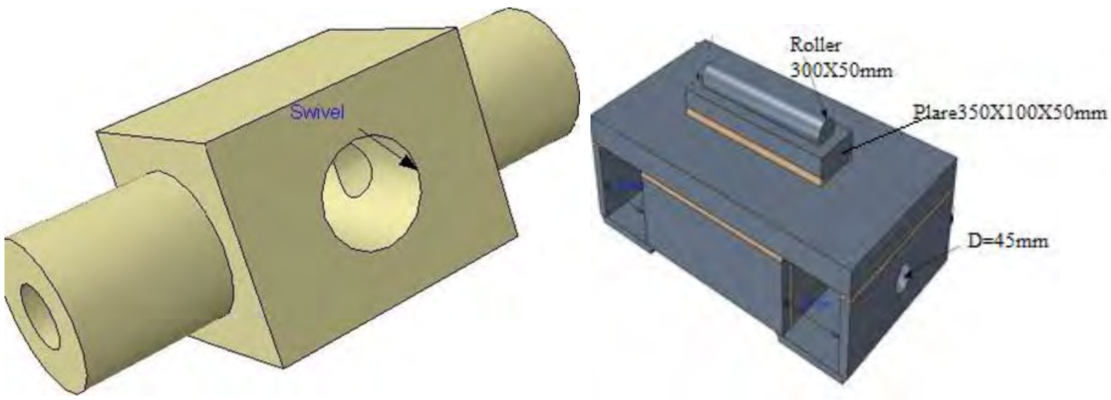

Figure 3.29: Position of column cap and swivel

Figure 3.30: Specimen installation

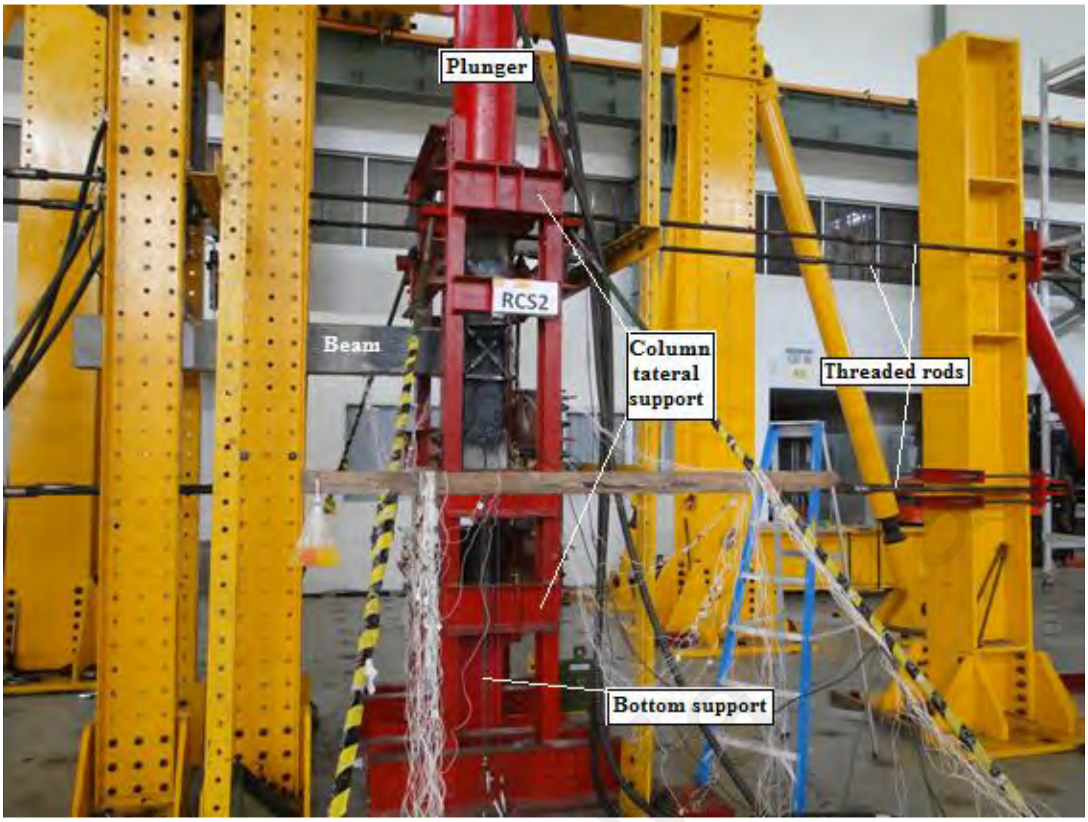

Figure 3.31: Schematic loading system and column lateral support

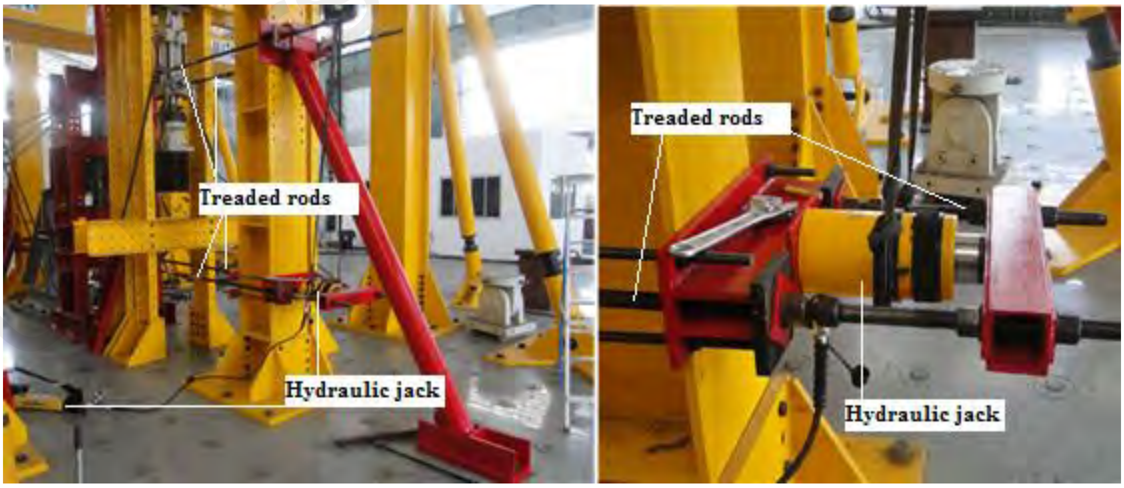

Figure 3.32: Load application to the threaded rods

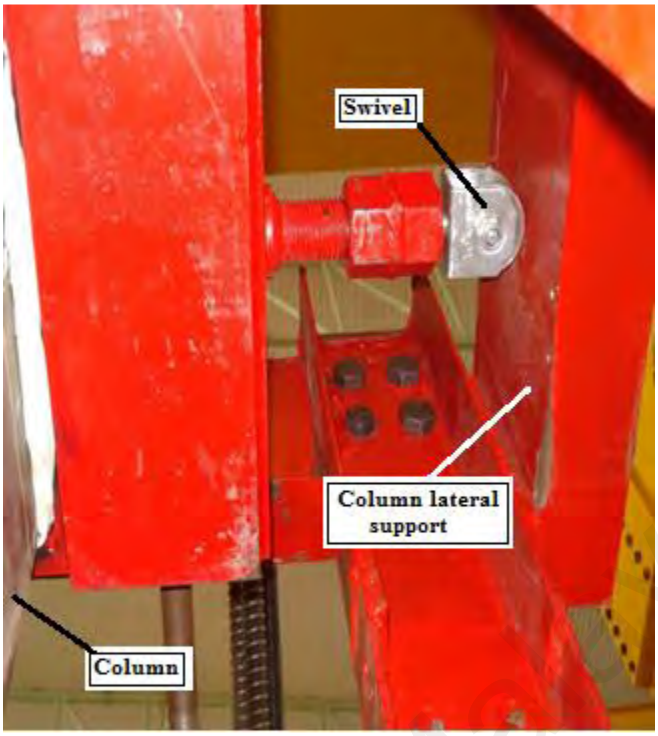

Figure 3.33: Position of lateral support for the column cap

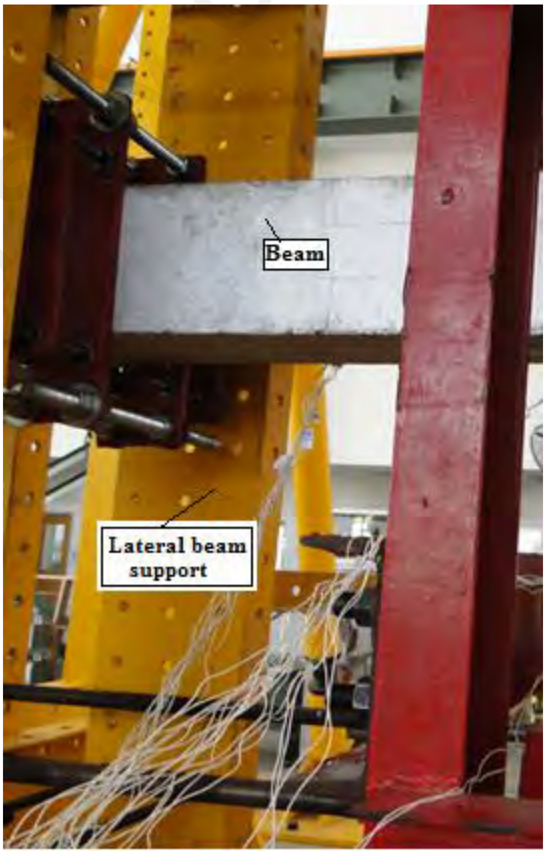

Figure 3.34: Beam lateral support

3.2.5 Instrumentation

The loads, displacements and strains applied at different locations on the specimens were measured. The loads applied and vertical displacements of the column top and beam end were measured using load cells attached to the related actuators. Although a linear voltage displacement transducer (LVDT) monitored the specimens' displacement (using nine LVDTs with a length of 300 mm), the vertical displacement of the column top and beam end was also measured by actuator strokes. Figures 3.35 to 3.38 show the typical LVDT location on the specimens to measure the beam end vertical displacement and the horizontal displacement at the lateral column points as well as a typical setup for measuring joint distortion. The typical locations of the strain gauges attached to the specimens are shown in Fig. 3.39 and 3.40. Fig. 3.41 displays the monitoring system. All instrumentation readings were recorded automatically using a data logger system controlled by a personal computer.

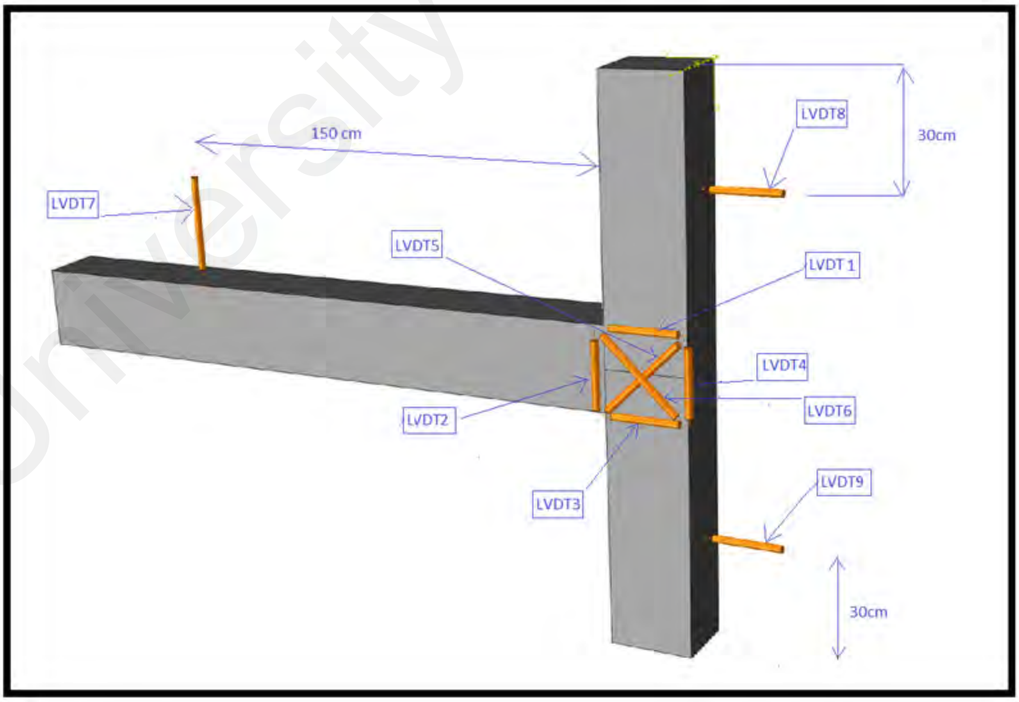

Figure 3.35: Typical LVDT location on the specimen

Figure 3.36: LVDT installed on the beam

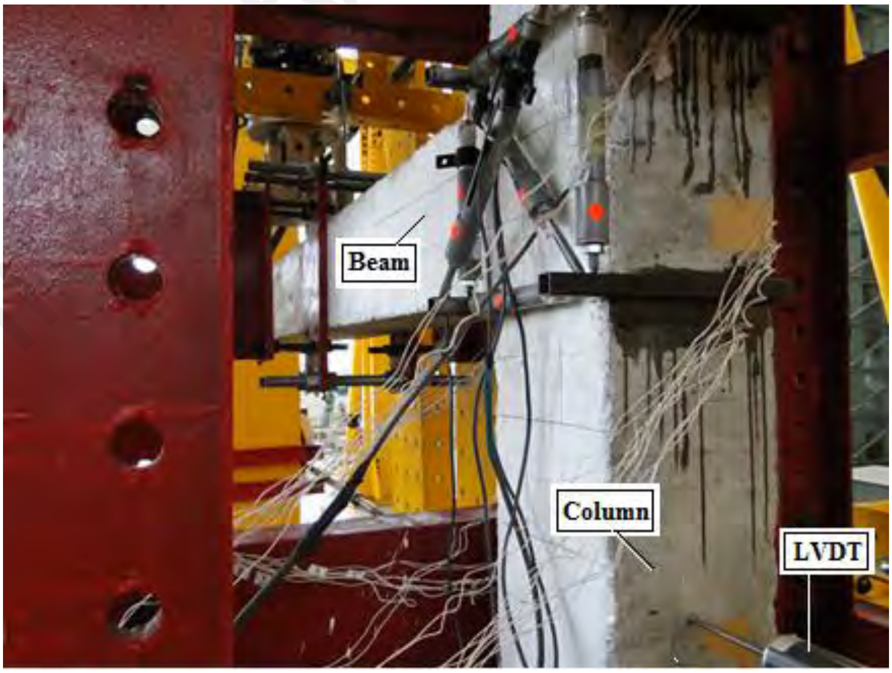

Figure 3.37: LVDT installed on the column

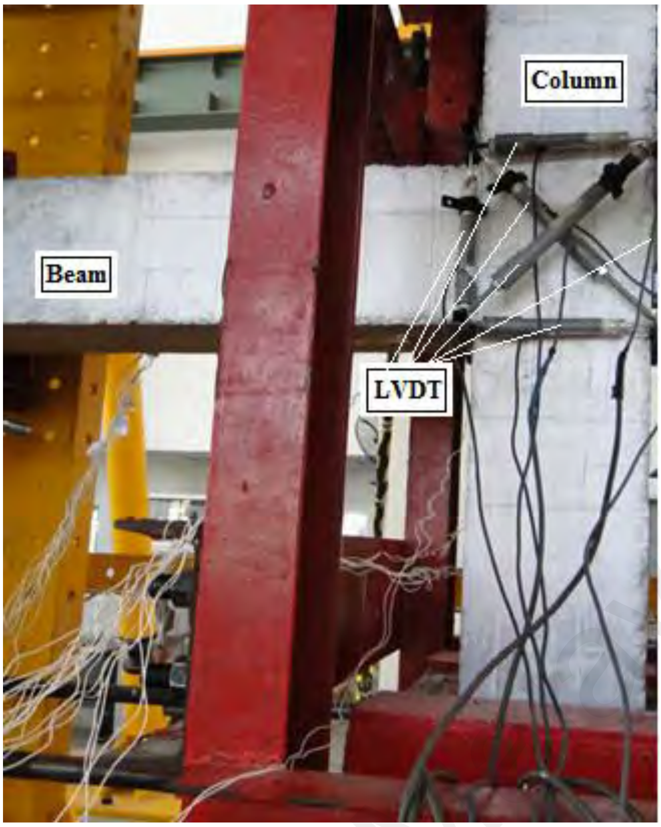

Figure 3.38: LVDT installed at the joint

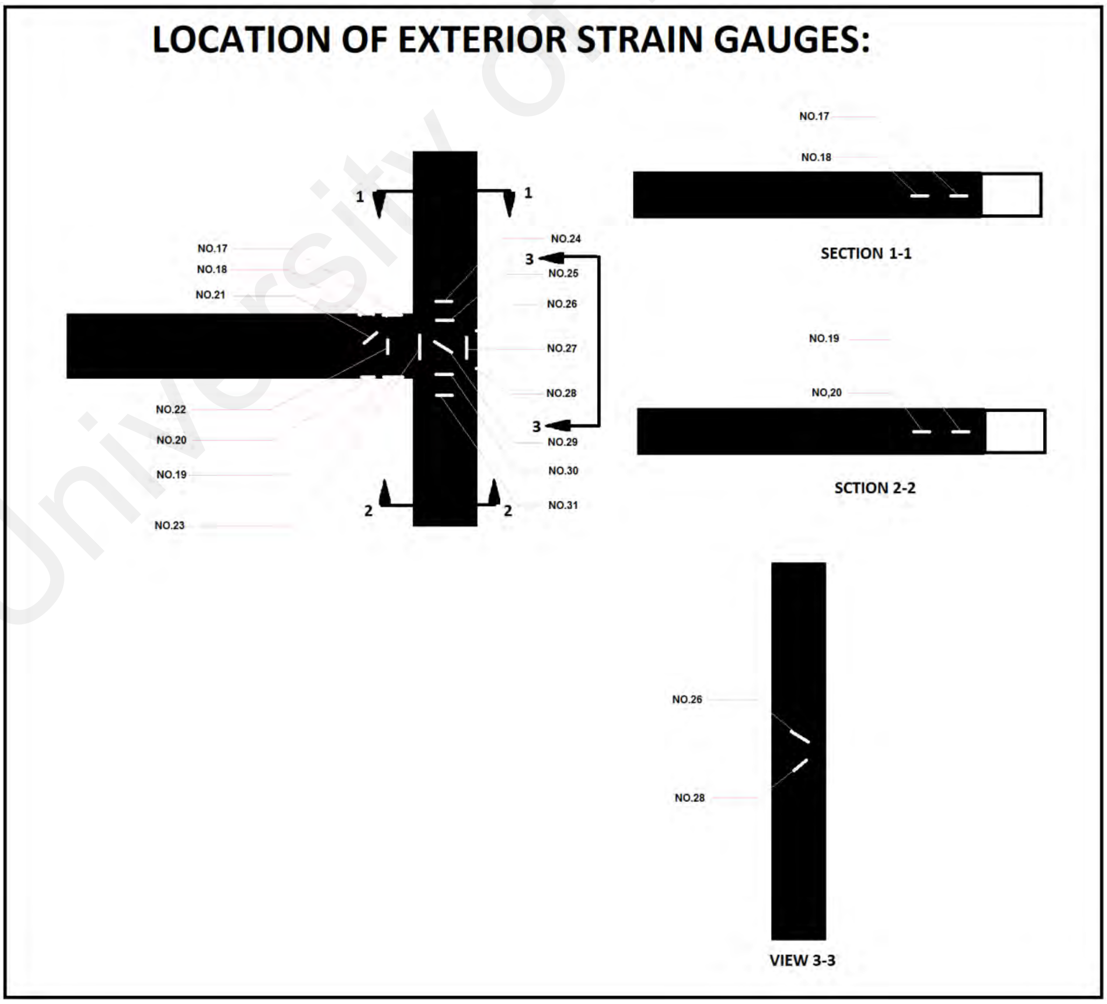

Figure 3.39: Typical locations of exterior strain gauges on the specimen

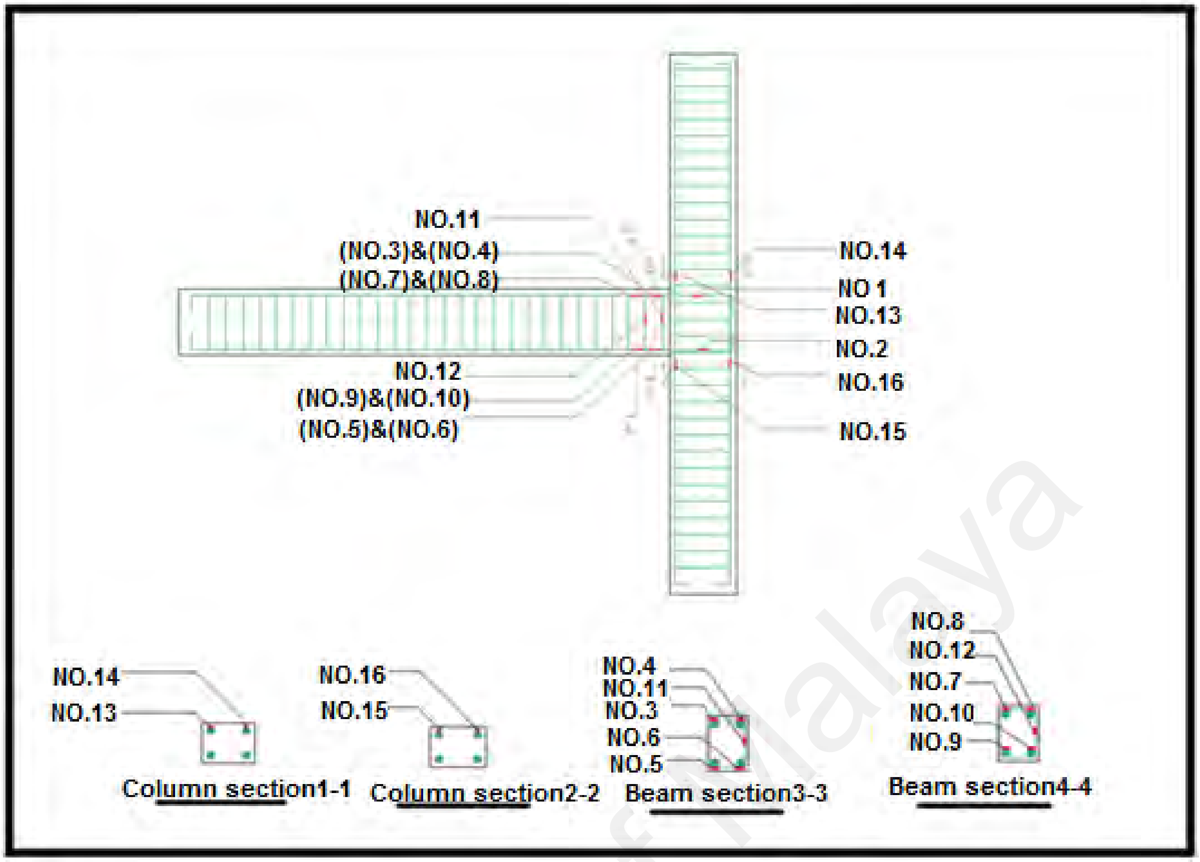

Figure 3.40: Typical locations of interior strain gauges on the specimen

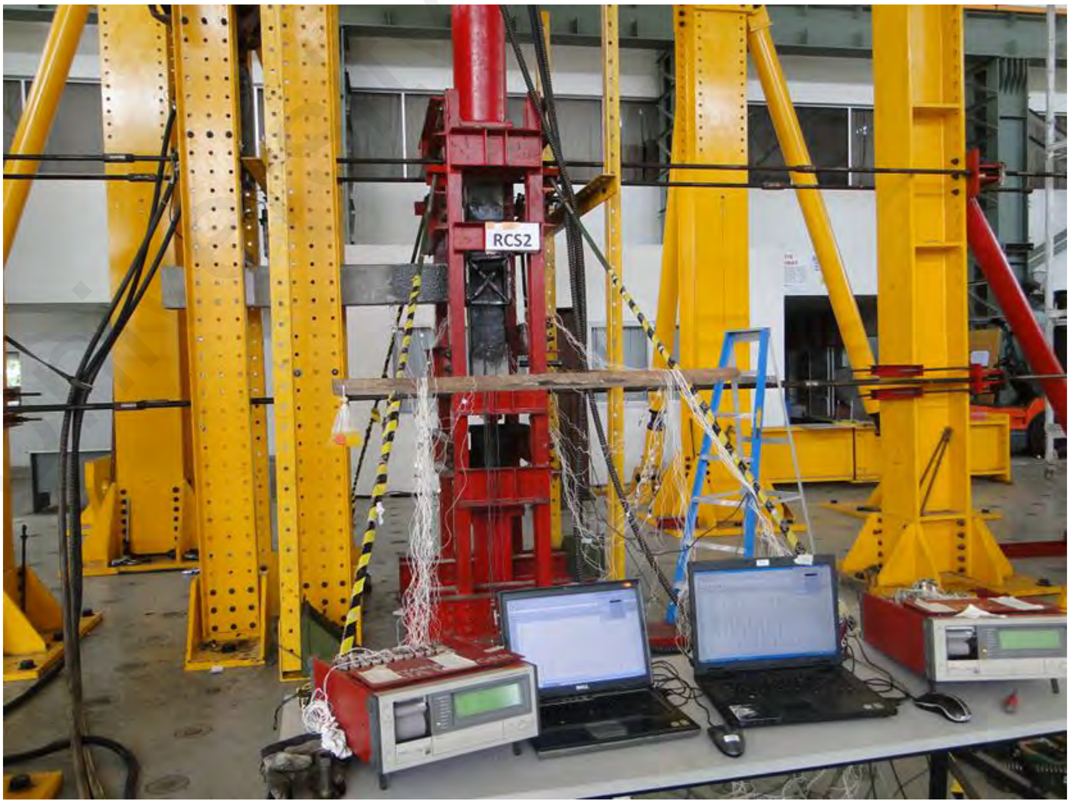

Figure 3.41: Data monitoring

3.3 Numerical Tools

Experimental testing is very costly and time consuming. Hence, accurate finite element modeling of connections is crucial for more extensive verification of the test parameters and also to achieve certain results that could not be observed through experimental testing. This objective is achievable through accurate modeling by considering parameters like the nonlinearity of materials, geometries (i.e. concrete crushing and cracking, contact interaction) and the elements suitable for modeling the interaction between steel and concrete, and also by providing appropriate solutions to overcome problem convergence. The accuracy of finite element modeling must be verified by comparing the numerical results with the experimental results. This section presents the modeling technique and finite element modeling details for the control and retrofitted specimens.

The specimens' finite element results were verified with the experimental test results. The results indicate good agreement in terms of the load-deformation relationship and maximum capacity of the connections. The finite element modeling of the specimens is described in the following sections.

3.3.1 Material Properties

3.3.1.1 Concrete

The stress-strain relationship according to EC2 was used to define the concrete behavior (En, 2004). Fig. 3.42 displays an equivalent uniaxial stress-strain curve for considering the nonlinear behavior of concrete under compression. The compression curve is divided into three parts, including the elastic range, the nonlinear parabolic portion and the descending slope. The value of the first part is the proportional limit stress of $0.4f_{ck}$ (En, 2004), where f_{ck} is defined as the concrete strength in the cylinder specimen and is equal to $0.8f_{cu}$, while f_{cu} is the concrete strength of the cubic specimen.

The strain (ε_{c1}) in relation to f_{ck} is equal to 0.0022 (En, 2004). The stress for the nonlinear parabolic part can be obtained with Eq. 3.3 to 3.5 (En, 2004):

$$\sigma = (\frac{Kn-n^2}{1+(K-2)n})f_{ck} \qquad (3.3)$$

where,

$$\mathrm{n} = \frac{\varepsilon_{\mathrm{c}}}{\varepsilon_{\mathrm{c1}}} \qquad (3.4)$$

$$\mathrm{K} = E_{cm}\, X\, \frac{\varepsilon_{c1}}{f_{ck}} \qquad (3.5)$$

The descending part can be used to define the concrete compression behavior post-failure in specimens in which concrete crushing occurred. The descending slope ceased at a stress value of rf_{ck}, where r is the reduction factor and can range between 0.5 and 1 equivalent to concrete cube strength in the range of 30 to 100 MPa. The value of r may be considered a constant of 0.85 (Ellobody et al., 2006). The ultimate strain of concrete at failure (Ɛcu) is equal to α Ɛc1 according to EC2 and BS 8110 Ɛcu is equal to 0.0035, which means that here α is equal to 1.75 (Bs, 1997).

The concrete density (γ) and Poisson's ratio (υ) are assumed to be 2,350 kg/m^3 and 0.2, respectively. The elasticity modulus (Ecm) is obtained from EC2 as per Eq. (3.6):

$$\mathrm{E_{cm}} = 9.5(\mathrm{f_{ck+}}8)^{\frac{1}{3}} \qquad (3.6)$$

Where Ecm is in GPa and Fck is in MPa.

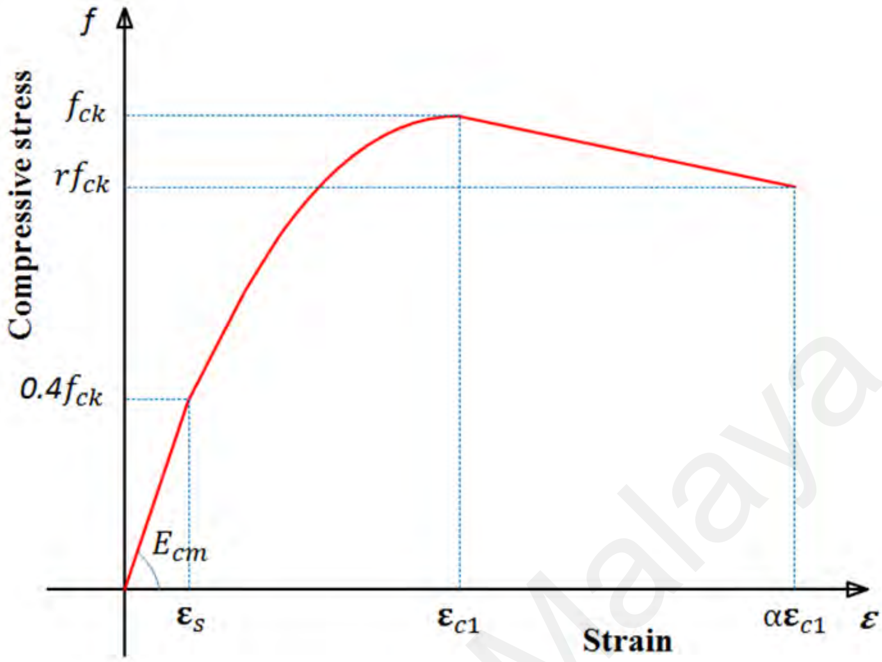

Figure 3.42: Stress-strain relationship for the compression behavior of concrete (En, 2004)

The nonlinear behavior of concrete under tension according to the uniaxial stress-strain curve is shown in Fig. 3.43. The tensile stress of concrete increased linearly with strain before the concrete cracked, and it decreased to zero upon concrete cracking. Fig. 3.44 presents the tension stress-crack displacement relationship. In the models, the damage plasticity for concrete cracking was defined for the specimens. The concrete damage plasticity model presumes a non-associated potential plastic flow. The material dilation angle (Ψ) and eccentricity (Ɛ) were taken as 25° and 0.1, respectively. The ratio of biaxial compressive strength to uniaxial compressive strength ($\frac{f_{bo}}{f_{co}}$) was taken as 1.16.

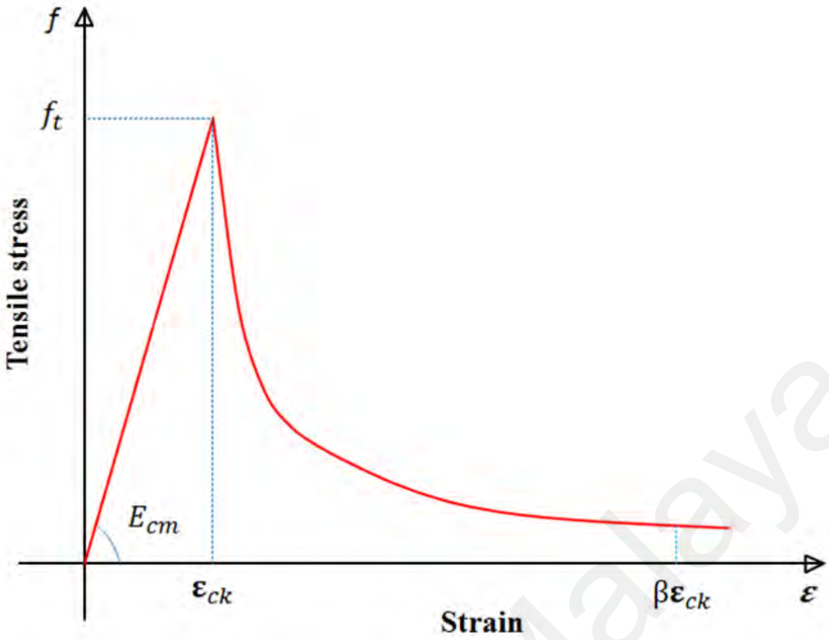

Figure 3.43: Stress-strain relationship for the tensile behavior of concrete (En, 2004)

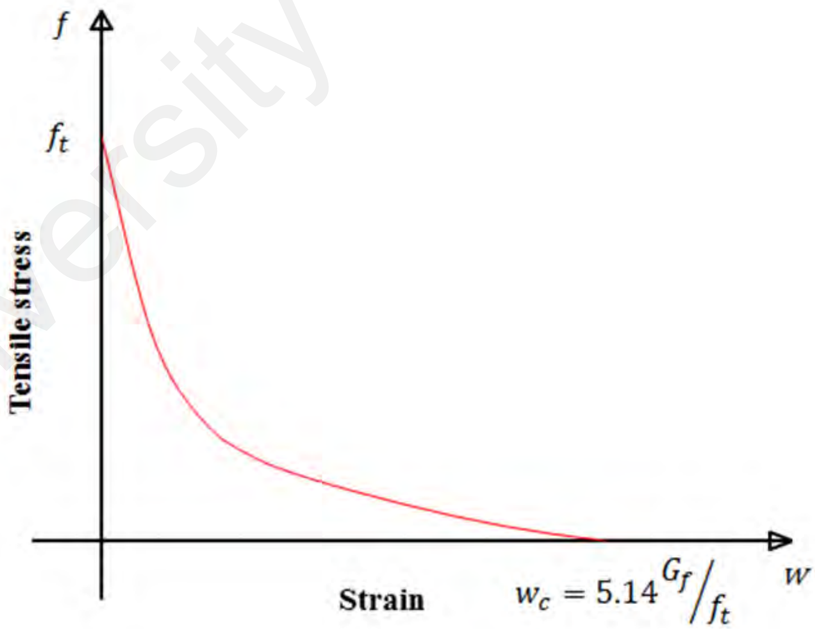

Figure 3.44: Function of tension softening model (Cornelissen et al., 1986)

3.3.1.2 Rebar Reinforcement

The longitudinal and transverse steel reinforcement rebars were incorporated in the FE model as an elastic-plastic material using a bilinear stress-strain curve. The stress-strain curve slope in the plastic stage was assumed to be about 1% of the modulus of elasticity for steel. The rebar truss element used in the FE model is shown in Fig. 3.45. The following properties were entered to define the reinforcement rebars:

1. Elastic modulus (Es).

2. Poisson's ratio (ν) = 0.3.

3. Tensile stress-inelastic strain curve for the steel reinforcement.

.

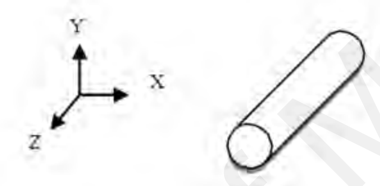

Figure 3.45: Steel Rebar Truss Element (T3D2)

3.3.1.3 Fiber Reinforcement Polymer (FRP)

The unidirectional laminate properties were incorporated in the model as an orthotropic material. The CFRP laminate mechanical properties are defined in the elastic laminate option. The CFRP shell element used in the FE model is presented in Fig. 3.46 and the following parameters were entered in the FE model:

1. Laminate module along and perpendicular to the fibers (E11 and E22).

2. Laminate shear modulus in the three orthogonal directions (G12, G13, and G23).

3. Laminate Poisson's ratio (ν12) = 0.3.

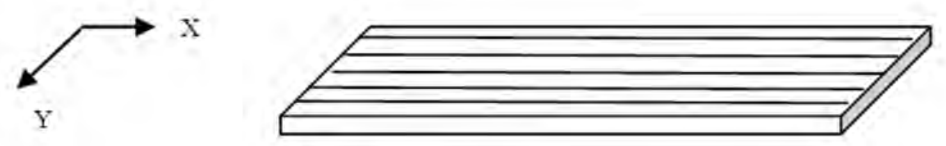

Figure 3.46: CFRP Shell Element (S4R)

The failure criterion for CFRP orthotropic materials is defined in the stress space. The input data for defining the failure criterion is based on the ultimate compressive, tensile and shear strengths of the CFRP laminate in two orthogonal directions. The renowned failure index, i.e. Tsai-Wu criterion, was applied to define the failure criteria of the FE analysis model (Tsai & Wu, 1971).

The failure criteria for the FE model are based on the following assumptions:

1. There is a full bond between the CFRP composite laminate and concrete surface. (Since none of the samples fail due to debonding CFRP sheets, this hypothesis does not affect the results).

2. The laminate material properties are homogeneous.

3. The material strength can be measured experimentally in simple tests.

The Tsai-Wu failure criterion for two-dimensional stress requires that:

$$I_F = F_1\sigma_{11} + F_2\sigma_{22} + F_{11}\sigma_{11}^2 + F_{22}\sigma_{22}^2 + F_{66}\sigma_{12}^2 + 2F_{12}\sigma_{11}\sigma_{22} \prec 1.0$$

Where I_F is the interaction equation of CFRP laminate stresses, and σ_{11}, σ_{22} and σ_{12} are the longitudinal, transverse and shear stresses applied, respectively.

The Tsai-Wu failure criterion coefficients are defined as follows:

$$F_1 = \frac{1}{X_t} + \frac{1}{X_c}$$

$$F_2 = \frac{1}{Y_t} + \frac{1}{Y_c}$$

$$F_{11} = -\frac{1}{X_t X_c}$$

$$F_{22} = -\frac{1}{Y_t Y_c}$$

$$F_{66} = \frac{1}{S^2}$$

Where:

Xt = ultimate tensile strength along the fiber direction,

XC = ultimate compressive strength along the fiber direction,

Yt = ultimate tensile strength perpendicular to the fiber direction,

Yc = ultimate compressive strength perpendicular to the fiber direction, and

S = ultimate shear strength of the fiber.

The criterion that determines on which branch of the quadratic curve the failure is located is based on the following discriminate value:

$$Discriminant = F_{11}F_{22} - F_{12}^2 \begin{cases} > 0 \text{ for ellipse} \\ = 0 \text{ for parallel line} \\ < 0 \text{ for hyperbola} \end{cases}$$

The normalized interaction term according to the Tsai-Wu criterion (Tsai & Wu, 1971) is expressed as:

$$F_{12} = f^* \sqrt{F_{11} F_{22}}$$

Where $-1.0 \leq f^* \leq 1.0$ is the range of normalized interaction term values for an elliptical solution.

For the Tsai-Wu failure criterion in the FE model, the normalized interaction term f* served as input data. In order to avoid infinite strength, the failure criterion has to represent a closed curve in the plane of normal stress components. To achieve this closed curve failure criterion, the discriminate f^* value served as input in the FE model and was equal to 0.5, which is commonly used in laminated composite failure analysis.

3.3.2 Specimen Modeling

To simulate the concrete beam-column connection specimens, a finite element model was proposed with the ABAQUS program (ABAQUS, 2011). To model the interaction between the components, surface element, tie constraint and merged element in ABAQUS, an explicit program was employed.

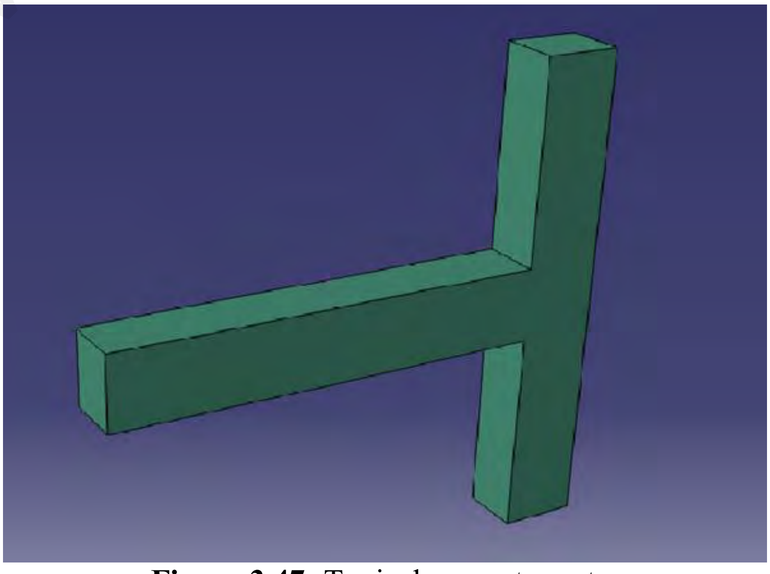

Figure 3.47: Typical concrete part

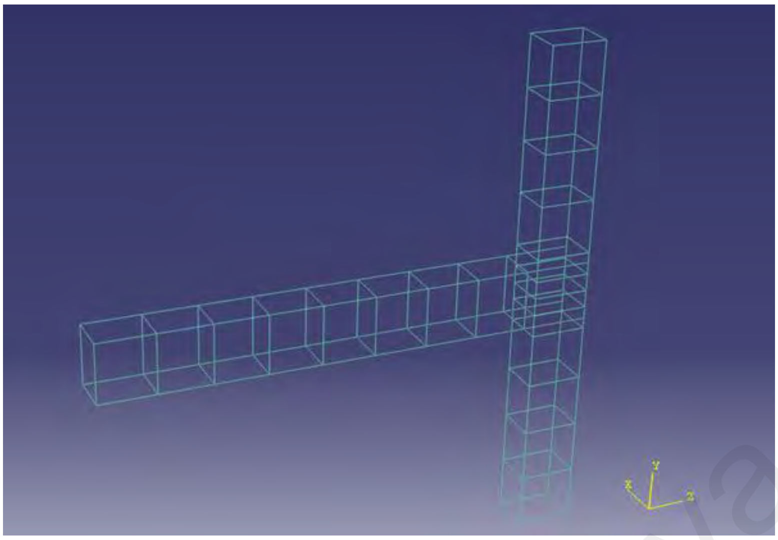

Figure 3.48: Typical steel part

3.3.3 Element Type

The element types used in finite element modeling are presented as follows. An eight-node solid element (C3D8R) was used to model the concrete core, which has three translational degrees of freedom at each node. This element can be used to consider concrete cracking and crushing in three orthogonal directions at each integration point.

The truss element (T3D2) was applied in modeling the longitudinal reinforcing bar in the specimens. This element has three translational degrees of freedom (translation in the x, y and z directions) at each node.

The fiber reinforcement polymer (FRP) composite laminate was modeled using four node shell elements. The shell element in the FE analysis model is called S4R.

3.3.4 Interaction

Finite element analysis is dependent on defining the relation between parts accurately. Subsequently, the interaction between parts will be described:

3.3.4.1 Tie constraint

A tie constraint was used to connect the laminate shell element to the concrete solid element. This constraint includes a master surface and slave surface. The concrete part was considered the master surface and CFRP sheet part was the slave surface. The slave surface was attached to the underlying element (master surface) by node to surface in the tie constraint. The initial position tab of the adjusted slave surface must be active in this process. Meshing should be refined for slave surfaces to achieve a more accurate result for the tie constraint (ABAQUS, 2011).

3.3.4.2 Embedded Element

The interaction between the reinforcing bars and concrete core was assumed to be a full bond with no slip between. Consequently, reinforcement rebar elements were connected to the surrounding concrete regions using an embedded element option. This option constrained the translational degrees of freedom of the embedded reinforcement rebar element node defined as a slave element to the degrees of freedom of the surrounding concrete element node defined as a host element.

3.3.5 Loading and Boundary Conditions

Two steps similar to the test specimen loading were considered for the loading in finite element analysis. First, axial load was applied on some nodes at the column top. The nodes were located on the line perpendicular to the main specimen plan. The load was kept constant until the end of analysis. The value of the axial load was the same as the axial load applied during the test. Second, vertical velocity loading was applied to the beam end. Velocity-controlled loading provides a more stable system in the nonlinear stage than force-controlled loading. A special 300 mm/s velocity rate was used monotonically as the loading rate. This rate was achieved by comparing the kinematic energy with the internal energy when the effect of dynamic analysis could be neglected. The real rate, which is much smaller than this rate, results in lengthy analysis with little effect on result accuracy.

To consider the pinned connection for the column bottom, the nodes on the center axis of the bottom column in the Y-direction were constrained for all translational displacements. The same condition was considered for the column top, except the displacement in the Z-direction was free because of the axial load applied on the column. The middle of the beam was also restrained against lateral movement.

3.3.6 The Finite Element Mesh

In order to obtain accurate FE modeling results, all elements in the model were purposely assigned the same mesh size to ensure that every two different materials shared the same node. The type of mesh selected in the model was structured. The mesh elements for concrete, rebar and FRP laminate were 3D solid, 2D truss, and shell, respectively. The length of 25 mm was considered for each dimension of the elements.

CHAPTER 4: RESULTS AND DISCUSSION

4.1 General

In this section, the laboratory results for the reinforced and prototype samples are compared, and the impact of different forms of CFRP reinforcement on the samples' bearing capacity and ductility is examined. Subsequently, the samples are modeled with ABAQUS software. A prototype is tested in order to validate the model and compare the numerical and experimental results. Following software model validation, samples RCS1 to RCS6 are modeled and analyzed. The numerical results are controlled with the experimental data. Since it is possible to control various parameters for all components, the samples' details are studied in the numerical analysis, which is simpler and less expensive than lab analysis. Therefore, different models are produced with various CFRP lengths and thicknesses. Numerical analysis is then applied to investigate the effect of reinforcing layer length and thickness in different configurations.

4.2 Experimental results

4.2.1 Introduction

After the six beam-column joint specimens were designed and constructed, they were tested as described in Chapter III. During each test, the cracking progress was recorded at each loading level and pictures were taken at the end of loading. The experimental tests on specimens RCS1 to RCS6 are explained in this chapter. In the first loading step, a constant axial load of 300 KN was applied to the column and maintained until the end of the test. In the second step, the beam end was loaded downward. The specimens' behavior is presented in terms of load-displacement relationship, failure modes and strain at different locations on the specimens. This data provides valuable information on the behavior and progress of failure in the specimens. Selected data is also useful for understanding the behavior of members and possible failure modes. The results are described for each specimen individually. The results are discussed by comparing the experimental test results for the specimens to identify their performance

4.2.2 Specimens cracking Behavior

In the control specimen (RCS1), flexural cracking of the beam section subjected to maximum bending moment initially appeared at a beam tip load of 6.7 kN. Cracks were detected simultaneously beside the beam close to the column. The onset of diagonal cracks in the joint area took place at a beam tip load of 10 kN. Additional cracks in the joint area appeared thereafter as loading progressed but remained within a very fine width throughout the test. The beam's longitudinal steel yielded at an average beam tip load of 12 kN and the corresponding average yield displacement (Dy) was 34 mm. Subsequently, the beam cracked extensively along a distance shorter than its depth from the column face. Finally, wide cracks developed in the hinge area at a beam tip load of 12.8 kN and the test was stopped as the beam capacity dropped substantially.

In specimen RCS2, two cross-shaped CFRP plates were bonded on both sides of the beam-column joint in the vertical plane, and then the column was wrapped around the joint. RCS2 was loaded until the first flexural crack was detected at a beam section adjacent to the column, which took place at a load of about 7.5 kN. Cracks were detected simultaneously on the beam end. As the loading proceeded, cracking progressed in the beam segment adjacent to the column and intensified due to the combination of high shear and normal stresses in this section. The degradation in strength progressed and the test was stopped at a load of about 19.1 kN.

Throughout the test, read strain on the FRP members indicated that their behavior remained elastic and did not fail.

Specimen RCS3 was retrofitted with two CFRP plate added to top and bottom of beam and the column were wrapped with CFRP on both sides as well as around the back of the beam. The CFRP plate ends were also wrapped in order to provide CFRP anchorage. The onset of diagonal cracks at the beam sides took place at a load of 6.5 kN. Additional cracks with uniform spacing appeared thereafter as loading progressed but remained within a very fine width throughout the test. At a load of 17 kN, the beam cracked extensively along a distance equal to its depth from the column face. The beam's transverse steel yielded at an average beam tip load of 16 kN and the cracks grew deeper. Then wide cracks developed in the area where the CFRP plate was connected to the beam, rubble began falling, and the beam lost most of its concrete. Hence, CFRP plate debonding occurred, stress in the longitudinal rebar suddenly increased and the rebar yielded at a load of 16.1 kN. The test was stopped as the beam capacity dropped substantially at a maximum recorded load of 17.81 kN.

Sample RCS4 was reinforced at the top and bottom corners of the connection with the L-shaped CFRP sheet layers, as described in Chapter 3. The CFRP layers on the beam caused the first bending cracks on the beam to shift to the closest region without CFRP to the column. At greater loading, diagonal cracks formed within the beam due to shear stress. Most cracks were at a distance with the beam depth from the column. As the loading further increased, the cracks grew wider and caused the transverse rebar to yield. Subsequently, the longitudinal rebar yielded at a suitable distance from the column. With transverse rebar yielding the cracks intensified, the CFRP layers ruptured and finally, an ultimate load (Fu) of 18.15 kN was recorded.

Despite a significant increase in loading capacity, the ductility did not increase effectively duo to shearing strength weakness. Evidently, it is possible to increase the ductility by selecting a suitable thickness for the CFRP layer. Moreover, selecting a suitable CFRP length can have an important role in determining the location and time of plastic hinge formation. This topic will be addressed in further sections via numerical analysis.

For sample RCS5, two reinforcing CFRP plates were used on both sides of the beam web. The first bending crack started at F=5.5 kN and the shear stress increased, but on account of the CFRP plates, shear cracking was controlled. At higher loads, new cracks formed paralleled to the beam.

According to strain gauge data, the top beam rebars yielded. The location where a plastic hinge formed was not sufficiently far from the column; therefore, by choosing suitable CFRP plate lengths and optimizing the CFRP thickness, it is possible to predict a more appropriate point on the beam for plastic hinge formation. The CFRP plates helped control the shear stress while the shear resistance of specimen RCS5 rose. The maximum stress of the longitudinal rebar reduced and the specimen became more ductile.

In the last sample, RCS6, in the vicinity of the joint, both beam and column were wrapped. A CFRP wrap covered the beam by around 35 cm near the joint. Due to the vertical presence of CFRP in this sample the shear strength increased, while CFRP located on top of the beam helped increment the bending strength. With increasing load the bending stress increased. Moreover, the present CFRP layers controlled the bending stresses of the steel close to the column, and the longitudinal rebars yielded at an acceptable distance from the column.

It was observed that sample RCS6 exhibited significant ultimate load due to the adequate shear and bending strength function. The strain gauges indicated that the plastic hinge formed sufficiently far from the column; therefore, by opting for a suitable beam length in reinforcing with CFRP and optimizing the CFRP thickness, it became possible to create a suitable point on the beam for plastic hinge formation.

4.2.3 Ductility factor and ultimate load

The first yield of the reinforcement rebar was calculated and determined based on data recorded for the beam and column section. When the data logger recorded the first yield that occurred to any of the steel reinforcement rebars, the corresponding displacement (Dy) was measured. The data logger also recorded displacement corresponding to ultimate load (Du). Dy and Du were used to calculate the experimental ductility factor (μ). The ductility factor is calculated with Eq. (4.1):

$$\mu = \frac{Du}{Dy} \qquad (4.1)$$

The ductility factor values for all specimens are given in Table 4.1.

The control specimen (RCS1) was tested by loading and the data logger measured its ultimate load. Then specimens RCS2-RCS6 were reinforced with various CFRP forms and tested. Reinforcing the specimens increased their ultimate loads significantly. A summary of the ultimate loads and strength increment is presented in Table 4.1.

Table 4-1: Summary of experimental test results

Specimen	Yielding load (F_Y)	Ultimate load (F_U)	D_Y	D_U	μ	Increase in Ultimate load
RCS1	12	12.8	34	65	1.91	0
RCS2	16.6	19.1	35	90	2.57	49%
RCS3	16.1	17.81	47.5	82	1.73	39%
RCS4	14.7	18.15	28.4	62.18	2.19	42%
RCS5	18.2	21.86	21.8	85	3.9	71%
RCS6	21.29	23.15	22.9	76.61	3.69	81%

4.2.4 Load-displacement curve

In the test, a data logger recorded the load and corresponding displacement. Figure 4.1 displays the load variations against displacement for all specimens. The presence of CFRP reinforcement affected the ultimate load and ductility factor of the specimens.

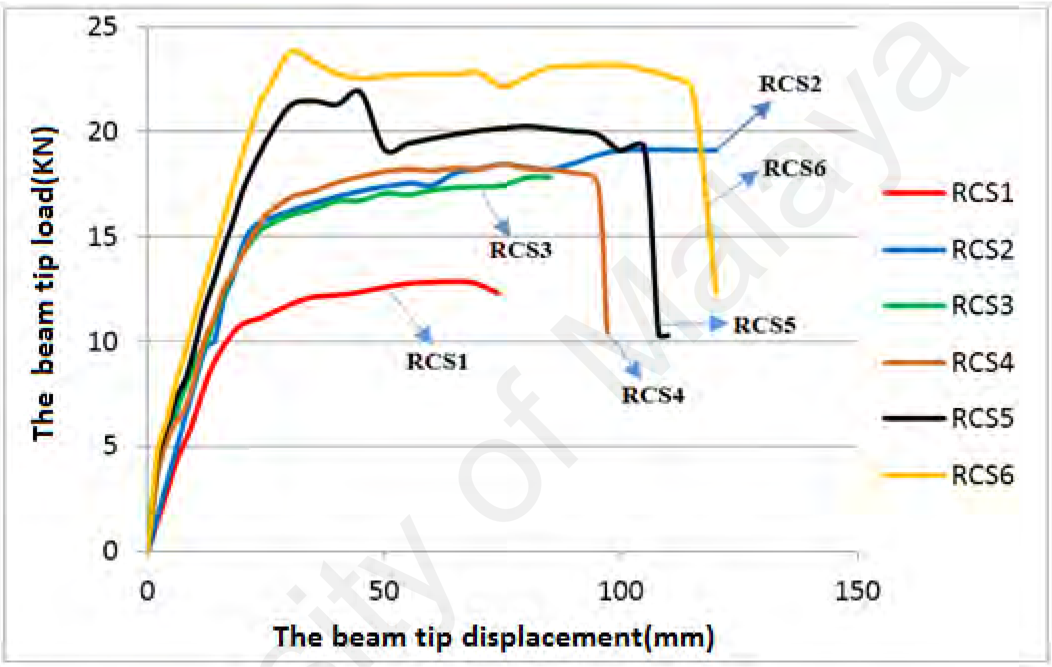

Figure 4.1: The load-displacement diagram of RCS6 sample

4.2.5 Remark and discussion

As the results in the previous sections revealed, applying CFRP reinforcement increased the beam-column connection's load capacity in all specimens. Nonetheless, the load capacity increase rate varied for each sample according to the geometry and location of the CFRP reinforcement applied. The CFRP dimensions had a different effect on the connection ductility factor. Accordingly, the presence of CFRP plates on the top and bottom of the beam in the RCS3 sample reduced the ductility factor, but the load capacity of this sample increased. The greatest effect on the increase in ductility factor was seen for sample RCS5, where two reinforcement plates were used on both sides of the beam web. Except for sample RCS3, the others exhibited an increment in the ductility factor due to the reinforcement. Table 4.2 provides a summary of the results obtained for the six samples tested experimentally. According to this table, the reinforcement plates in the beam web influenced the ductility factor increment considerably. On the other hand, sample RCS6, in which parts of the beam and column at the top and bottom of the connection point were wrapped with CFRP layers, performed well. Unfortunately, implementing CFRP reinforcement in the forms of samples RCS2 and RCS6 is not applicable in practice due to the three-dimensional structure of actual concrete frames and the presence of frames perpendicular to the frame concerned. Hence, to examine the most effective form of reinforcement, only the RCS3 and RCS5 sample models are studied in upcoming sections, whereby the CFRP reinforcement varies in length and thickness.

Table 4-2: Ductility factor and ultimate load increment of samples

Specimen	RCS1	RCS2	RCS3	RCS4	RCS5	RCS6
Ductility factor	1.91	2.57	1.73	2.19	3.9	3.69
Increase in strength (%)	0	49%	39%	42%	71%	81%

4.3 Numerical results

This section presents the finite element (FE) analysis results for specimens RCS1 to RCS6. The specimens' behavior is presented in terms of the load-displacement relationship, and the strain and stress at various locations on the specimens. The finite element results are verified against the experimental test results where possible. The results are discussed by comparing the finite element results among specimens.

4.3.1 Verification of Finite Element Results

In this part, the ability of the finite element method to present the behavior of the specimens is verified using an exterior beam-column connection tested previously by Mahini et al. (2007). The prototype structure is a typical eight-story residential RC (reinforced concrete) building located in Brisbane, Australia, as shown in Fig. 4.2. The controlling design criterion for this structure is the strength required to resist the gravity and lateral loads applied. The prototype was designed as an Ordinary Moment Resisting Frame (OMRF) according to Australian Concrete Code AS3600 with details similar to non-ductile RC frames designed in line with ACI-318. A scaled-down frame was modeled by applying similitude requirements that relate the model to the prototype using the Buckingham theorem. The scaled-down joints were extended to the column mid-high and beam mid-span corresponding to the inflection points of the bending moment diagram under lateral loading. The scaled-down frame was loaded, analyzed and designed according to AS3600.

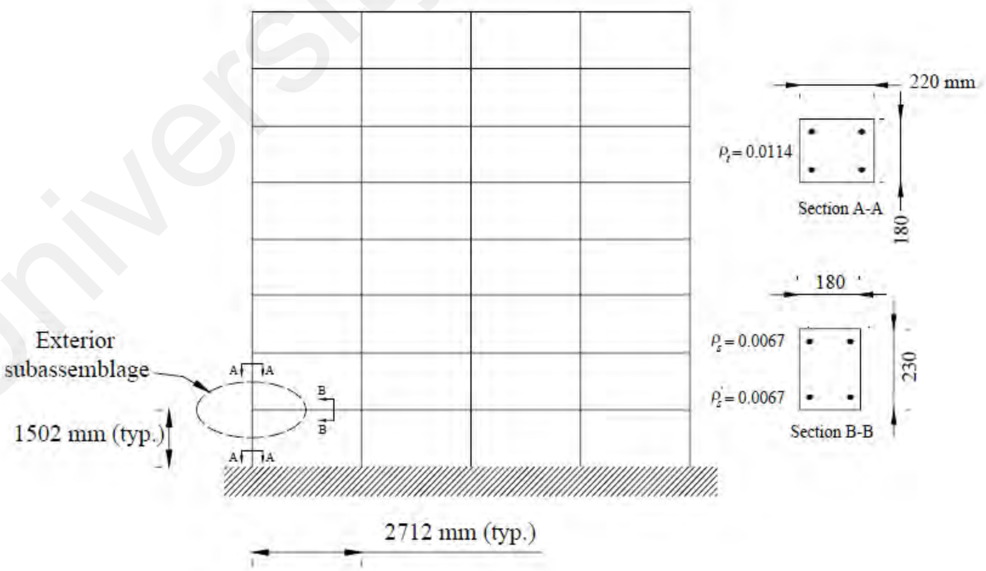

Figure 4.2: typical eight story residential RC building

Mahini et al. (2007) used a down-scale exterior reinforced concrete beam-column joints. Fig. 4.3 shows the test specimen details. The specimen consisted of a 180 mm wide x 230 mm deep beam and a 220 mm x 180 mm column. Four N12 rebars (φ12 mm) were used for both the vertical column reinforcement and the longitudinal beam reinforcement. R6.5 bars (φ 6.5 mm) were used as stirrups at a spacing of 15 mm in both the beam and column.

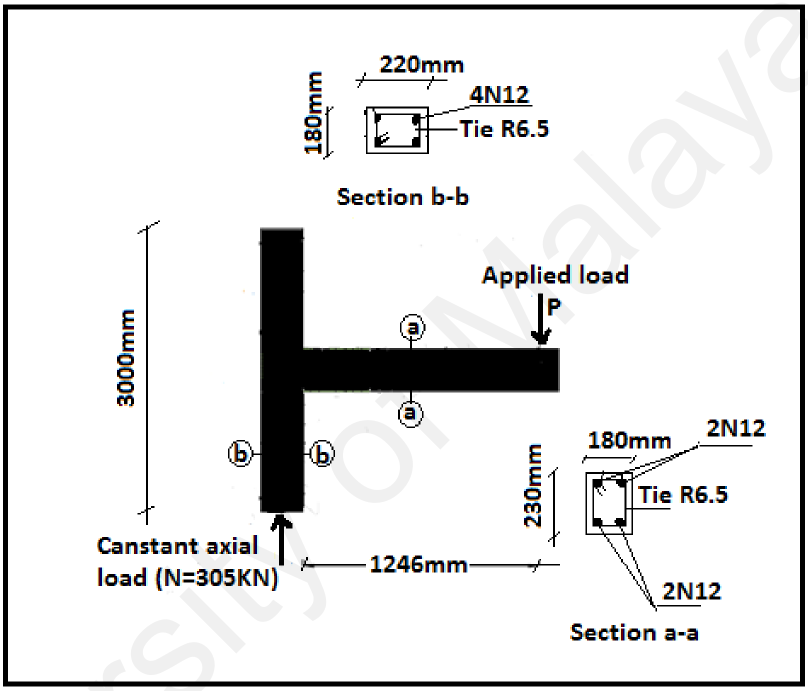

Figure 4.3: Typical test specimen details

A 30 mm concrete cover was considered for the beam and column reinforcements which is about half of the corresponding cover in prototype. Yield strength of the main steel reinforcements, N12 was around 500 MPa and the modulus of elasticity was equal to 200 GPa. The columns was reinforced with four N12 reinforcing bars, with one bar positioned at each corner of the columns. The stirrups had yield strength of 382 MPa and a modulus of elasticity of 200 GPa. Ties were also placed in the joints region in accordance with the requirements of AS3600. The concrete had a compressive strength around 40 MPa and a modulus of elasticity around 27.6 GPa. The results from the FEM analysis were then compared with the experimental results.

The load-deflection curve for the control beams-column connection is shown in figure 4.14. As shown, there is good agreement between the FEM model and experimental result. The load-deflection curve for the control beams-column connection is shown in figure4.14. As shown, there is good agreement between the FEM model and experimental result.

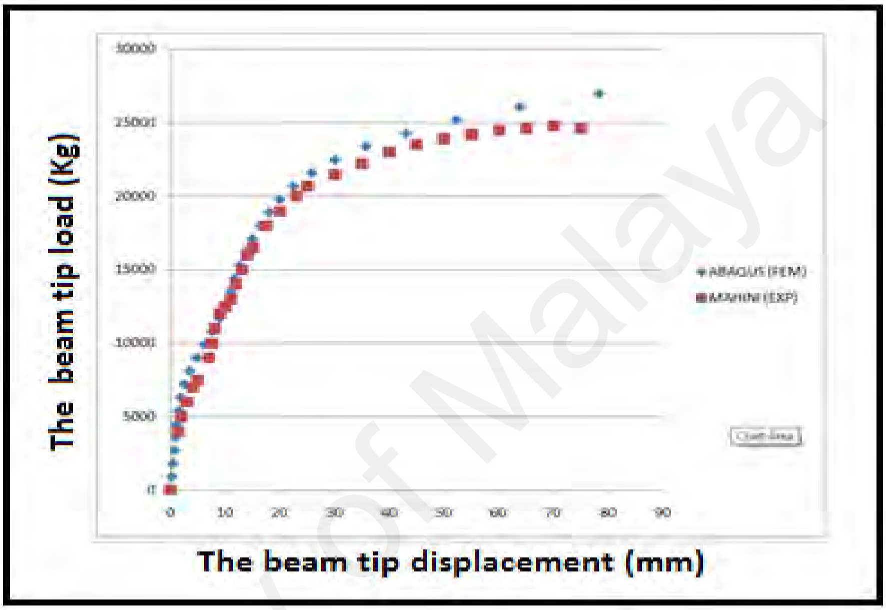

Figure 4.4: Load-displacement comparison between FEA and experimental test for the control specimen

4.3.2 Finite Element Results of Control Specimen (RCS1)

4.3.2.1 Model Description

To validate the experimental test data, the exterior RC beam-column joint was modeled and analyzed under both gravity and lateral load. The gravity load was applied in the first step of analysis, followed by lateral incremental displacement load applied tangentially at the end of the beam in the second step. The elements and material properties are defined as mentioned in sections 3.3.1 and 3.3.3. The boundary conditions at the column ends served as model input to mimic the supporting system of the actual specimen. The analysis results are presented in the following sections.

4.3.2.2 Load Displacement Curve

The load displacement curve was generated numerically for the end of the beam in the FE model analysis similar to the experimental test. The curve demonstrates that the lateral load increased linearly up to 9.3 kN, after which nonlinearity was initiated. In the nonlinear portion of the curve, the specimen reached a maximum lateral load of 13.2 kN with 65 mm lateral displacement. After reaching the peak point, strength degradation began in the specimen's joint, which continued until the end of the numerical run. This section presents a comparison between the load displacement envelope generated from the down-scale tests of the control specimen and that obtained from numerical FE model analysis using ABAQUS software. The load displacement curves (experimental versus analysis) for the control specimen are presented in Fig. 4.5. This figure signifies good agreement between the experimental data and FE model, specifically in the linear range. In the nonlinear range, the experimental load displacement curve underestimated the control joint's strength by an order of magnitude of about 3% compared to the numerical data results.

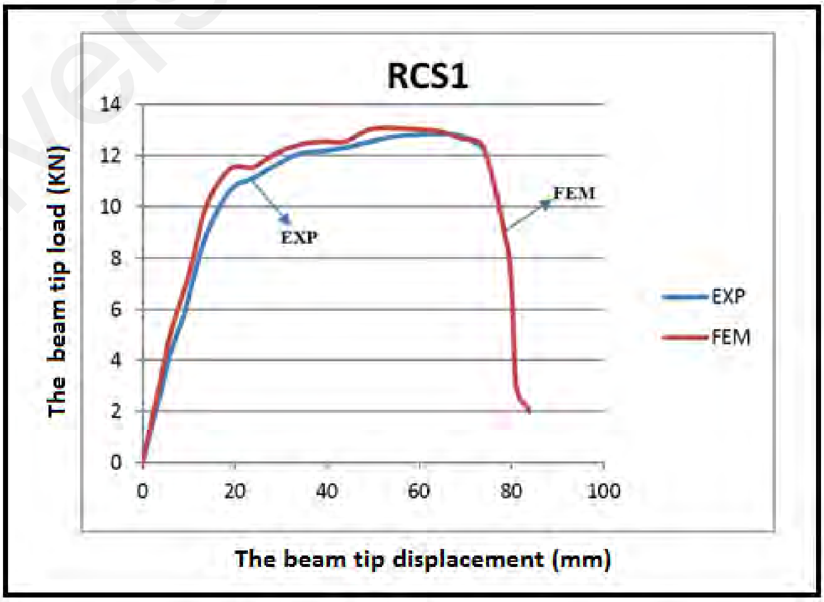

Figure 4.5: Experimental and FE Model Load Displacement Curves for the Control Specimen (RCS1)

4.3.2.3 Stresses and Strains

The stresses and strains were calculated through the step increments in the lateral loading phase. The output results were presented at the end of the lateral loading steps. First, the beam experienced flexural cracking at top of the beam close to the column. Cracks were detected simultaneously beside the beam in the zone near the column. The cracking pattern of concrete is shown in Fig. 4.6(a), which validates the numerical test result shown in Fig. 4.6(b).

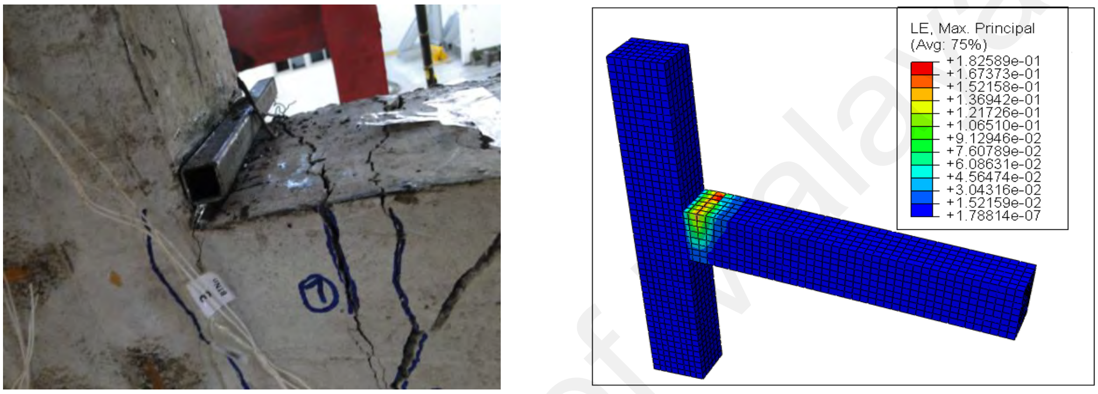

(a) Experimental specimen (RCS1) (b) Numerical specimen (RCS1)

Figure 4.6: Experimental and numerical comparison of cracking in RCS1

The stresses and strains in the rebar are shown in Fig. 4.7. The highest rebar stress and strain are located at the beam's longitudinal steel reinforcement, which is attributed to moment induced from lateral loading at the end of the beam.

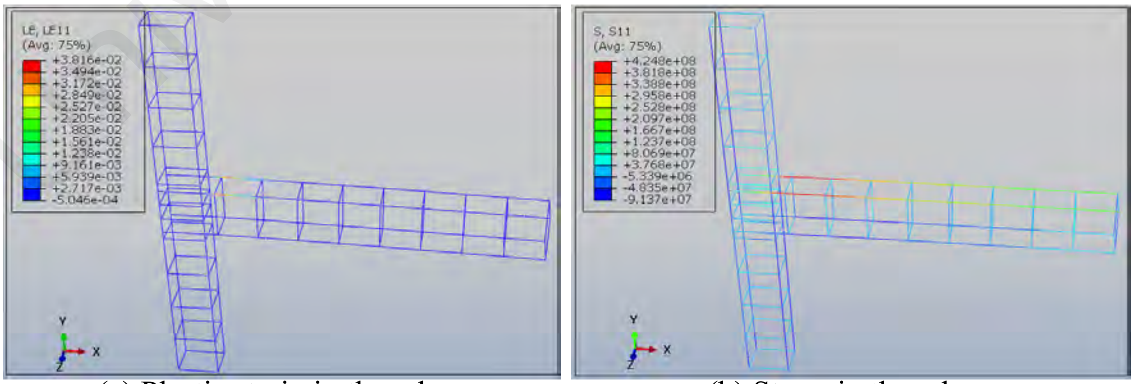

(a) Plastic strain in the rebar (b) Stress in the rebar

Figure 4.7: Rebar Stresses and strains in RCS1

4.3.2.4 State of Damage

As mentioned earlier, specimen failure was attributed to the yield of the longitudinal steel reinforcement at the end of the beam. Consequently, the beam cracked extensively along a distance shorter than its depth from the column face. At last, the concrete in the hinge area experienced compression crushing and the test was stopped as the beam capacity dropped substantially.

4.3.3 Finite Element Results of Specimen RCS2

4.3.3.1 Model Description

In retrofitted specimen RCS2, two cross-shaped CFRP plates were bonded to the beam-column joint. A full bond was assumed between the CFRP composite plate and the concrete substrate. The FE results achieved for the load displacement envelope, stress, strain and Tsai-Wu failure criterion (1971) for the CFRP composite are discussed in the next section and compared with the experimental results in the following chapter.

4.3.3.2 Load Displacement Curve

A comparison of the load displacement curves for the experimental and FE models is presented in Fig. 4.8. The numerical FE analysis results show overall good agreement with the experimental test data. The specimen reached a maximum load of 19.25 kN in the last step (designated herein as failure) during the lateral loading phase. Following this load increment, the beam’s longitudinal steel reinforcement yielded close to the column. Moreover, displacement increased and strength degradation was initiated in the joint specimen, which continued until the end of the numerical run.

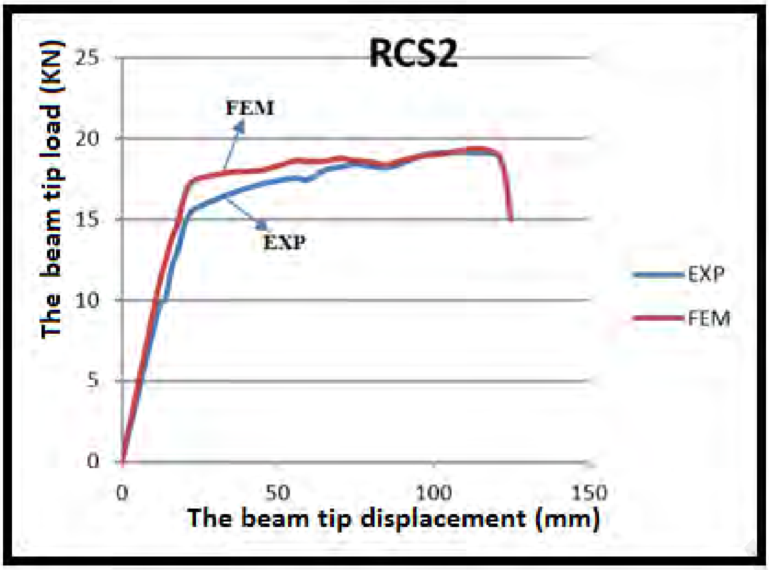

Figure 4.8: Experimental and FE Model Load Displacement Curves for Retrofitted Specimen RCS2

4.3.3.3 Stresses and Strains

As part of FE model analysis, the stresses and strains were computed for the concrete, rebars and CFRP composite laminates at each load step increment. The stress and strain contours in the concrete, reinforcement rebars and CFRP laminate are presented at the end of the analysis. As the beam's longitudinal rebars yielded, the most damaging stress concentrations were located in the zone near the column due to tensile and compressive damage to the concrete. A plastic hinge developed close to the joint. The maximum rebar stress was located in the top longitudinal beam rebar close to the column. These simulation results are in good agreement with the experimental data results from the test. The principal strains in the rebar and CFRP laminate are presented in Fig 4.9.

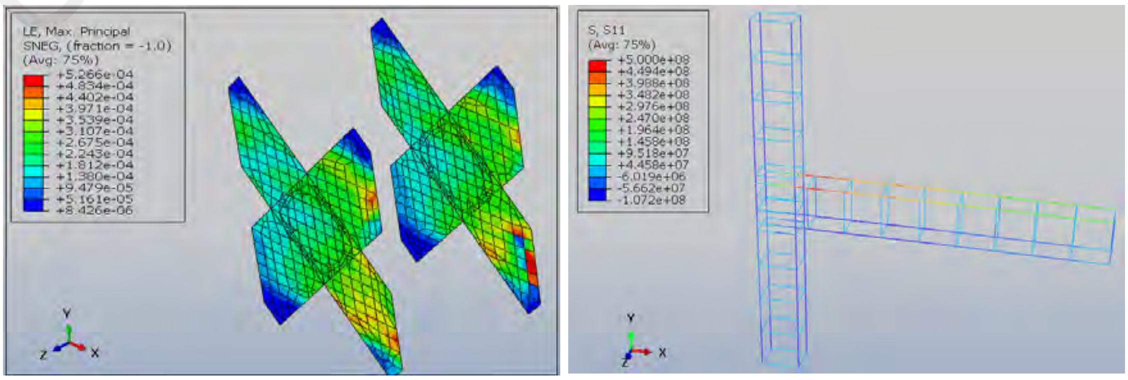

Figure 4.9: Principal strain in RCS2 parts

4.3.3.4 State of Damage

1. In the concrete part, cracks occurred when the tensile stress exceeded the tensile strength in concrete. As loading proceeded, damage progressed in the beam segment adjacent to the column and intensified due to the combination of high shear and normal stresses in this section, as shown in Fig. 4.10. Strength degradation continued and the test was stopped at a load of about 19.1 kN.

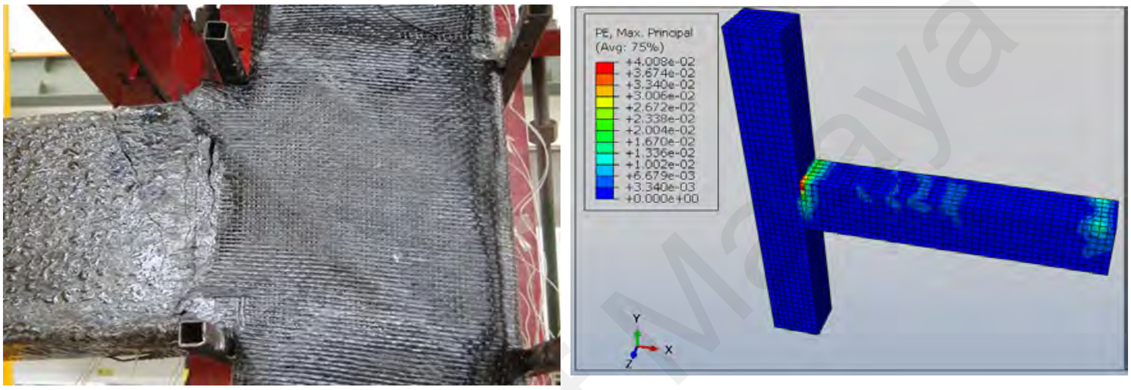

Figure 4.10: Concrete damage in RCS2

As mentioned earlier, most damage stress concentrated in the zone close to the column due to tensile and compressive damage to the concrete after the beam's longitudinal rebar yielded in this area. Throughout the test, the strain recorded for the CFRP members indicated that the behavior of these members remained elastic and did not fail.

The Tsai-Wu failure criterion (1971) was also applied to check the CFRP composite laminate. CFRP laminate rupture signaled the end of strength analysis.

4.3.4 Finite Element Results of Specimen RCS3

4.3.4.1 Model Description

Two CFRP plates were added to the top and bottom of the beam in the RCS3 specimen. Moreover both sides of the column as well as the back of the beam were wrapped with CFRP. A full bond was assumed between the CFRP composite laminate and the concrete substrate. The FE model analysis results are discussed in the following sections.

4.3.4.2 Load Displacement Curve

As for other joint models described earlier, the load displacement of this specimen was calculated with the FE model at the same location as the measurement in the experimental test. The specimen was subjected to incremental displacement load until failure. A comparison between the load displacement curves for the experimental and FE models is presented in Fig. 4.11. The FE analysis results show good overall agreement with the experimental test data. As seen in the figure, the linear portion of the curve ends at 10.3 kN. The load kept increasing nonlinearly until the solution diverged at an ultimate load of 18.1 kN.

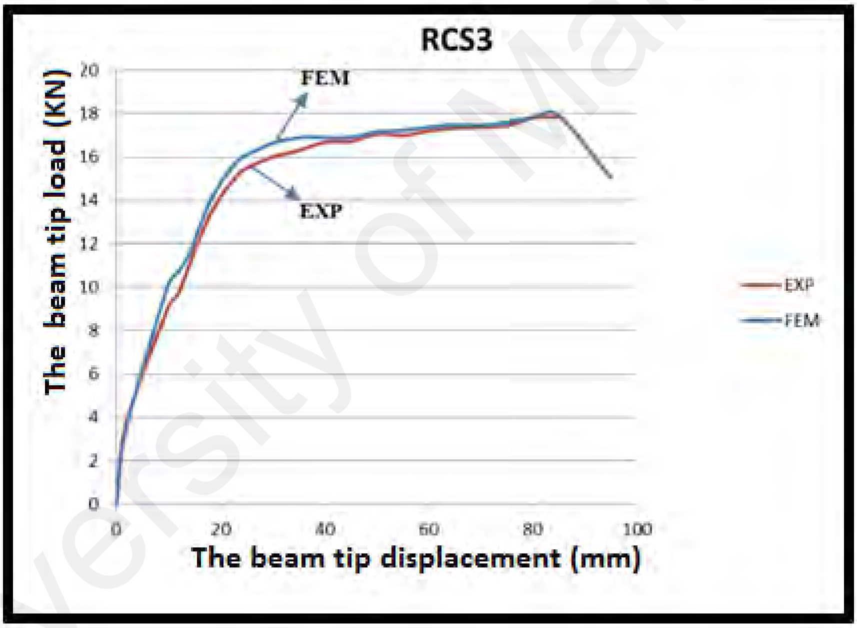

Figure 4.11: Experimental and FEM Load Displacement curves for RCS3

4.3.4.3 Stresses and Strains

The concrete principal stress contour for numerical specimen RCS3 is compared with the experimental contour after failure in Fig. 4.12. According to this figure, the damage concentrated at the beam web, which may be attributed to the excessive shear stress. However, most of the high strain concentration appeared to populate both sides of the beam due to shear stress. The principle stresses and strains in the joint's reinforcing composite laminates are presented in Fig. 4.13. In order to evaluate the failure in the laminate, the Tsai-Wu failure criterion (1971) was adopted for retrofitted specimen RCS3.

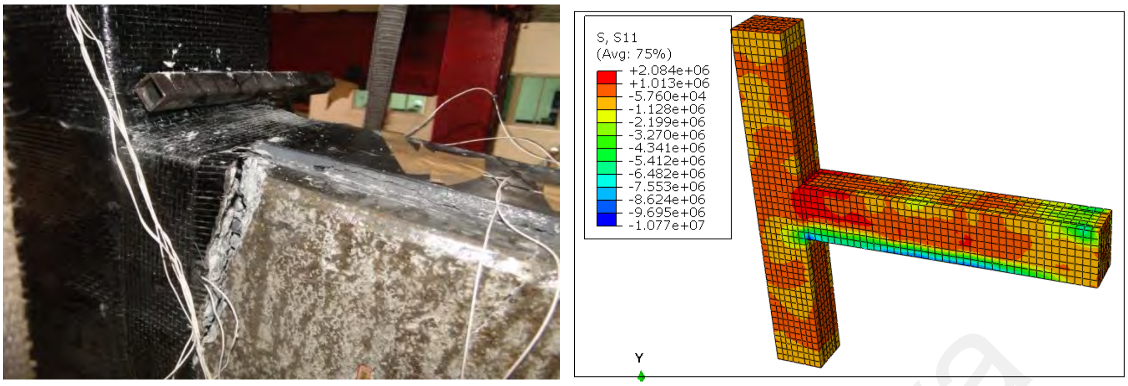

Figure 4.12: Comparison of experimental concrete cracking with the concrete principal stress contour of numerical specimen RCS3

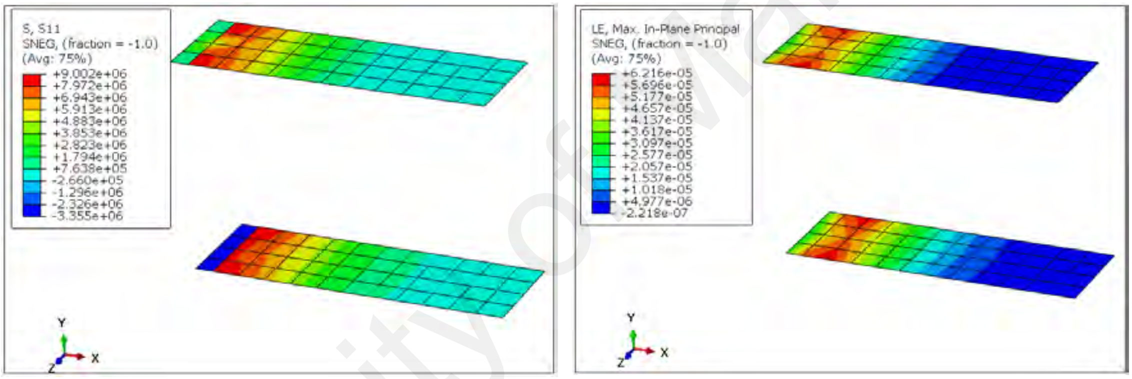

(a) Stress **(b) Strain**

Figure 4.13: CFRP plate principal stresses and strains in RCS3

4.3.4.4 State of Damage

Again, specimen failure was attributed to shear strength degradation in the beam's web region. The beam was damaged extensively along a distance equal to its depth from the column face. The stress in the beam's transverse steel was reached to steel yield strength and the cracks grew deeper. Next, wide cracks developed where the CFRP plate was connected to the beam, rubble started falling, and the beam lost most of its concrete. Hence, CFRP plate debonding happened, stress in the longitudinal rebar suddenly increased and the rebar yielded. The analysis was terminated as the beam capacity dropped substantially. Finally, the maximum beam load recorded was 18.1 kN for specimen RCS3.

4.3.5 Finite Element Results for Specimen RCS4

4.3.5.1 Model Description

Specimen RCS4 was reinforced at the top and bottom corners of the connection with the L-shaped CFRP layer and both sides of the column as well as the back of the beam were wrapped with CFRP. A full bond was assumed between the CFRP composite laminate and the concrete substrate. The FE model analysis results are discussed in the following sections.

4.3.5.2 . Load-Displacement Curve

The load displacement for specimen RCS4 was calculated in the FE model at the same location as in the experimental test. The specimen was subjected to incremental displacement load until ultimate load. As the FE model load displacement curve indicates, the linear portion of the curve ended at 11.85 kN. The load kept increasing nonlinearly until the solution diverged at an ultimate load of 18.7 kN. The load displacement curves (experimental versus FE analysis) for specimen RCS4 are presented in Fig. 4.14. This figure exhibits an excellent correlation between the numerically simulated and laboratory specimens.

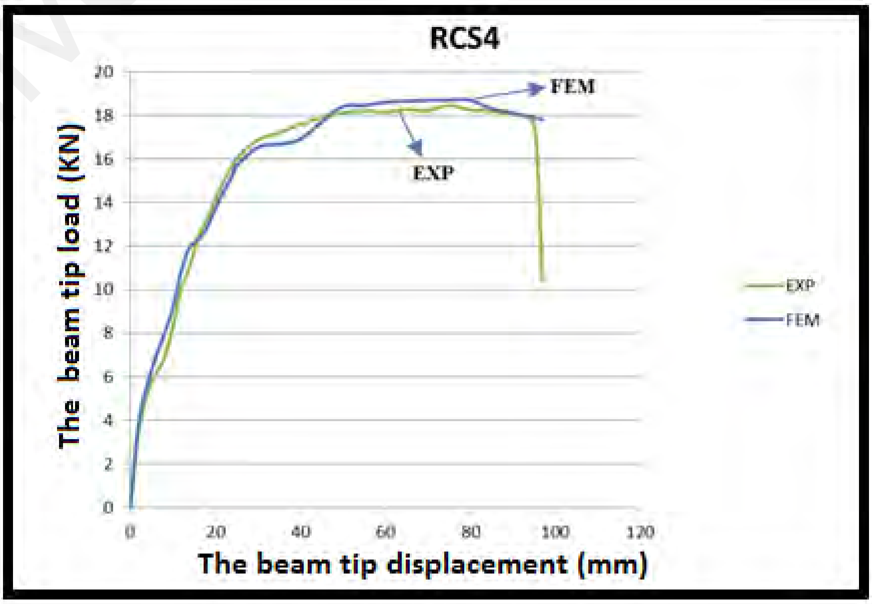

Figure 4.14: Experimental and FE Load Displacement curves for RCS4

4.3.5.3 Stresses and Strains

An advantage of the FE model is that a part of the specimen can be removed to see the other parts clearly. Hence, by removing the CFRP layers, the principal plastic strain at the concrete surface is visible as per Fig. 4.15. Figure 4.16 shows the strains in the beam-column joint specimen's rebar. Here, the beam's top rebars yielded at a suitable distance from the joint region.

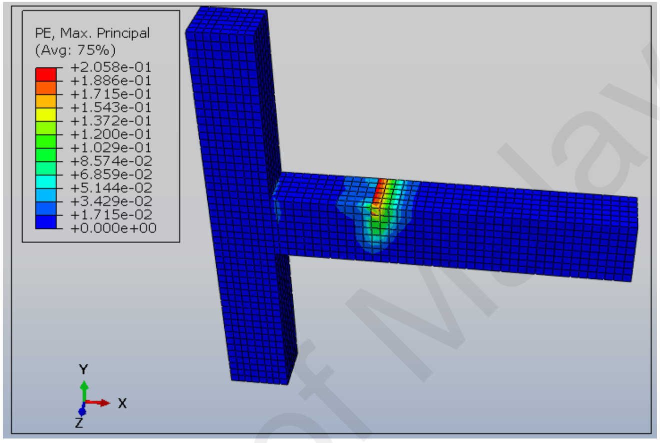

Figure 4.15: Principal plastic strain in concrete for RCS4

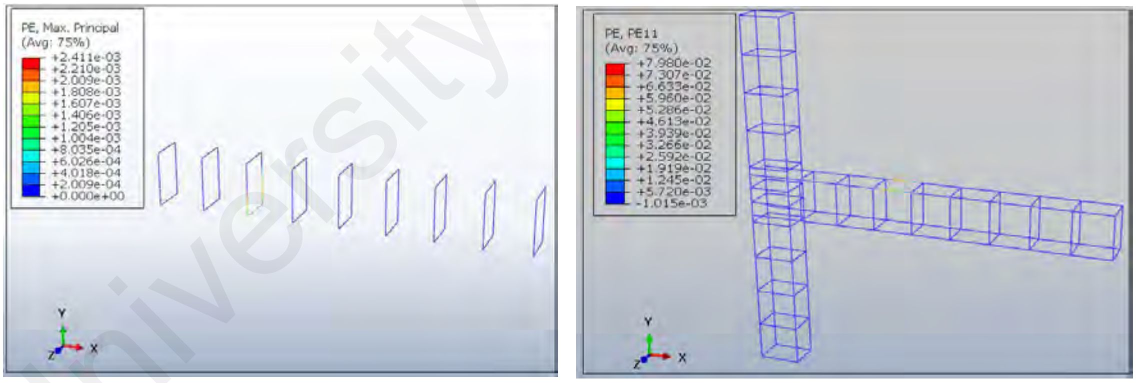

(a) Transverse rebars (b) Longitudinal rebars Figure

Figure 4.16: Steel rebar plastic strain for RCS4 (plastic hinge formation)

4.3.5.4 State of Damage

As illustrated in Fig. 4.15, the concrete was damaged at the top of the beam. Thereafter, as per Fig. 4.16(a), the transverse rebars yielded, after which the longitudinal rebars yielded at a suitable distance from the column (Fig. 4.16(b)). As the longitudinal rebars yielded, displacement increased and analysis was stopped.

4.3.6 .Finite Element Results for Specimen RCS5

4.3.6.1 Model Description

Two reinforcing CFRP plates were used on both sides of the beam web in RCS5. Moreover, the same as for the other retrofitted specimens, both sides of the column as well as the back of the beam were wrapped with CFRP. A full bond was assumed between the CFRP composite laminate and the concrete substrate. The FE model analysis results are discussed in the following sections.

4.3.6.2 Load Displacement Curve

The load displacement curve for the end of the beam was generated numerically in the FE model analysis, similar to the experimental test. The load displacement curves (experimental versus FE analysis) for specimen RCS5 are presented in Fig. 4.17. Overall, the FE analysis results are in good agreement with the experimental data. The numerical curve shows that the lateral load increased linearly until 10.8 kN, after which nonlinearity was initiated. In the nonlinear portion of the curve, the specimen reached a maximum 21.4kN lateral load displacement. Subsequent to the peak point, strength degradation was initiated in the joint specimen, which continued until the end of the numerical run.

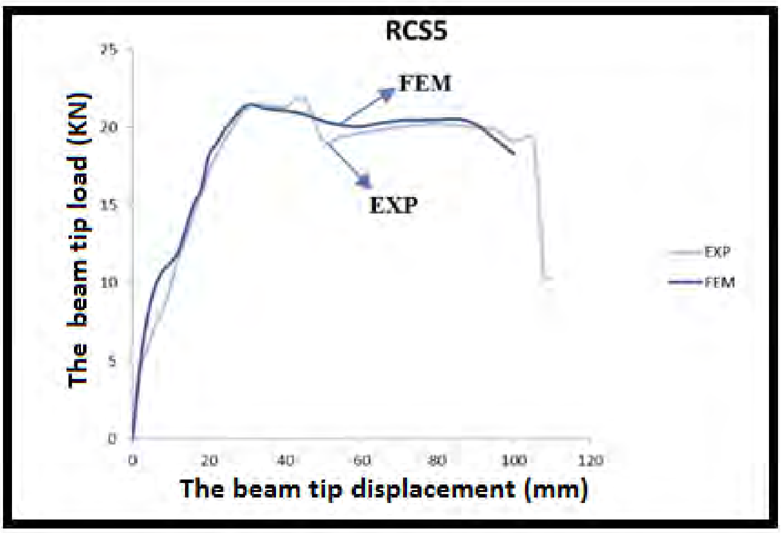

Figure 4.17: Experimental and FE load displacement curves for specimen RCS5

4.3.6.3 Stresses and Strains

The presence of CFRP plates in the beam web controlled the shear stress, and damage was concentrated at the top of the beam due to tensile stress (Fig. 4.18). The stresses in the longitudinal rebars are presented in Figure 4.19.

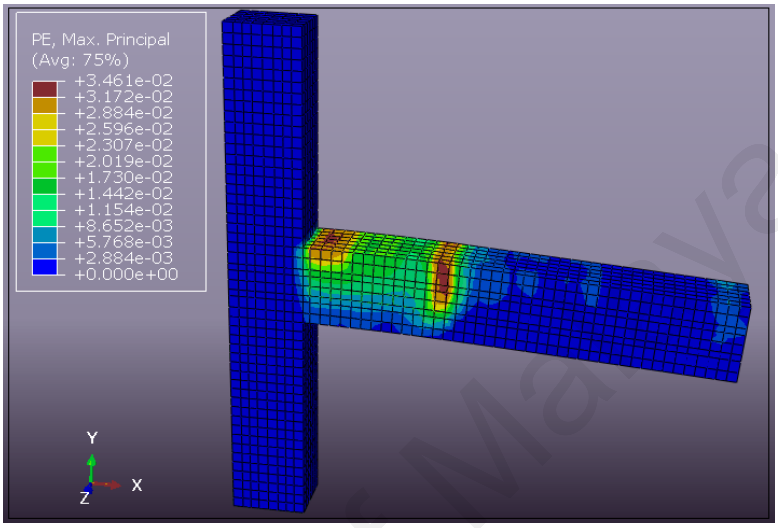

Figure 4.18: Concrete plastic strains in specimen RCS5

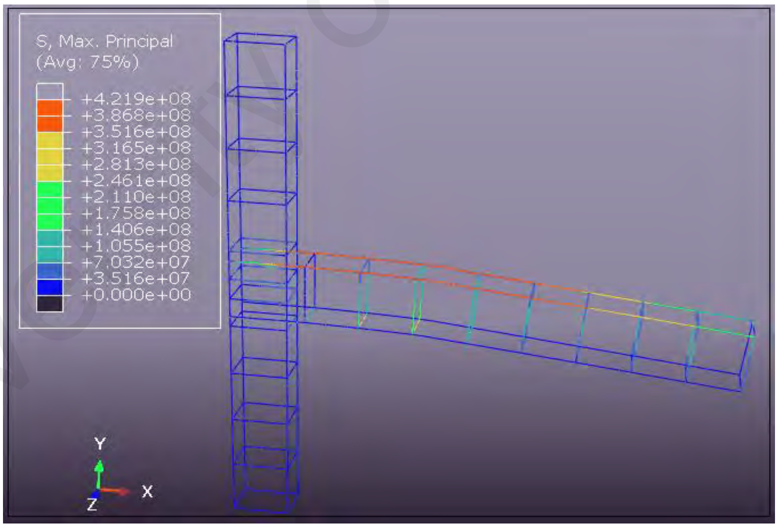

Figure 4.19 : Steel rebar stresses in specimen RCS

In order to evaluate the failure in the laminate, the Tsai-Wu failure criterion (1971) was adopted for retrofitted specimen RCS5. The principal stresses and strains are presented in Fig. 4.20(a, b)

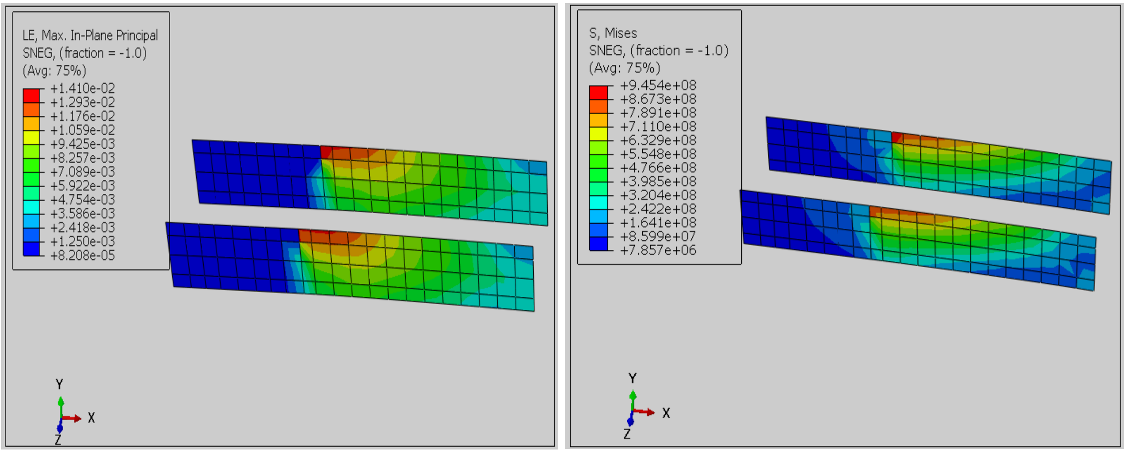

(a)Strains (b) stresses

Figure 4.20: CFRP principal stresses and strains in specimen RCS5

4.3.6.4 State of Damage

With increasing load, bending cracks formed paralleled to the beam and the concrete was damaged extensively. Then the beam's longitudinal rebars yielded, the displacement increased sharply and finally, the sample ruptured. As mentioned in the experimental section, the plastic hinge did not form far enough from the column; therefore, choosing suitably long CFRP plates and optimizing the CFRP thickness would facilitate predicting a more suitable point on the beam for plastic hinge formation.

4.3.7 Finite Element Results of Control Specimen RCS6

4.3.7.1 Model Description

In sample RCS6, in addition to the some parts of the column in the vicinity of the connection, the end of the beam 35cm from the column was wrapped with layers of CFRP. Contrary to the experiment where the surface of the concrete was not visible, by removing the CFRP layers from the numerical sample the concrete surface became visible. A full bond was assumed between the CFRP composite laminate and the concrete substrate. The FE model analysis results are discussed in the following sections.

4.3.7.2 Load Displacement Curve

The specimen was subjected to incremental displacement load until the specimen failed. The FE model and experimental load displacement curves for specimen RCS6 are presented in Fig. 4.21. The load increased nonlinearly until the longitudinal rebars yielded and the displacement increased sharply, after which the solution diverged. An ultimate load of 23.8 kN was recorded and the analysis was stopped. The ultimate load for the FE model is 3% greater in peak load than experimental load.

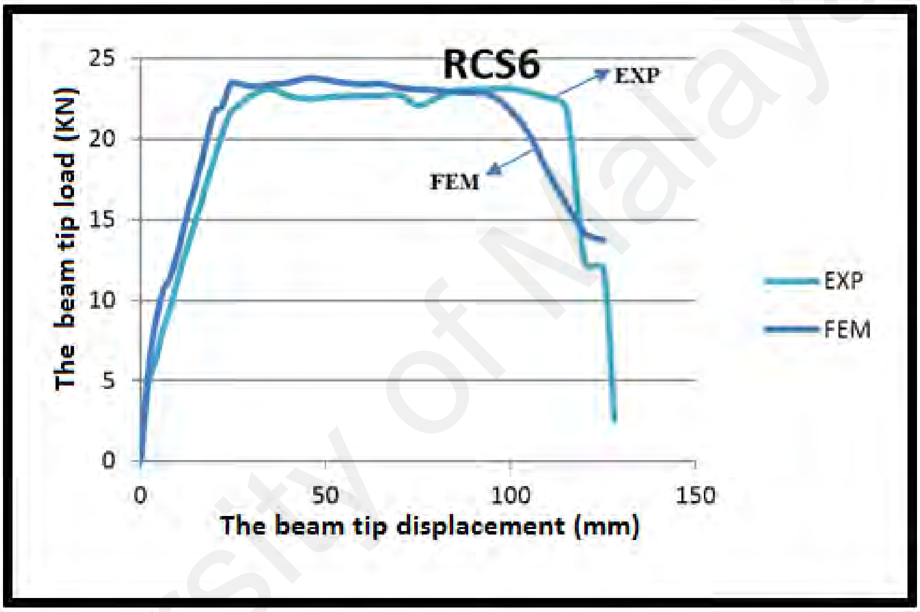

Figure 4.21: Experimental and FE load displacement curves for specimen RCS6

4.3.7.3 Stresses and Strains

The concrete principal strain contours for specimen RCS6 is shown in Fig. 4.22. According to this figure, the highest amount of tensile stress was concentrated at the top of the beam due to bending. The presence of vertical CFRP layers at the beam web controlled the shear stress. Fig. 4.23 shows the stresses and strains in the specimen's longitudinal rebars. In order to evaluate the failure in the laminate, the Tsai-Wu failure criterion (1971) was adopted for retrofitted specimen RCS6. The principal stresses and strain are presented in Fig. 4.24.

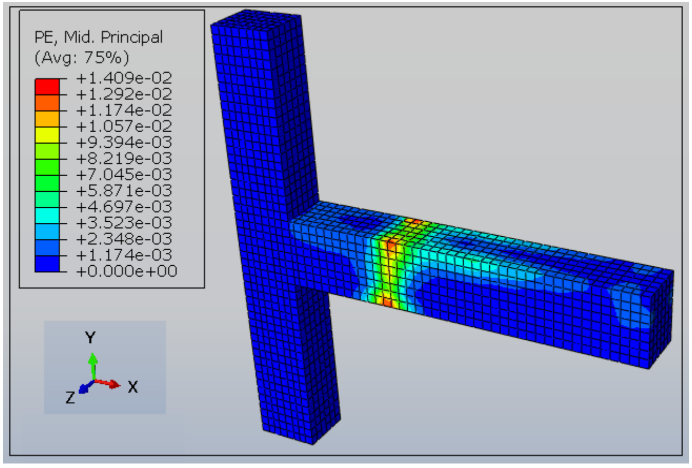

Figure 4.22 : Principal plastic strains of concrete in specimen RCS6

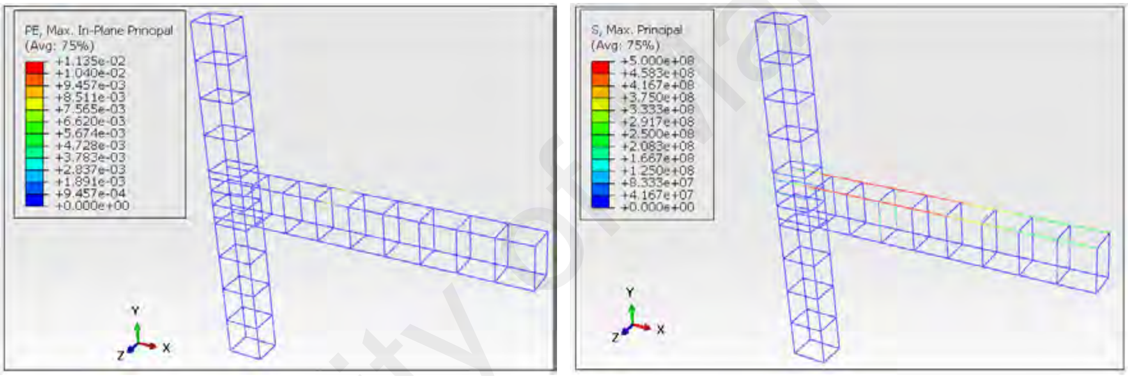

Figure 4.23: Principal plastic strains and stresses in the steel rebars of specimen RCS6

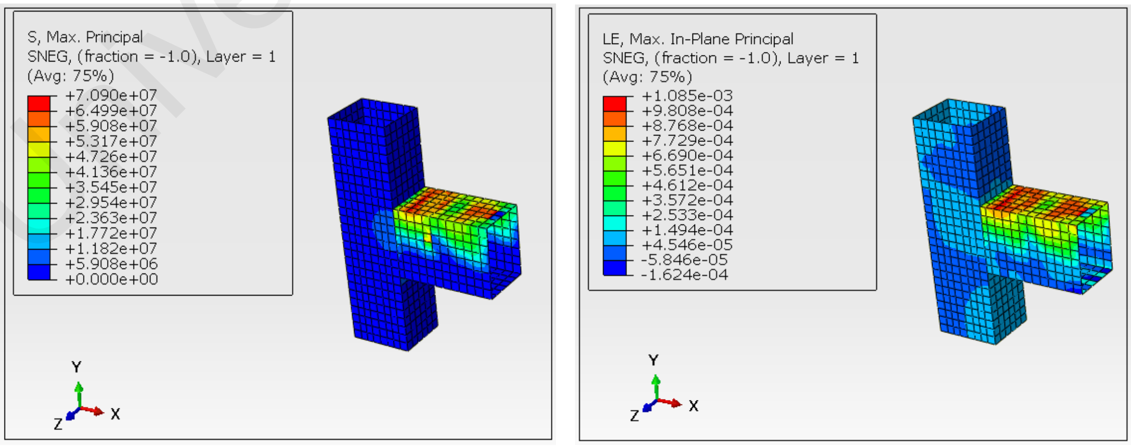

Figure 4.24: CFRP principal stresses and strains of RCS6

4.3.7.4 State of Damage

As mentioned earlier, the CFRP layers helped to withstand the longitudinal rebars' load. With increasing load, the longitudinal rebars yielded at a suitable distance from the column. The beam rebar yield was accompanied by large displacement and the analysis stopped. In specimen RCS6, the plastic hinge formed sufficiently far from the column, as shown in Fig. 4.23(a).

4.4 Comparison of experimental and numerical results and discussion

According to previous sections, the numerical analysis (Finite Element Method: FEM) results complied with the experimental results acceptably. Table 4.3 presents a summary of the maximum capacity of the samples according to the experimental as well as numerical analysis (FEM) results. These results are compared.

Table 4-3: Summary of maximum load of samples according to Finite Element and Experimental results

Specimen	Maximum load Experimental (kN)	Maximum load -- Numerical (kN)	Difference Percentage
RCS1	12.8	13.2	-3% *
RCS2	19.1	19.25	-1% *
RCS3	17.81	18.1	-2% *
RCS4	18.15	18.7	-3% *
RCS5	21.86	21.2	+3% **
RCS6	23.15	23.8	+3% **

* Negative difference means numerical amount is more than experimental amount

** Positive difference means numerical amount is less than experimental amount

These differences are small and acceptable. The reasons for the differences are summarized as follows:

1- Difference between the actual supporting system behavior in the experimental test and the model's boundary conditions.

2- Full bond assumption of the rebar embedded inside the concrete; however, the rebar slipped in the actual specimen due to rebar elongation.

3- Full bond assumption between the CFRP composite laminate and the concrete surface for FE model simplicity.

The concrete damage plasticity (CDP) model was used in ABAQUS software to model the concrete. As such, the actual performance of concrete was modeled. Concrete sections where the stress level reached the maximum strength of the concrete were considered damaged concrete. This applies to both tension stresses and compression stresses (George et al., 2017). Therefore, the application displayed the concrete damage sites clearly. An advantage of ABAQUS software over the experimental method is based on the fact that it provides sufficient time to check all the parts, as the crack development and expansion trends of concrete exist in all directions. In addition, the software features allows easy inspection of some parts of the samples where the concrete was placed below the CFRP reinforcement layers and was not visible in the laboratory. Hence, the CFRP layers can be removed in the visualization module and the concrete section below these layers can be observed.

Examining the cracking and concrete failure stages derived from numerical analysis shows that the process was consistent with what occurred in the experimental specimens. However, the rebars were not visible with the experimental method. To evaluate their performance, the relevant strain amount can be determined only at a few limited points by installing strain gauges. Accordingly, the approximate location and time of rebar yield may be determined. By using the software and removing the concrete and CFRP sections in the visualization module, the rebars can be checked easily with precision and sufficient time. Thus, the stress and strain in the rebars are visible at each point and any moment of the loading process. Therefore, it is possible to determine the time and location of plastic hinge formation effortlessly. In the next sections, some of the reinforced beam-column connections with varying CFRP plate lengths and thicknesses will be analyzed.

Obviously, testing this number of samples experimentally would be very time-consuming and costly. Nonetheless, the result analysis would not be as straightforward as a numerical analysis with the software. In fact, this is the most important advantage of using good numerical software. Although the assumptions of perfect concrete and rebar bonding as well as full CFRP layer-to-concrete adhesion caused a slight difference in the results from the actual amount, almost negligible (about 1% to 3%), and did not affect the problem results in general, it can be ignored. Moreover, the beginnings and ends of the CFRP plates in the experimental samples were wrapped with strips of CFRP fabric to prevent CFRP debonding from concrete. Hence, the full bonded CFRP assumption is closer to reality.

4.5 The effect of CFRP plate length and thickness on plastic hinge relocation

4.5.1 Introduction

As stated earlier, ABAQUS software with its unique features is one of the most powerful applications for fine reinforced concrete element modeling. Owing to the software's ability to model rebars inside concrete such that their behavior matches reality to a great extent, it is feasible to monitor the rebars' behavior details.

One of the main goals of this research was to determine the appropriate length and thickness of carbon fiber-reinforced plastic (CFRP) reinforcement panel plates in order to improve the beam-column concrete connections. This should ultimately have the greatest impact on the plastic hinge transfer from within the connection toward the concrete beam.

This section evaluates the effect of changes in CFRP plate length and thickness on the plastic hinge transfer in two types of enhanced connections, including:

i) CFRP reinforcement on both sides of the beam web (RCS5), and

ii) CFRP reinforcement at the top and bottom of the beam (RCS3)

Therefore, for both reinforced RCS3 and RCS5 connections, some samples were modeled and analyzed for different lengths and thicknesses.

In each analysis, the strain results were evaluated in the concrete beam's longitudinal rebars. By evaluating the strain in the beam's longitudinal rebars, the location of plastic hinge formation was determined. The best design includes a plastic hinge formed at an appropriate distance from the column..

4.5.2 Analysis of joints reinforced with CFRP plates on the beam web

In this section, sample RCS5 with CFRP reinforcement panels of different lengths and thicknesses is evaluated. The width of all plates was fixed at 10 cm. Plates with thicknesses of 1, 1.2, 1.4, 1.6 and 1.8 mm were modeled. For each thickness, lengths of 30, 40, 50, 60, 70, and 80 cm were considered. Moreover, for plates with thicknesses of 2, 2.2 and 2.4 mm, lengths of 70 and 80 cm were modeled.

4.5.2.1 Sample RCS5 reinforced with 1 mm thick plates bonded on the beam web

First, six samples 10cm wide and 1 mm thick, all with two reinforcement CFRP plates on both sides of the beam web were modeled. Different lengths of 30, 40, 50, 60, 70 and 80 cm were considered, and the samples were denoted as RCS5L30T10, RCS5L40T10, RCS5L50T10, RCS5L60T10, RCS5L70T10 and RCS5L80T10, respectively. The specifications of all samples are summarized in Table 4.4.

Table 4-4: specification of web bonded sample with 1 mm thickness plates

Sample	Length (cm)	Width (cm)	Thickness (mm)
RCS5L30T10	30	10	1
RCS5L40T10	40	10	1
RCS5L50T10	50	10	1
RCS5L60T10	60	10	1
RCS5L70T10	70	10	1
RCS5L80T10	80	10	1

Modeling was done similar to previous sections and all dimensions and sizes were considered fixed except for the reinforcement plate lengths. The boundary conditions and loading were also as mentioned in previous chapters. The strain graphs of the top longitudinal beam rebars for these six samples are shown in Fig. 4.25(a-f).

As seen in Fig. 4.25(a), for the sample with a plate 1 mm thick, using a length of 30 cm caused maximum strain for both longitudinal rebars (R1, R2) to occur at the end of the CFRP layer. However, given the fact that the 30 cm length started from the back of the column, the end of the CFRP plate was only 8 cm from the beam-column connection point, which is not a reliable distance.

According to Fig. 4.25(b), the 1 mm thick and 40cm long plate had a more suitable condition than other lengths. This caused maximum strain of the two longitudinal reinforcements (R1, R2) to occur at the end of the CFRP layer, indicating that plastic hinge relocation was somewhat successful.

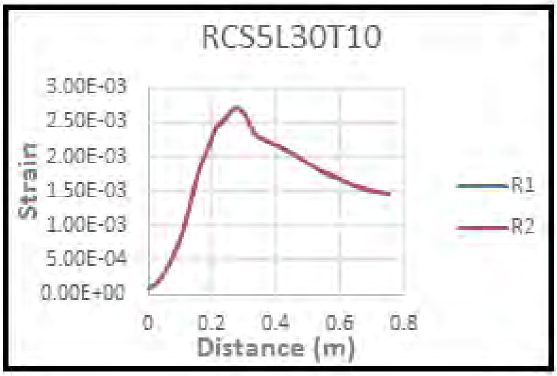

(a) Plate length: 30 cm

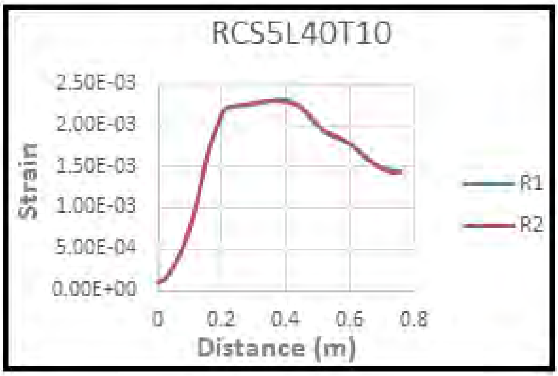

(b) Plate length: 40 cm

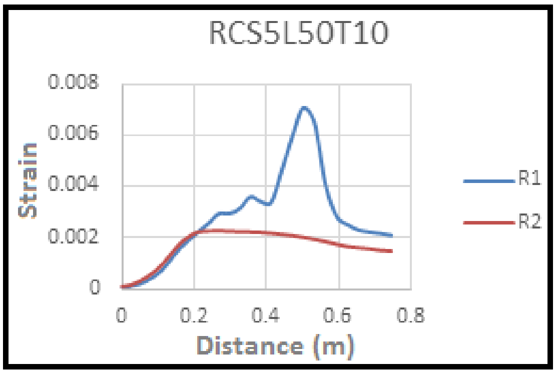

(c) Plate length: 50 cm

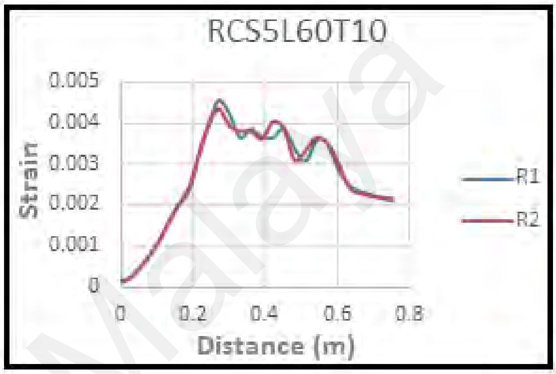

(d) Plate length: 60 cm

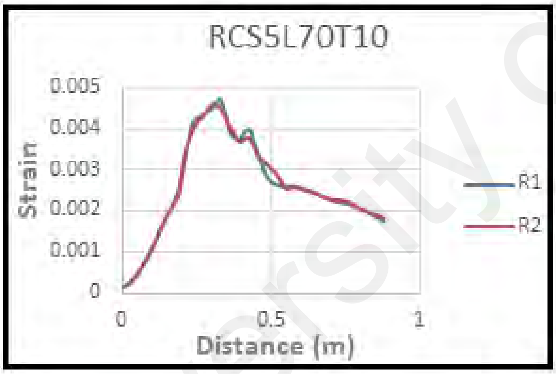

(e) Plate length: 70 cm

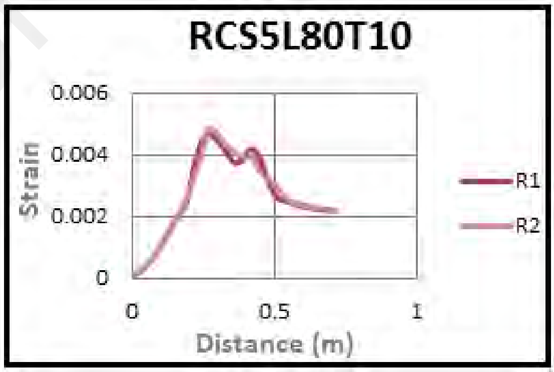

(f) Plate length: 80 cm

Figure 4.25: Steel strain distribution diagram for reinforced specimen with web bonded plates 1 mm in thickness (R1&R2 are upper longitudinal rebars)

However, as shown in Fig. 4.25(c), the increase in CFRP plate length up to 50 cm not only did not help improve the plastic hinge movement. On the contrary, it led to maximum strain only at the longitudinal rebar R1 at the end of the CFRP and at the longitudinal rebar R2 on the column. This also suggests the reduced successful percentage of plastic hinge transfer in these conditions.

It is worth noting that successful plastic hinge transfer implies the occurrence of maximum strain on all longitudinal rebars at the end of the CFRP plate, while it is at least 20% more than their strain close to the column.

Figure 4.25(d) also indicates that for a CFRP plate of the same thickness and 60cm long, the difference between the strain at the end of the CFRP and beside the column decreased. This decrease continued until the 1 mm thick CFRP length increased to 70 and 80 cm (Fig. 4.25(e, f)), when the maximum strain of all tensile longitudinal rebars occurred at the column. Apparently, the plastic hinge relocation was completely unsuccessful at these lengths.

4.5.2.2 Sample RCS5 reinforced with 1.2 mm thick plates bonded on the beam web

Sample RCS5 was modeled once again. This time, the thickness of the web reinforcement plate was increased to 1.2 mm. The sample was analyzed for CFRP reinforcement plates with lengths of 30, 40, 50, 60, 70 and 80 cm. Details of the modeled samples are given in Table 4.5.

Table 4-5: Specifications of samples with 1.2 mm thick web bonded plates

Sample	Length (cm)	Width (cm)	Thickness (mm)
RCS5L30T12	30	10	1.2
RCS5L40T12	40	10	1.2
RCS5L50T12	50	10	1.2
RCS5L60T12	60	10	1.2
RCS5L70T12	70	10	1.2
RCS5L80T12	80	10	1.2

At the end of each analysis, a strain distribution diagram was drawn for the upper longitudinal rebars depending on the distance between points and the column. Fig. 4.26 Illustrates these graphs for the six models. As seen in Fig. 4.26(a), the sample with a 30cm long and 1.2 mm thick plate was effective on plastic hinge transfer. However, due to the insufficient length of the CFRP reinforcement, the joint was not spaced away from the connection enough. Fig. 4.26(b) indicates that the length of 40 cm was relatively effective on plastic joint transfer and both R1 and R2 longitudinal rebars yielded at the end of the CFRP plate. However, sample RCS5L50T12 did not successfully relocate the plastic joint, and only one of the rebars yielded at a distance from the column equal to the plate length while the R1 rebar yielded near the column as shown in Fig. 4.26(c).

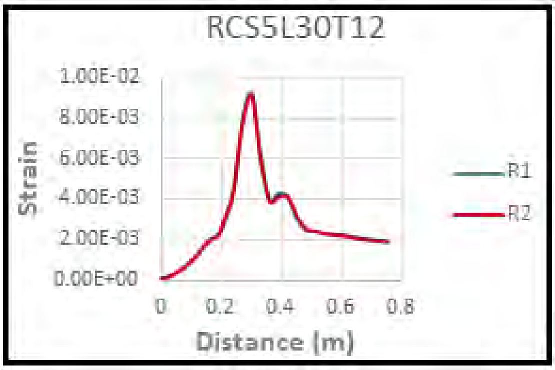

(a) Plate length: 30 cm

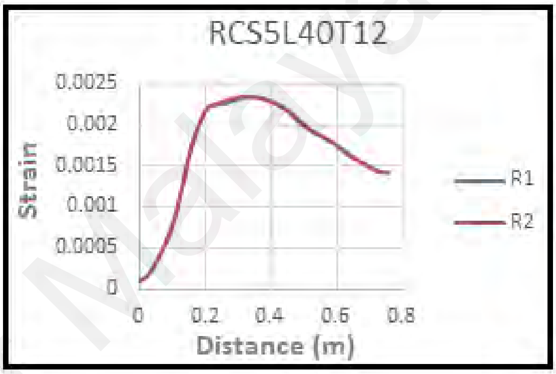

(b) Plate length: 40 cm

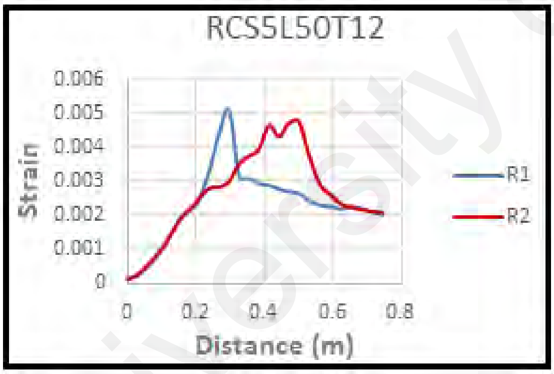

(c) Plate length: 50 cm

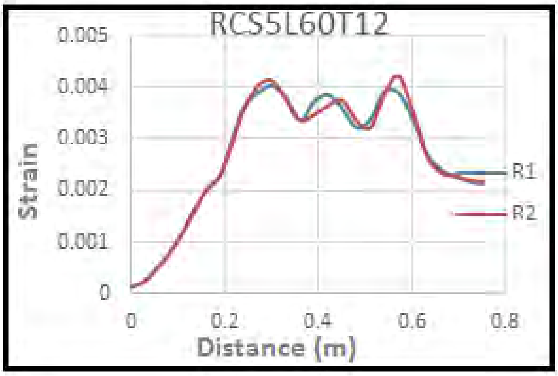

(d) Plate length: 60 cm

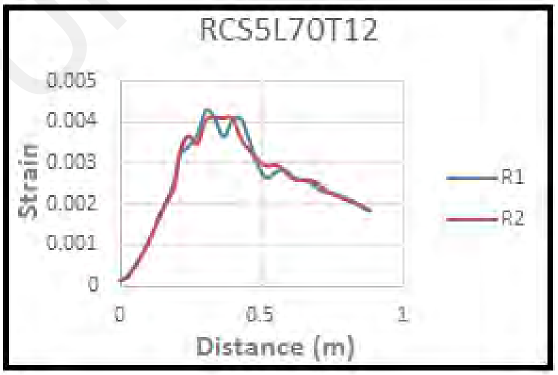

(e) Plate length: 70 cm

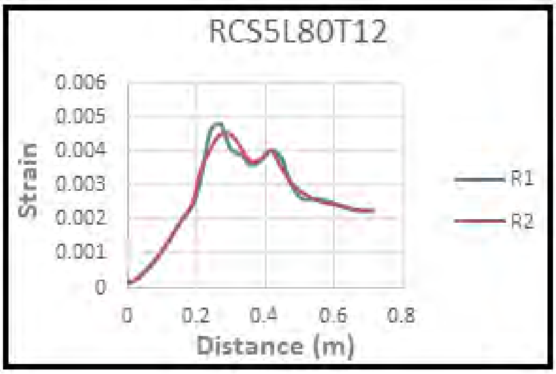

(f) Plate length: 80 cm

Figure 4.26: Steel strain distribution diagram for reinforced specimen with web bonded plates 1.2 mm in thickness (R1&R2 are upper longitudinal rebars)

Figures 4.26(d-f) show that a plastic hinge formed in samples RCS5L60T12, RCS5L70T12 and RCS5L80T12 near the column. Therefore, the lengths and thicknesses of the reinforcement plates were not suitable for these three samples.

4.5.2.3 Sample RCS5 reinforced with 1.4 mm thick plates bonded on the beam web

The same samples from the previous sections with 1.4 mm thick web CFRP reinforcement plates are analyzed. Details of these samples are given in Table 4.6, while the strain distribution results are shown in Fig. 4.27.

Sample	Length (cm)	Width (cm)	Thickness (mm)
RCS5L30T14	30	10	1.4
RCS5L40T14	40	10	1.4
RCS5L50T14	50	10	1.4
RCS5L60T14	60	10	1.4
RCS5L70T14	70	10	1.4
RCS5L80T14	80	10	1.4

Table 4-6: Specifications of samples with 1.4 mm thick web bonded plates

It is evident that this time, in addition to the 30 cm and 40 cm lengths, the 50cm long plate was also effective. Thus, with a thicker CFRP reinforcement plate, sample RCS5L50T14 also exhibited successful plastic hinge transfer. In addition, the location of the plastic hinge in this sample was more appropriate than in samples RCS5L30T14 and RCS5L40T14. According to Fig. 4.27(d-f), the 60, 70 and 80 cm lengths failed.

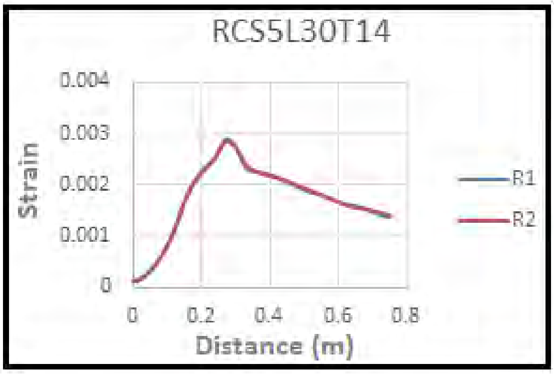

(a) Plate length: 30 cm

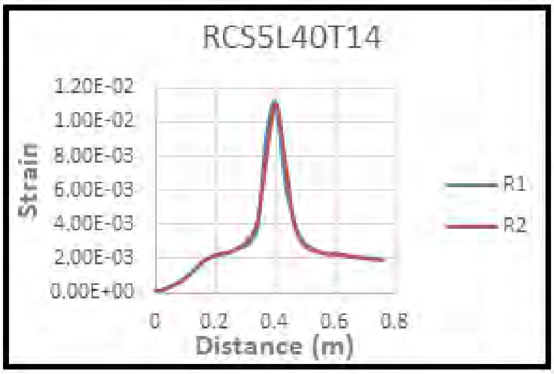

(b) **Plate length: 40 cm**

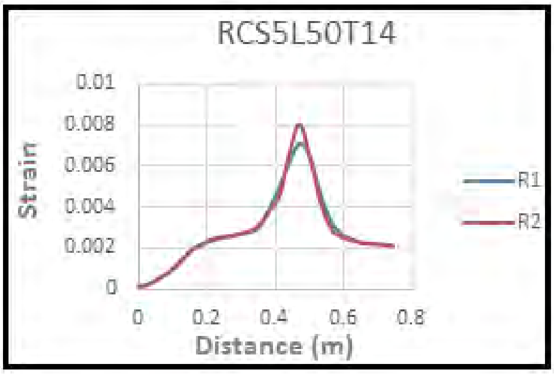

(c) **Plate length: 50 cm**

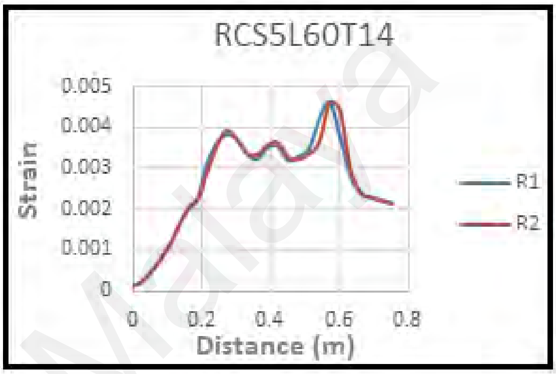

(d) Plate length: 60 cm

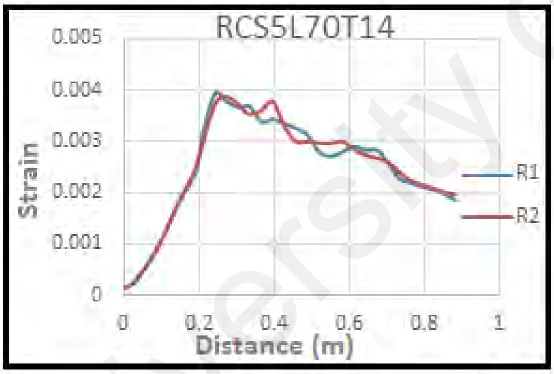

(e) **Plate length: 70 cm**

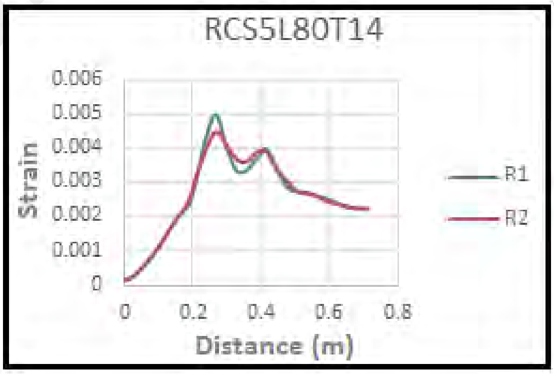

(f) Plate length: 80 cm

Figure 4.27 : Steel strain distribution diagrams for specimens reinforced with 1.4 mm thick web bonded plates (R1&R2 are upper longitudinal rebars)

4.5.2.4 Sample RCS5 reinforced with 1.6 mm thick plates bonded on the beam web

This group of samples were modeled using 1.6 mm thick web bonded CFRP plates. Details of these samples are provided in Table 4.7.

Table 4-7: Specifications of samples with 1.6 mm thick web bonded plates

Sample	Length (cm)	Width (cm)	Thickness (mm)
RCS5L30T16	30	10	1.6
RCS5L40T16	40	10	1.6
RCS5L50T16	50	10	1.6
RCS5L60T16	60	10	1.6
RCS5L70T16	70	10	1.6
RCS5L80T16	80	10	1.6

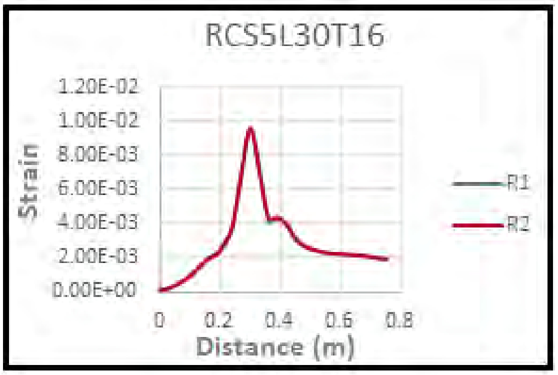

(a) Plate length: 30 cm

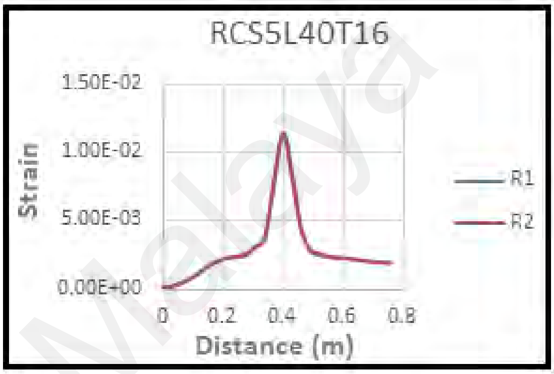

(b) Plate length: 40 cm

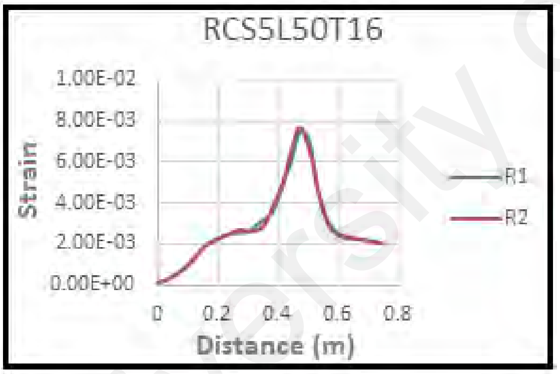

(c) Plate length: 50 cm

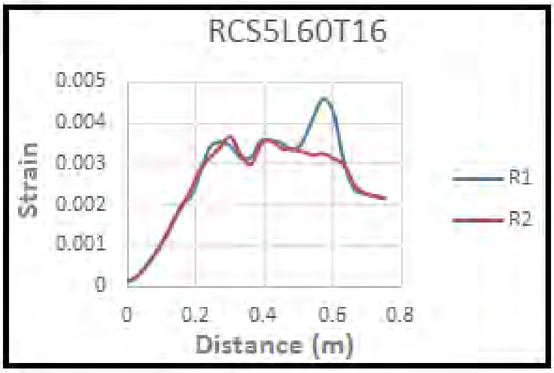

(d) Plate length: 60 cm

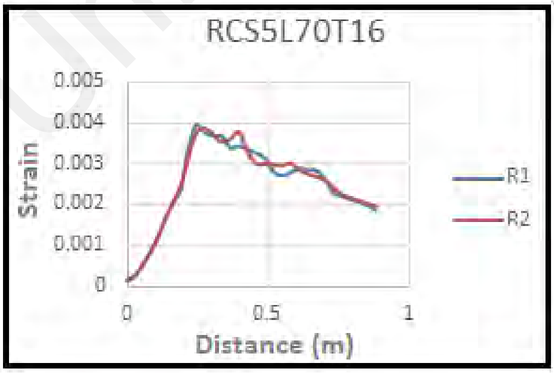

(e) Plate length: 70 cm

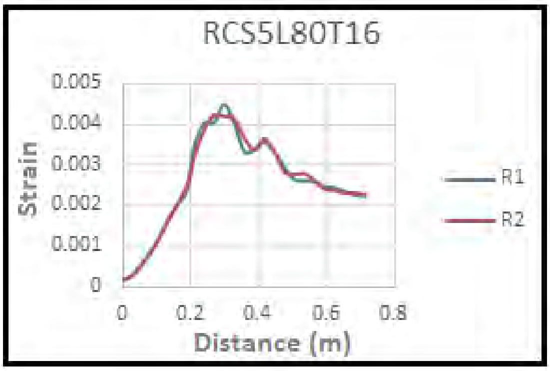

(f) Plate length: 70 cm

Figure 4.28: Steel strain distribution diagrams for specimens reinforced with 1.6 mm thick web bonded plates (R1&R2 are upper longitudinal rebars)

4.5.2.5 Sample RCS5 reinforced with 1.8 mm thick plates bonded on the beam web

In this section, the web bonded CFRP reinforcement plate thickness was increased to 1.8 mm. Table 4.8 presents the details of the six samples analyzed in this section.

Table 4-8: Specifications of samples with 1.8 mm thick web bonded plates

Sample	Length (cm)	Width (cm)	Thickness (mm)
RCS5L30T18	30	10	1.8
RCS5L40T18	40	10	1.8
RCS5L50T18	50	10	1.8
RCS5L60T18	60	10	1.8
RCS5L70T18	70	10	1.8
RCS5L80T18	80	10	1.8

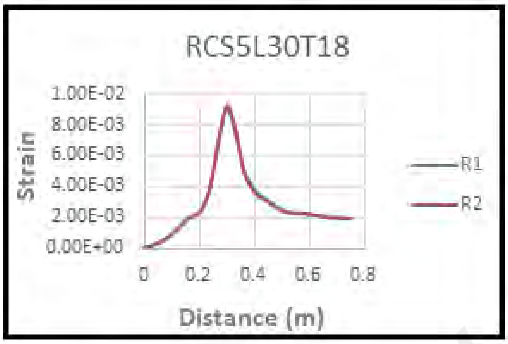

(a) Plate length: 30cm

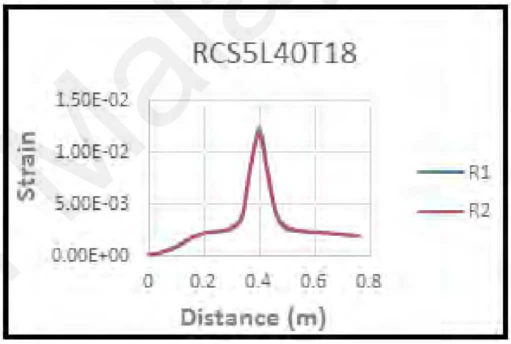

(b) Plate length: 40cm

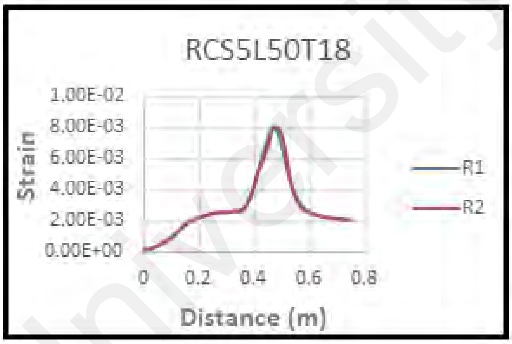

(c) Plate length: 50cm

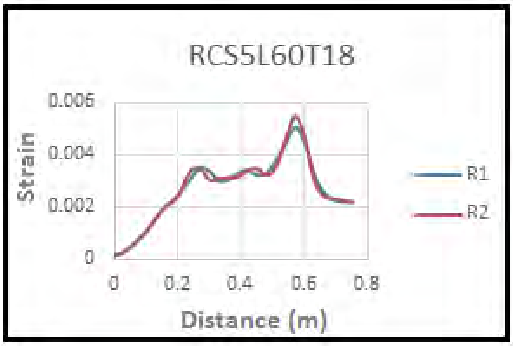

(d) Plate length: 60cm

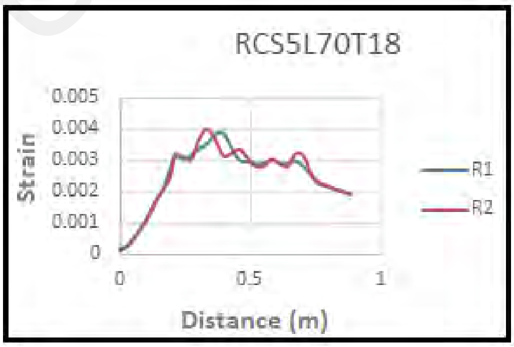

(e) Plate length: 70cm

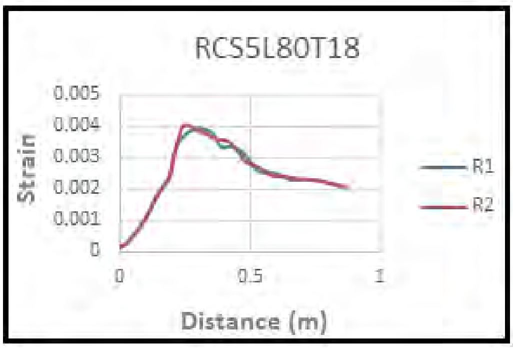

(f) Plate length: 80cm

Figure 4.29: Steel strain distribution diagrams for specimens reinforced with 1.8 mm thick web bonded plates (R1&R2 are upper longitudinal rebars)

As seen in Figs. 4.29(d-f), 60 cm was also an effective length for 1.8 mm thick sheets, but the 70 and 80 cm lengths did not produce positive results.

4.5.2.6 Sample RCS5 reinforced with 2, 2.2 and 2.4 mm thick web bonded plates

An attempt was made to find out whether increasing the plate thickness would produce favorable results for the samples reinforced with 70 and 80cm long CFRP plates. To this end, the RCS5 sample with 10cm wide and 70 and 80cm long reinforcement plates on both sides of the web was analyzed by increasing the plate thickness to 2 mm, 2.2 mm, and 2.4 mm. Table 4.9 provides details of the six samples analyzed in this section.

Table 4-9: Specifications of samples with 2.0, 2.2 and 2.4 mm thick web bonded plates

Sample	Length (cm)	Width (cm)	Thickness (mm)
RCS5L70T20	70	10	2.0
RCS5L80T20	80	10	2.0
RCS5L70T22	70	10	2.2
RCS5L80T22	80	10	2.2
RCS5L70T24	70	10	2.4
RCS5L80T24	80	10	2.4

However, as seen in Figs. 4.30 to 4.32 plastic hinge transfer did not occur in any of these samples. Thus, it can be concluded that the effect of increasing the reinforcing plate length limited the plastic joint movement. The increase in length was limited to about twice the beam height.

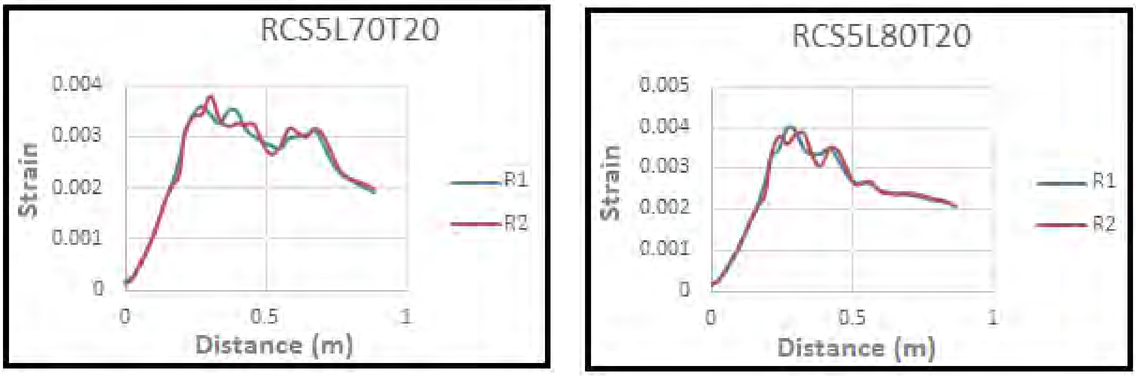

(a) Plate length: 70 cm **(b) Plate length: 80 cm**

Figure 4.30: Steel strain distribution diagrams for specimens reinforced with 2 mm thick web bonded plates (R1&R2 are upper longitudinal rebars)

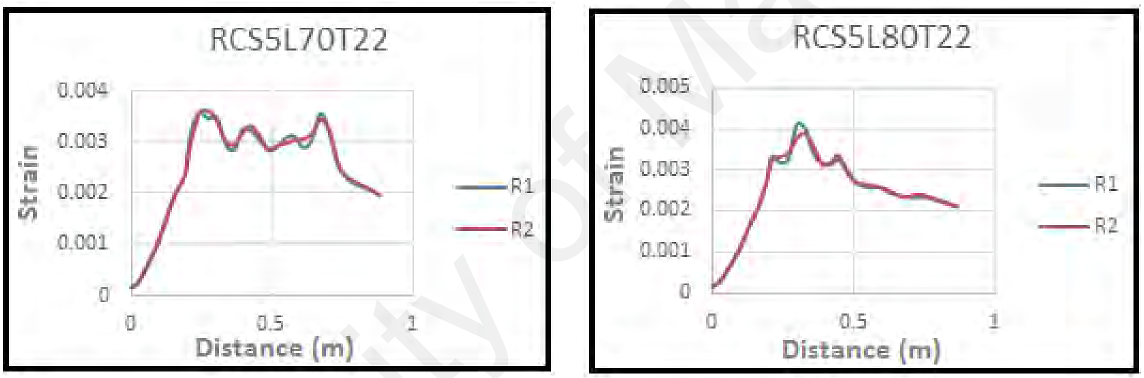

(a) Plate length: 70 cm **(b) Plate length: 80 cm**

Figure 4.31: Steel strain distribution diagrams for specimens reinforced with 2.2 mm thick web bonded plates (R1&R2 are upper longitudinal rebars)

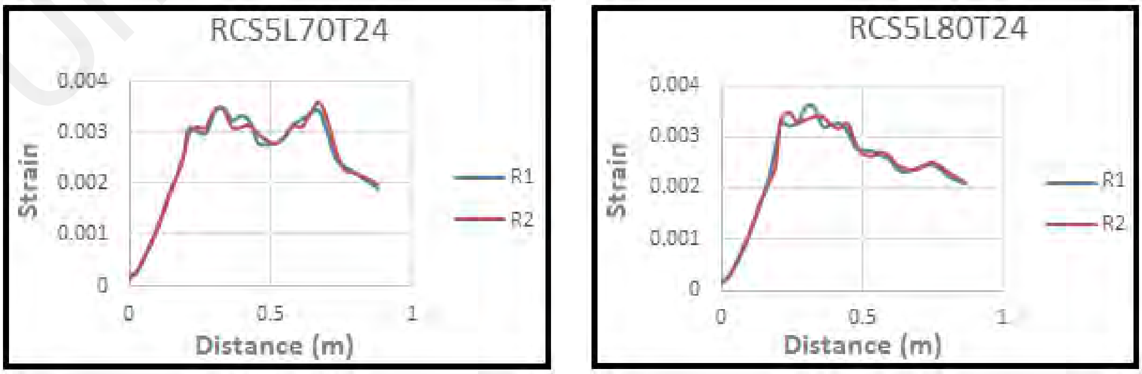

(a) Plate length: 70 cm **(b) Plate length: 80 cm**

Figure 4.32: Steel strain distribution diagrams for specimens reinforced with 2.4 mm thick web bonded plates (R1&R2 are upper longitudinal rebars)

4.5.3 Analysis of joints reinforced with CFRP plates on the beam flanges

It is known that adding CFRP reinforcement plates to the beam web, as discussed in previous sections, is not feasible practically in the case of actual three-dimensional reinforced concrete frames. As an alternative, reinforcing the beam-column connection using CFRP plates on the beam flanges can be effective (Azarm et al., 2017). In the following sections, the RCS3 sample model is used. Reinforcement plates of different lengths and thicknesses were applied to the beam flanges and samples were modeled and analyzed. The aim is to evaluate the effects of CFRP reinforcement plate length and thickness on plastic hinge transfer from the proximity of the connection to the beam.

4.5.3.1 Sample RCS3 reinforced with 1 mm thick plates on the beam flanges

In this section, 1 mm thick and 10cm wide CFRP plates were used on the beam flanges to reinforce the beam-column connection. Lengths of 30, 40, 50, 60 and 70 cm were considered. Details of the modeled samples are given in Table 4.9.

Table 4-10: Specifications of samples with 1 mm thick plates on the flanges

sample	Length (cm)	Width (cm)	Thickness (mm)
RCS3L30T10	30	10	1
RCS3L40T10	40	10	1
RCS3L50T10	50	10	1
RCS3L60T10	60	10	1
RCS3L70T10	70	10	1

Upon analysis completion, the strain variations in the beam tensile rebars were compared for the above samples in Fig. 4.33(a-e).

As shown in Fig. 4.33(a), the connection reinforced using 1 mm thick and 30cm long CFRP plates exhibited a more favorable situation compared to other lengths. This caused maximum strain in both longitudinal rebars (R1 and R2) to occur at the end of the CFRP plates. It was found that the plastic hinge transfer was somewhat successful.

However, as per Fig. 4.33(b), increasing the CFRP plate length to 40 cm not only did not help improve the plastic hinge location, but on the contrary, it led to maximum strain at the end of the CFRP plates in the R1 longitudinal rebar and in the R2 rebar near the column. Therefore, the success of plastic hinge transfer diminished.

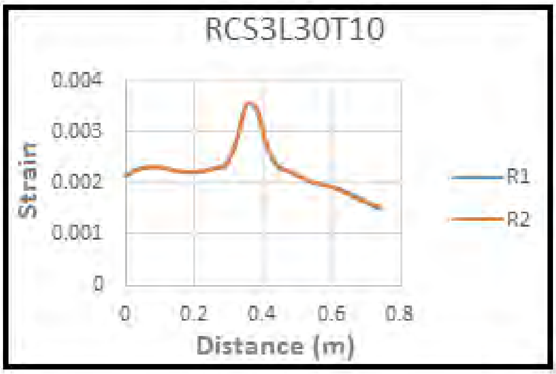

(a) Plate length: 30 cm

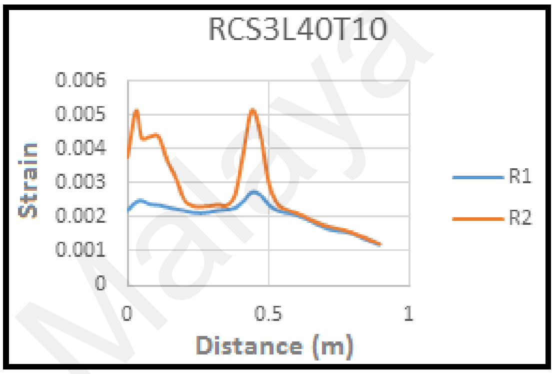

(b) Plate length: 40 cm

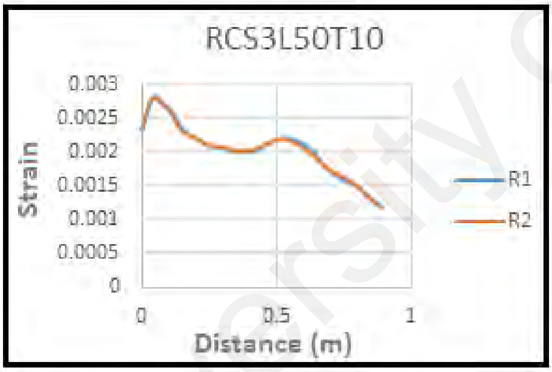

(c) Plate length: 50 cm

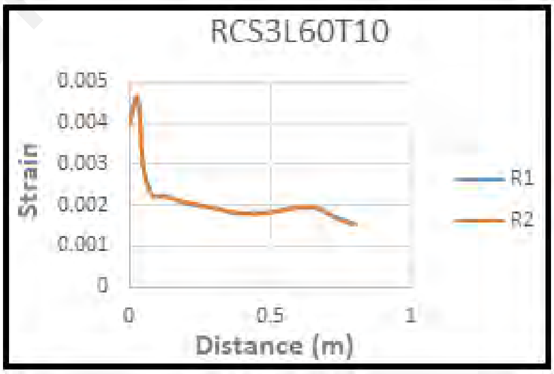

(d) Plate length: 60 cm

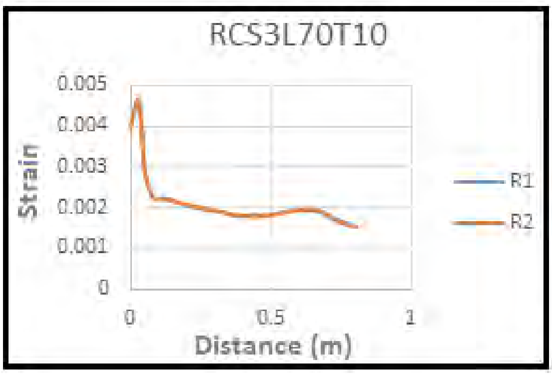

(e) Plate length: 70 cm

Figure 4.33: Steel strain distribution diagrams for specimens reinforced with 1 mm thick plates on the flanges (R1&R2 are upper longitudinal rebars)

Fig. 4.33(c) indicates that by increasing the plate length, the difference between rebar strains at the end of the CFRP plate and in the region near the column decreased. Fig. 433(d, e) show that for lengths of 60 and 70 cm, maximum strain occurred in the region close to the column for both R1 and R2 longitudinal rebars. Therefore, the reinforcement plates with these lengths were unsuccessful in plastic hinge transfer.

4.5.3.2 Sample RCS3 reinforced with 1.2 mm thick plates on the beam flanges

In this section, samples RCS3 with 1.2 mm thick CFRP reinforcement plates with different lengths of 30, 40, 50, 60 and 70 cm are analyzed. The details of these samples are given in Table 4.11. The rebars' tensile strain graphs for the five samples modeled are shown in Fig. 4.34(a-e). According to Fig. 4.34(a), the sample with a 30cm long CFRP reinforcement plate was superior to other lengths and led to maximum strain on both R1 and R2 rebars at the end of the CFRP plates. Therefore, the plastic hinge transfer was partly successful. In addition, compared with a sample reinforced with a 30cm long and 1 mm thick plate in Fig. 4.33(a), it is evident that by increasing the thickness from 1 mm to 1.2 mm, the joint transfer was more favorable, and the strain at the end of the reinforcement plate was different from the strain near the column.

Table 4-11: Specifications of samples with 1.2 mm thick plates on the flanges

Sample	Length (cm)	Width (cm)	Thickness (mm)
RCS3L30T12	30	10	1.2
RCS3L30T12	40	10	1.2
RCS3L30T12	50	10	1.2
RCS3L30T12	60	10	1.2
RCS3L30T12	70	10	1.2

Fig. 4.34(b) indicates that despite a relative success, the length of 40 cm was not 100% successful. The reason is that the strain difference between the end of the CFRP plate and near the column was negligible. Fig. 4.34(c) shows that CFRP plates with a thickness of 1.2 mm and length of 50 cm were not useful in handling the plastic hinge,

as the maximum strain was transferred only in the R1 rebar next to the CFRP plate. However, maximum strain also occurred in the R2 longitudinal rebar near the column. It should be noted that completely successful plastic hinge relocation denotes instances when maximum strain occurs in all longitudinal tensile rebars at the end of the CFRP plates and is at least 20% more than the strain near the column.

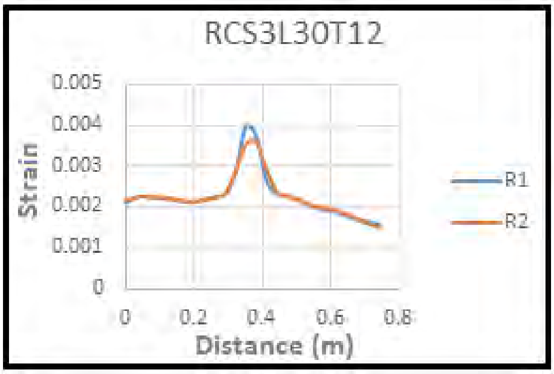

(a) Plate length: 30 cm

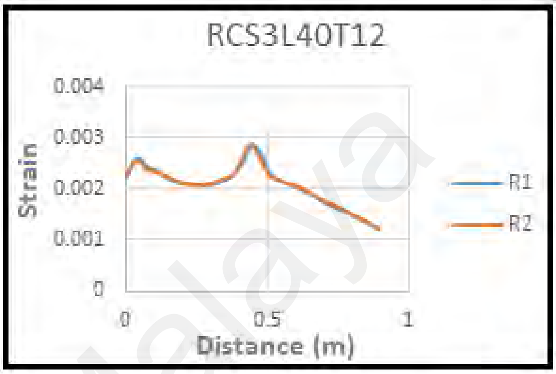

(b) Plate length: 40 cm

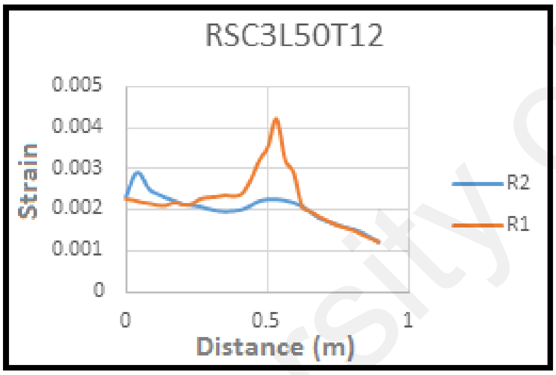

(c) Plate length: 50 cm

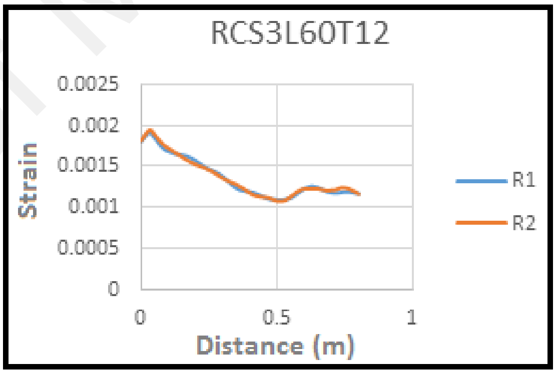

(d) Plate length: 60 cm

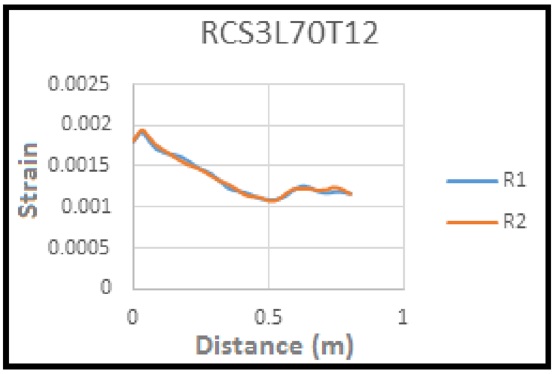

(e) Plate length: 70 cm

Figure 4.34: Steel strain distribution diagrams for specimens reinforced with 1.2 mm thick plates on the flanges (R1&R2 are upper longitudinal rebars)

Fig. 4.34(d) shows that increasing the sheet length to 60 cm (same thickness of 1.2 mm) led to a decrease in the strain difference between the CFRP plate end region and near the column. Subsequently, according to Fig. 4.34(e), using a length of 70 cm and the same thickness caused maximum strain in both R1 and R2 rebars near the column. This implies that using a 70cm long and 1.2 mm thick plate was completely unsuccessful in plastic hinge transfer.

4.5.3.3 Sample RCS3 reinforced with 1.4 mm thick plates on the beam flanges

In this section, 1.4 mm thickness was selected for the reinforcement plates, and samples with different lengths were modeled. Table 4.12 contains details of these samples.

Table 4-12: Specifications of samples with 1.4 mm thick plates on the flanges

sample	Length (cm)	Width (cm)	Thickness (mm)
RCS3L30T14	30	10	1.4
RCS3L40T14	40	10	1.4
RCS3L50T14	50	10	1.4
RCS3L60T14	60	10	1.4
RCS3L70T14	70	10	1.4
RCS3L90T14	90	10	1.4

The strain variations along the beam for the upper rebars in these specimens are shown in Fig. 4.35(a,b).

Fig. 4.35(a) demonstrates that the connection with a 1.4 mm thick and 30cm long reinforcement plate was superior to other lengths. Here, the strain reached its maximum on both longitudinal R1 and R2 rebars at the end of the CFRP plates. A comparison of Figures 4.35(a), 4.34(a) and 4.33(a) indicates that the 30cm long and 1.4 mm thick plate was more appropriate than the 1.1 and 1.2 mm thick plates. As seen in Fig. 4.35(b), increasing the plate length to 40 cm aided the plastic hinge transfer condition and both R1 and R2 rebars experienced maximum strain at the end of the CFRP plates.

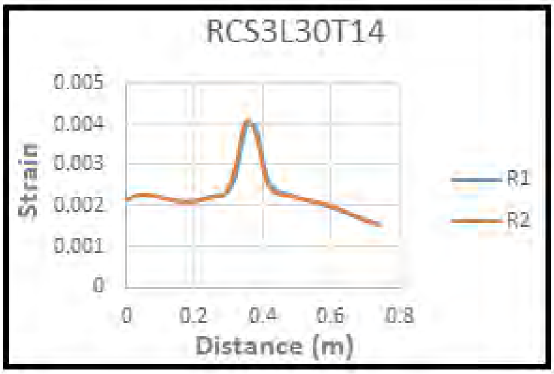

(a) **Plate length: 30 cm**

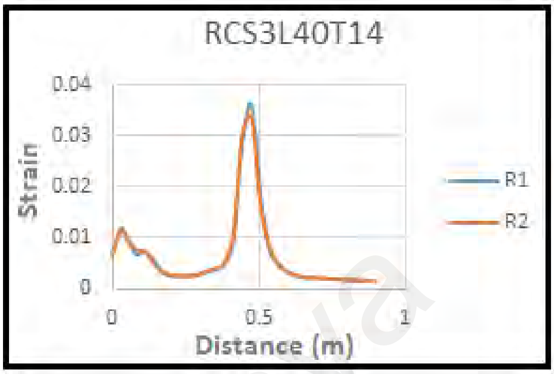

(b) **Plate length: 40 cm**

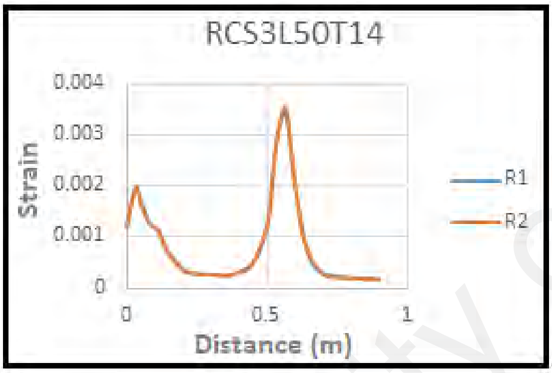

(c) **Plate length: 50 cm**

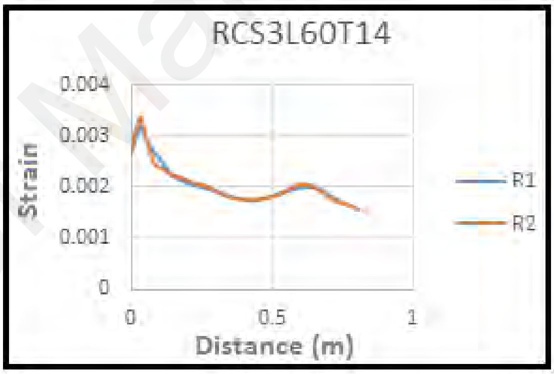

(d) **Plate length: 60 cm**

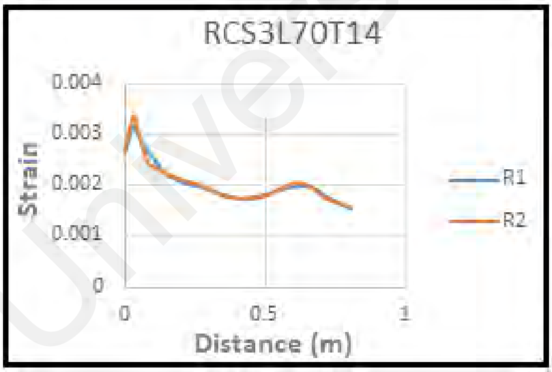

(e) **Plate length: 70 cm**

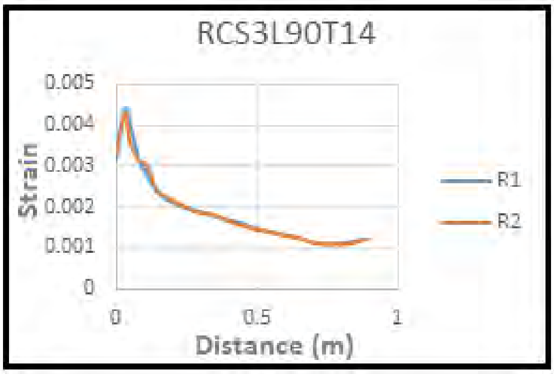

(f) **Plate length: 90 cm**

Figure 4.35: Steel strain distribution diagrams for specimens reinforced with 1.4 mm thick plates on the flanges (R1&R2 are upper longitudinal rebars)

According to Fig. 4.35(c), the plastic hinge relocation became more favorable for the 50 cm length. However, according to Fig. 4.35(d), relocation was not successful for a length of 60 cm. Fig. 4.35(e) shows that by increasing the plate length to 70 cm, maximum strain occurred in the R2 rebar in the connection zone, suggesting the unsuccessful function of this sample. Furthermore, in Fig. 4.35(f), for the sample with a 90cm long CFRP plate, the maximum strain in both R1 and R2 rebars occurred near the column.

4.5.3.4 Sample RCS3 reinforced with 1.6 mm thick plates on the beam flanges

Once again, the reinforcing plate thickness was increased. Now the samples were modeled by selecting a thickness of 1.6 mm and lengths of 30, 40, 50, 60, 70 and 90 cm for the plates. Table 4.13 tabulates the sample details.

Table 4-13: Sample RCS3 reinforced with 1.6 mm thick plates on the flanges

Sample	Length (cm)	Width (cm)	Thickness (mm)
RCS3L30T16	30	10	1.6
RCS3L40T16	40	10	1.6
RCS3L50T16	50	10	1.6
RCS3L60T16	60	10	1.6
RCS3L70T16	70	10	1.6
RCS3L90T16	90	10	1.6

Following analysis, the strain distribution diagrams for all samples are given in Fig. 4.36(a-f). According to these graphs, the lengths of 30, 40, 50 and 60 cm were successful in plastic joint transfer, with the 60 cm length having been the most successful.

The 70 cm length was not suitable for the reinforcement plates, since in this sample, the maximum strain value occurred near the column. In the sample with a 90cm long reinforcement plate, the maximum rebar strain occurred near the column, which rendered this sample unsuccessful.

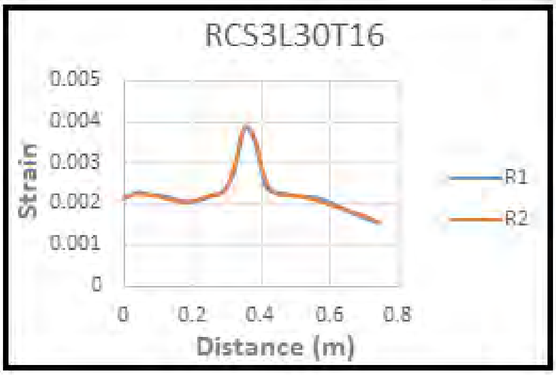

(a) Plate length: 30 cm

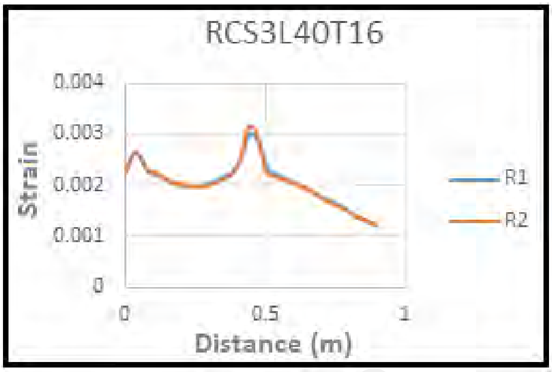

(b) Plate length: 40 cm

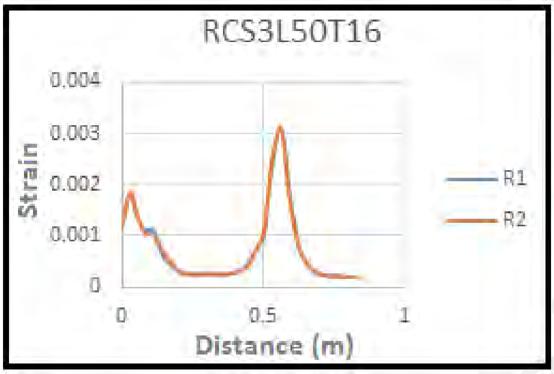

(c) Plate length: 50 cm

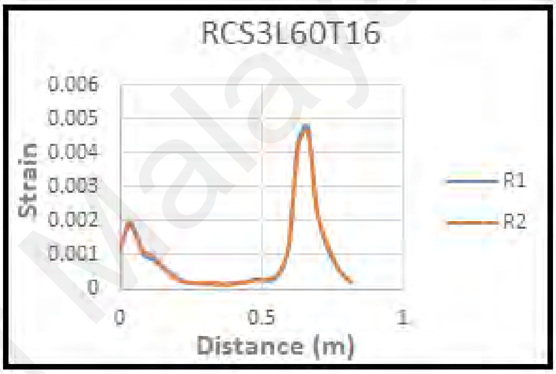

(d) Plate length: 60 cm

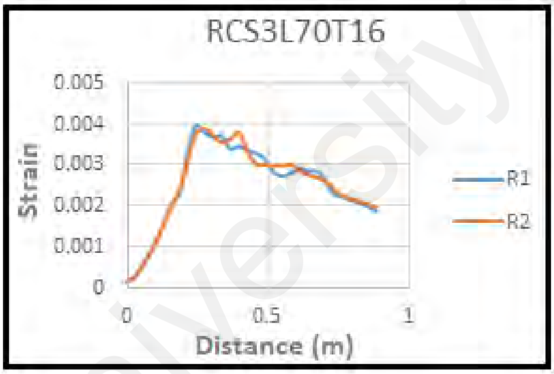

(e) Plate length: 70 cm

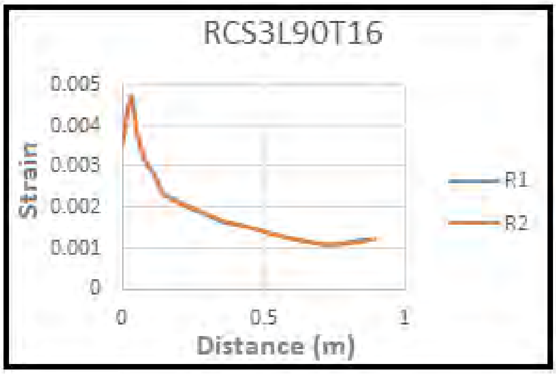

(f) Plate length: 90 cm

Figure 4.36: Steel strain distribution diagrams for specimens reinforced with 1.6 mm thick plates on the flanges (R1&R2 are upper longitudinal rebars)

4.5.3.5 Samples RCS3 reinforced with 1.8 mm thick plates on the beam flanges

The thickness of the reinforcement plates was increased again. This time, modeling was done with 1.8 mm thick plates and a summary of the specimen features is presented in Table 4.14.

Table 4-14: Specifications of 1.8 mm thick plates on the flanges

Sample	Length (cm)	Width (cm)	Thickness (mm)
RCS3L30T18	30	10	1.8
RCS3L40T18	40	10	1.8
RCS3L50T18	50	10	1.8
RCS3L60T18	60	10	1.8
RCS3L70T18	70	10	1.8
RCS3L90T18	90	10	1.8

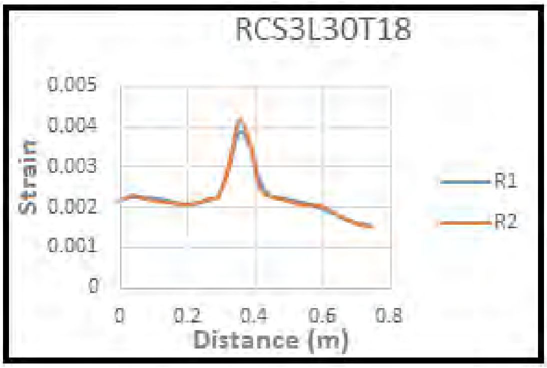

(a) Plate len gth: 30 cm

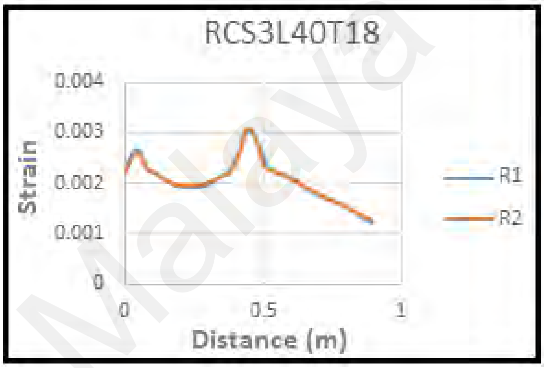

(b) Plate length: 40 cm

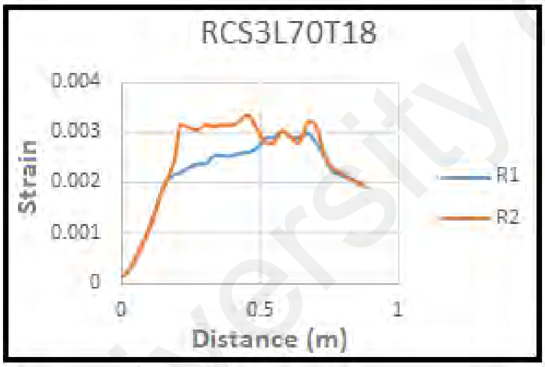

(c) Plate length: 50 cm

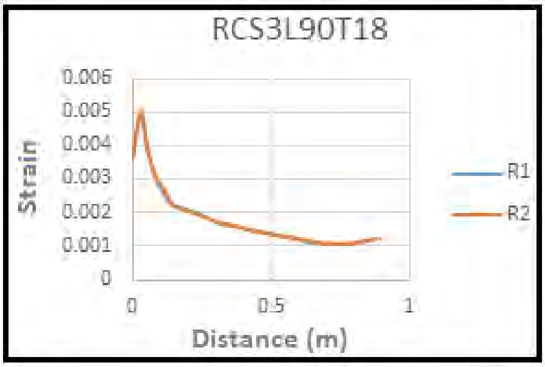

(d) Plate length: 60 cm

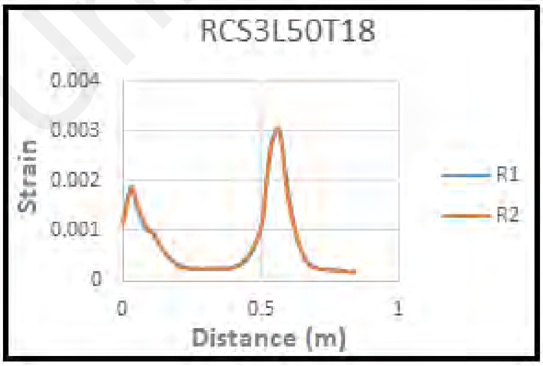

(e) Plate length: 70 cm

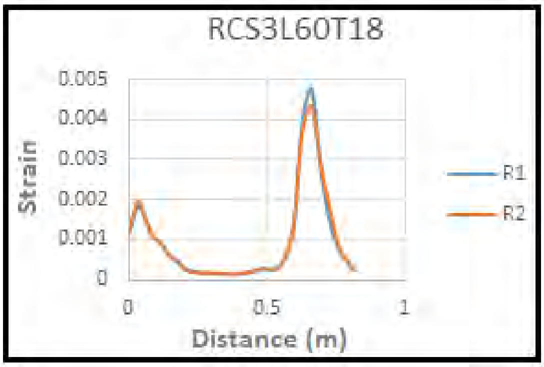

(f) Plate length: 90 cm

Figure 4.37: Steel strain distribution diagram for reinforced specimens with flange installed plates 1.8 mm in thickness (R1&R2 are upper longitudinal rebars)

Modeling was done for plates 30, 40, 50, 60, 70 and 90 cm in length. The strain distribution diagrams for these specimens are shown in Fig. 4.37(a-f). A review of the graphs indicates that the 30, 40 and 50 cm lengths were successful in plastic joint transfer. The sample reinforced with 60cm long and 1.8 mm thick plates performed better than with previous thicknesses. However, for 70 cm length, one of the longitudinal rebars (R2) exhibited maximum strain near the column. Figure 4.37(f) shows that selecting 90 cm for the length was not successful.

4.5.3.6 Samples RCS3 reinforced with 2.0 mm thick plates on the flanges

Finally, 2 mm thickness was selected for CFRP reinforcement plates with lengths of 30, 40, 50, 60, 70 and 90 cm. Details of these samples are given in Table 4.15, and the analysis results for the strain distribution in the longitudinal rebars are provided in Fig. 4.38(a-f).

Table 4-15: Specifications of 2 mm thick plates on the flanges

Sample	Length (cm)	Width (cm)	Thickness (mm)
RCS3-T2-L30	30	10	2
RCS3-T2-L40	40	10	2
RCS3-T2-L50	50	10	2
RCS3-T2-L60	60	10	2
RCS3-T2-L70	70	10	2
RCS3-T2-L90	90	10	2

These graphs reveal that increasing the plate thickness at this stage had little impact on plastic joint transfer, but the 50 and 60 cm lengths were somewhat better.

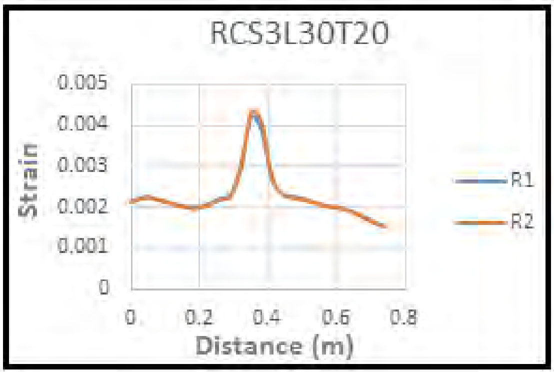

(a) Plate length: 30 cm

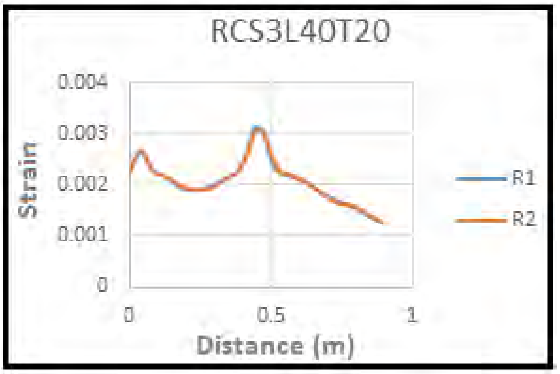

(b) Plate length: 40 cm

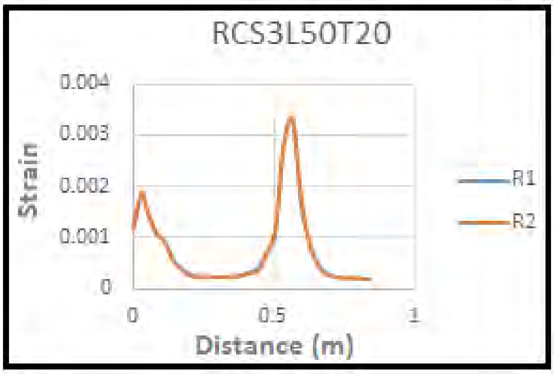

(c) Plate length: 50 cm

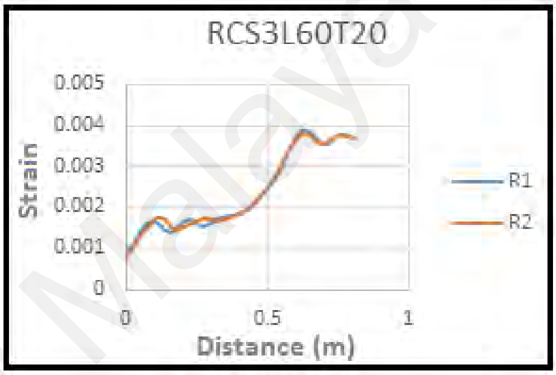

(d) Plate length: 60 cm

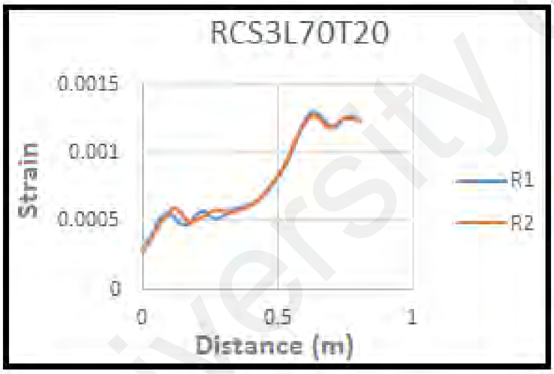

(e) Plate length: 70 cm

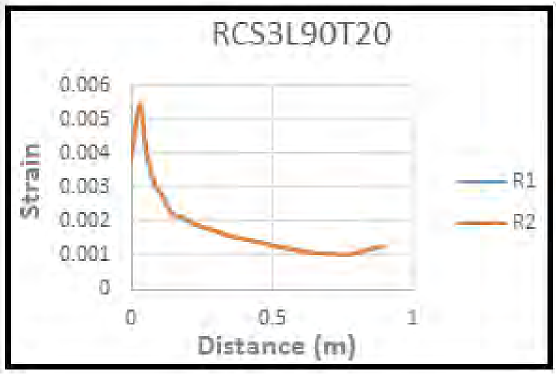

(f) Plate length: 90 cm

Figure 4.38: Steel strain distribution diagrams for specimens reinforced with 2 mm thick plates on the flanges (R1&R2 are upper longitudinal rebars)

4.5.4 Remarks and discussion

The samples reinforced with CFRP plates in various patterns and designs to relocate the plastic hinge away from the column face were analyzed. The samples fell mainly in two categories:

1. Samples reinforced with CFRP plates on both sides of the beam web
2. Samples reinforced with CFRP plates on the upper and lower beam flanges

In all cases, the width of the CFRP plates was the same (10 cm) and the effect of varying plate lengths and thicknesses was examined.

In the first category, where CFRP plates were installed on both sides of the beam web, 1 mm thick reinforcing plates with lengths of 30, 40, 50, 60, 70 and 80 cm were analyzed. The results showed that with 30 and 40cm long plates, the plastic hinge was relocated to the end of the CFRP plates. However, other lengths did not succeed in relocating the plastic hinge. In the next step, the CFRP plate thickness was increased to 1.2 mm and results similar to the first stage were obtained. The status of the sample with a 40cm long reinforcement plate improved slightly. However, the lengths of 50, 60, 70 and 80 cm did not fulfill the expected plastic hinge transfer. Subsequently, the CFRP plate thickness was increased to 1.4 mm. This time, it was observed that in addition to the lengths of 30 and 40 cm, the 50cm long plate was successful in transferring the plastic hinge. Lengths greater than 50 cm did not perform well. With increasing the plate thickness in the next steps, it appeared that the 60 cm length and 1.8 mm thickness also functioned suitably. However, 1.8mm thick and 70 and 80cm long plates were not suitable. Next, suitable thicknesses for the 70 and 80cm long reinforcement plates were evaluated. Here, the samples analyzed contained 2, 2.2 and 2.4 mm thick and 70 and 80cm long reinforcement plates. The results revealed that none of these patterns were effective on shifting the plastic hinge. Thus, it can be concluded that despite the ability to increase the effective length of the CFRP plates by increasing their thickness to create a plastic hinge at the end of the CFRP plates, there were some limitations. As such, it was not possible to increase the reinforcement plate length, and thereby the plastic hinge distance from the column as much as anticipated. It was deduced that the maximum effective CFRP plate length, or in other words the distance from the plastic joint formation on the column, can be considered to be about twice the height of the beam.

The second group of samples, to which reinforcement plates were added above and below the beam, were studied and analyzed like the first group by using fixed-width reinforcement plates of various lengths and thicknesses. As mentioned before, given that the actual frames are three-dimensional and due to the presence of floors and roofs, in most cases it is not possible to instal reinforcing plates on both sides of the beam web. Frame reinforcement is more practical by installing reinforcing plates on and under the beam.

The analysis results for 1 mm thick plates suggest that using 30cm long plates was effective for plastic joint transfer, but not plates 40 cm and longer. By increasing the thickness to 1.2 mm, the sample with a 30cm long plate exhibited a better condition. However, the samples with longer plates remained ineffective as reinforcement plates. In the next step, when a thickness of 1.4 mm was considered for the CFRP plates, the sample quality enhanced at lengths of 30, 40 and 50 cm. The 60cm long plate was relatively successful, but the lengths of 70 and 90 cm failed. A plate thickness of 1.6 mm with lengths of 30, 40, 50 and 60 cm succeeded in transferring the plastic hinge, but the 50 cm length revealed superior performance. Meanwhile, the lengths of 70 and 90 cm continued to fail. Finally, 2 mm thickness was selected for the plates and the samples were analyzed. The results indicate that increasing the plate thickness did not greatly affect the samples' performance. Although the samples with plates 50 and 60cm long performed slightly better, those with lengths of 70 and 90 cm remained unsuccessful in plastic joint transfer.

Therefore, in both samples (beam web and flanges) reinforced with CFRP plates, increasing the reinforcing plate thickness increased the plates' effective length for plastic hinge transfer. However, this increase is limited and excessive thickening may have negative effects.

CHAPTER 5: CONCLUSION

5.1 General

This chapter presents the conclusions from this study and recommendations for future work. This research study was based on five interrelated tasks:

(i) Design and selection of sample dimensions and details as well as the test setup.

(ii) Experimental evaluation of the different techniques using down-scale testing.

(iii) Numerical simulation of as-built and retrofitted joints using the Finite Element Method (FEM) and analysis.

(iv) Comparison of experimental results and FE numerical analysis.

(v) Modeling and analysis of several samples with different lengths and thicknesses of CFRP reinforcement in order to relocate the plastic hinge away from the column face.

The purpose of this research was to evaluate the ability of CFRP reinforcement to enhance strength and ductility. Meanwhile, the aim of this study was to prevent plastic hinge formation at the column face in the exterior beam-column joint by using an advanced CFRP laminate.

5.2 Main finding and Conclusions

The main findings of this research can be listed such as:

1) Applying the CFRP reinforcement increased the load capacity of the beam-column connections in all specimens. The ductility factor of sample RCS3 (CFRP plates on the top and bottom of the beam) reduced smoothly, but the ductility factor of the other samples increased.

2) The control specimen and retrofitted joints were simulated in Finite Element (FE) modeling software (ABAQUS) and then analyzed. The behavior of the numerical specimens was completely consistent with that of the experimental specimens.

3) By increasing the reinforcing plate thickness, the plate effective length on plastic hinge transfer increased. Increasing the plate effective length is limited (60cm) and excessive thickening may have negative effects. The optimum effective CFRP plate length can be considered a distance about twice the height of the beam from behind the column.

in the next section a summary of the conclusions will be descripted.

5.3 Summary

1) In the experimental program, six scaled-down RC exterior joints were tested under moderately monotonic loads. One specimen was the control while the five other specimens were strengthened with CFRP of various designs. Applying the CFRP reinforcement increased the load capacity of the beam-column connections in all specimens. The ductility factor of sample RCS3 (CFRP plates on the top and bottom of the beam) reduced smoothly, but the ductility factor of the other samples increased. The greatest effect on the ductility factor was seen in sample RCS5 (almost 100%), where two reinforcement plates were bonded to both sides of the beam web.

2) The control specimen and retrofitted joints were simulated in Finite Element (FE) modeling software (ABAQUS) and then analyzed. The numerical analysis results seemed to be in acceptable compliance with the experimental results, except for a slight difference in the results from the actual values of about 1% to 3%. Following numerical analysis with ABAQUS, the stress and strain contours were examined and compared with experimental observations, and the results were recorded in a data logger. The

behavior of the numerical specimens was completely consistent with that of the experimental specimens. The locations of cracking and concrete damage as well as plastic hinge in the rebars were in good agreement in both numerical and experimental methods. The most important advantage of the numerical method over the experimental method is that this method allows enough time to examine different parts. Moreover, the parts that are not visible in the lab can be observed and studied in detail via numerical analysis and ABAQUS software. In addition, a large number of samples can be investigated with minimum cost, whereas the same process in the laboratory is very costly and time-consuming.

3) After numerical method validation, several CFRP-reinforced samples with different plate lengths and thicknesses were analyzed for their ability to relocate the plastic hinge away from the column face. These samples were mainly in two categories:

i: Samples reinforced with CFRP plates on both sides of the beam web.

ii: Samples reinforced with CFRP plates on the upper and lower beam flanges.

Specimen RCS2 in which the beam-column connection had been reinforced attained a relatively good ductility coefficient. But in practice, as the actual frames are three-dimensional, it is not possible to reinforce the connection site. Furthermore, specimen RCS6, which was wrapped at the end of the beam, not only had an increased ductility coefficient but also a dramatically higher ultimate load. In practice, however, due to the presence of a concrete slab it is not feasible to implement this type of wrapped reinforcement. Therefore, samples RCS3, RCS4 and RCS6 are more suitable in practice. Of these, sample RCS3 was reinforced at the beam web and the other two were reinforced in the beam flange region. Owing to the use of reinforcement plates in the RCS5 sample, this sample was more appropriate than RCS4 in which sheets were used for comparison with RCS3. Thus, in the final section of this study, samples RCS3 and RCS5 were selected, for which plates with various lengths and thicknesses were modeled.

The results demonstrated that the effective length of a CFRP plate to relocate the plastic hinge is dependent on its thickness. It was found for both groups of samples reinforced with CFRP plates in the beam web and flanges that by increasing the reinforcing plate thickness, the plate length effective on plastic hinge transfer increased. However, this increase is limited and excessive thickening may have negative effects. The optimum effective CFRP plate length can be considered a distance about twice the height of the beam from behind the column.

5.4 Recommendations for future research

Based on the results of this study, the following recommendations for future research are offered:

a) In this research, monotonic loading was used in the tests, but cyclic loading is recommended in future work. Because, in the case of seismic loading, where the column and beam moments transferred to contrary directions, the BCCs experience high magnitude of horizontal and vertical shear forces and becomes more critical

b) An exterior beam-column connection was evaluated in the present work, considering that each framed structure includes both external and internal connection, an internal beam-column connection could be evaluated in future.

c) It is advised that connection loading be performed without column axial force or with different values and the impact of the axial force be evaluated, because the column axial load is effective on beam-column connections behavior.

d) In this study, it was assumed there was a full bond between the rebars and the concrete part, and also between the concrete and the CFRP layers. Since the studies of this project were more behavioral, these assumptions did not have a significant impact on the results. In future work, this subject should be reviewed. If the connection between the components is assumed more realistically, it may result in a slight change. For example, the effect of rebar slip or CFRP layer debonding could be evaluated.

REFERENCES

Abdel-Wahed, O., ElNesr, O., ElGhandour, A., and Saad Eldin, W. (2005). *Behavior of reinforced concrete beam–column joint with FRP*. Paper presented at the Eleventh international colloquium on structural and geotechnical engineering, 11th ICSGE. Egypt: Ain Shams University, Faculty of Engineering.

Abdullah, A., and Takiguchi, K. (2000). Experimental Investigation on Ferrocement as an Alternative Material to Strengthen Reinforced Concrete Column. *Journal of Ferrocement, 30*(2), 177-190.

ACI-318-2008. 318 (2008) Building Code Requirements for Structural Concrete (ACI 318-08) and Commentary (ACI 318R-08). *American Concrete Institute (ACI), Detroit, Mich*.

ACI. (2014). Building code requirements for reinforced concrete.

Al-Salloum, Y. A., and Almusallam, T. H. (2007). Seismic response of interior RC beam-column joints upgraded with FRP sheets. I: Experimental study. *Journal of Composites for Construction, 11*(6), 575-589.

Al-Sulaimani, G., and Basunbul, I. (1991). Behavior of ferrocement material under direct shear. *Journal of ferrocement, 21*(2), 109-117.

Ali, O., Bigaud, D., and Riahi, H. (2018). Seismic performance of reinforced concrete frame structures strengthened with FRP laminates using a reliability-based advanced approach. *Composites Part B: Engineering, 139*, 238-248.

Antonopoulos, C. P., and Triantafillou, T. C. (2002). Analysis of FRP-strengthened RC beam-column joints. *Journal of composites for construction, 6*(1), 41-51.

Antonopoulos, C. P., and Triantafillou, T. C. (2003). Experimental investigation of FRP-strengthened RC beam-column joints. *Journal of composites for construction, 7*(1), 39-49.

Arya, A. (1981). A manual of earthquake-resistant non-engineered construction. *Indian Society of Earthquake Technology, Roorkee*.

Ascione, F., Lamberti, M., Razaqpur, A., and Spadea, S. (2017). Strength and stiffness of adhesively bonded GFRP beam-column moment resisting connections. *Composite Structures, 160*, 1248-1257.

Aslam, M., Shafigh, P., Jumaat, M. Z., and Shah, S. (2015). Strengthening of RC beams using prestressed fiber reinforced polymers–A review. *Construction and Building Materials, 82*, 235-256.

Association, C. S. (2002). *Design and construction of building components with fibre-reinforced polymers*: Canadian Standards Association.

Azarm, R., Maheri, M. R., and Torabi, A. (2017). Retrofitting RC Joints Using Flange-Bonded FRP Sheets. *Iranian Journal of Science and Technology, Transactions of Civil Engineering, 41*(1), 27-35.

Badawi, M., and Soudki, K. (2009). Flexural strengthening of RC beams with prestressed NSM CFRP rods–experimental and analytical investigation. *Construction and Building Materials, 23*(10), 3292-3300.

Bakis, C. E., Ganjehlou, A., Kachlakev, D. I., Schupack, M., Balaguru, P., Gee, D. J., et al. (2002). Guide for the design and construction of externally bonded FRP systems for strengthening concrete structures. *Reported by ACI Committee, 440*(2002).

Beres, A., El-Borgi, S., White, R. N., and Gergely, P. (1992). Experimental results of repaired and retrofitted beam-column joint tests in lightly reinforced concrete frame buildings *Technical Report NCEER* (Vol. 92): US National Center for Earthquake Engineering Research.

Beres, A., Pessiki, S. P., White, R. N., and Gergely, P. (1996). Implications of experiments on the seismic behavior of gravity load designed RC beam-to-column connections. *Earthquake Spectra, 12*(2), 185-198.

Bonacci, J., and Pantazopoulou, S. (1993). Parametric investigation of joint mechanics. *ACI Structural Journal, 90*, 61-71.

Bs, B. S. I. (1997). Structural use of concrete. Part I: Code of practice for design and construction. *British Standards Institution, UK*.

Busel, J., and Lockwood, J. (2000). Product selection guide: FRP composite products for bridge applications. *Market Development Alliance (MDA) of the FRP Composites Industry, New York, NY*, 122-157.

Choudhury. (2010). *Study on Size Effect of RC Beam-Column Joints with and without Retrofitting Under Cyclic Loading: Author, 2010.*

Choudhury, Dutta, A., and Deb, S. (2010). *Study on Size effect of Retrofitted beam-column joint with Beam Weak in Flexure under Cyclic Loading‖*. Paper presented at the Proceedings of 35 th Conference on our world in concrete & structures.

Chutarat, N., and Aboutaha, R. S. (2003). Cyclic response of exterior reinforced concrete beam-column joints reinforced with headed bars—experimental investigation. *Structural Journal, 100*(2), 259-264.

Clyde, C., and Pantelides, C. (2002). *Seismic evaluation and rehabilitation of R/C exterior building joints.* Paper presented at the Proceeding of the 7th US national conference on earthquake engineering, 7NCEE, Earthquake Engineering Research Institute, Berkeley, Calif.

Corazao, M., and Durrani, A. J. (1989). *Repair and strengthening of beam-to-column connections subjected to earthquake loading*: National Center for Earthquake Engineering Research, State University of New York at Buffalo.

Cornelissen, H. A. W., Hordijk, D. A., and Reinhardt, H. W. (1986). Experimental determination of crack softening characteristics of normalweight and lightweight concrete. *HERON, 31 (2), 1986*, 45-56.

D'Ayala, D., Penford, A., and Valentini, S. (2003). *Use of FRP fabric for strengthening of reinforced concrete beam-column joints.* Paper presented at the Proceedings of the 10th International conference on structural faults and repair, London.

Daly, A., and Witarnawan, W. (1997). *Strengthening of bridges using external post-tensioning.* Paper presented at the Conference of eastern Asia society for transportation studies, Seoul, Korea.

Danesh, F., Esmaeeli, E., and Alam, M. F. (2008). Shear strengthening of 3d rc beam-column connection using GFRP: FEM study. *Asian Journal of Applied Sciences, 1*(3), 217-227.

De Lorenzis, L., Nanni, A., and La Tegola, A. (2000). *Strengthening of reinforced concrete structures with near surface mounted FRP rods.* Paper presented at the International Meeting on Composite Materials, PLAST 2000, Proceedings, Advancing with Composites.

De Lorenzis, L., and Teng, J. (2007). Near-surface mounted FRP reinforcement: An emerging technique for strengthening structures. *Composites Part B: Engineering, 38*(2), 119-143.

Deng, Z.-c., and Xiao, R. (2011). Flexural performance of RC beams strengthened with prestressed AFRP sheets: Part I. Experiments *Advances in FRP Composites in Civil Engineering* (pp. 699-703): Springer.

Dowrick, D. J. (2003). *Earthquake risk reduction*: John Wiley & Sons.

Ehsani, M. R., and Wight, J. K. (1985). *Exterior reinforced concrete beam-to-column connections subjected to earthquake-type loading.* Paper presented at the ACI Journal Proceedings.

Ei-Mikawi, M., and Mosallam, A. S. (1996). A methodology for evaluation of the use of advanced composites in structural civil engineering applications. *Composites Part B: Engineering, 27*(3), 203-215.

El-Hacha, R., and Gaafar, M. (2011). Flexural strengthening of reinforced concrete beams using prestressed, near-surface-mounted CFRP bars. *PCI journal, 56*(4), 134-151.

Ellobody, E., Young, B., and Lam, D. (2006). Behaviour of normal and high strength concrete-filled compact steel tube circular stub columns. *Journal of Constructional Steel Research, 62*(7), 706-715.

Elsouri, A. M., and Harajli, M. H. (2015). Repair and FRP strengthening of earthquake-damaged RC shallow beam-column joints. *Advances in Structural Engineering, 18*(2), 237-249.

En. (2004). Eurocode 2: Design of concrete structures-Part 1-1: General rules and rules for buildings. *European Committee for Standardization*.

Engindeniz, M., Kahn, L. F., and Zureick, A.-H. (2005). Repair and strengthening of reinforced concrete beam-column joints: State of the art. *ACI structural journal, 102*(2).

Engindeniz, M., Kahn, L. F., and Zureick, A.-H. (2008). Performance of an RC corner beam-column joint severely damaged under bidirectional loading and rehabilitated with FRP composites. *Seismic Strengthening of Concrete Buildings Using FRP Composites*, 19-36.

Estrada, J. I. (1990). *Use of steel elements to strengthen a reinforced concrete building*.

Feroldi, F., and Russo, S. (2016). Structural behavior of all-FRP beam-column plate-bolted joints. *Journal of Composites for Construction, 20*(4), 04016004-04016001-04016012.

Filiatrault, A., Pineau, S., and Houde, J. (1995). Seismic behavior of steel-fiber reinforced concrete interior beam-column joints. *ACI Structural Journal, 92*(5), 543-552.

French, C. W., and Moehle, J. P. (1991). Effect of Foor Slab on Behavior of Slab-Beam-Column Connections. *ACI Special Publication, 123*, 225-258.

Fujii, S., and Morita, S. (1991). Comparison Between Interior and Exterior R/C Beam-Column Joint Behavior. *ACI Special Publication, 123*, 145-166.

Ganesan, N., Indira, P., and Abraham, R. (2007). Steel fibre reinforced high performance concrete beam-column joints subjected to cyclic loading. *ISET Journal of Earthquake Technology, 44*(3-4), 445-456.

Garden, H., and Hollaway, L. (1998). An experimental study of the failure modes of reinforced concrete beams strengthened with prestressed carbon composite plates. *Composites Part B: Engineering, 29*(4), 411-424.

Gencoglu, M., and Mobasher, B. (2007). *The strengthening of the deficient RC exterior beam-column joints using CFRP for seismic excitation.* Paper presented at the Proceedings of the 3 rd international conference on structural engineering, mechanics and computation.

George, J., Rama, J. K., Kumar, M. S., and Vasan, A. (2017). Behavior of Plain Concrete Beam subjected to Three Point Bending using Concrete Damaged Plasticity (CDP) Model. *Materials Today: Proceedings, 4*(9), 9742-9746.

Gergely, J., Pantelides, C. P., and Reaveley, L. D. (2000). Shear strengthening of RCT-joints using CFRP composites. *Journal of composites for construction, 4*(2), 56-64.

Ghobarah, A., Aziz, T. S., and Biddah, A. (1997). Rehabilitation of reinforced concrete frame connections using corrugated steel jacketing. *ACI Structural Journal, 94*(3), 282-294.

Ghobarah, A., and El-Amoury, T. (2005). Seismic rehabilitation of deficient exterior concrete frame joints. *Journal of Composites for Construction, 9*(5), 408-416.

Ghobarah, A., and Said, A. (2001). Seismic rehabilitation of beam-column joints using FRP laminates. *Journal of Earthquake Engineering, 5*(1), 113-129.

Ghobarah, A., and Said, A. (2002). Shear strengthening of beam-column joints. *Engineering structures, 24*(7), 881-888.

Gupta, A., Agarwal, P., . (2012). *Performance Evaluation Of Exterior Rc Beam Column Joint strengthened With Frp Under Cyclic Load.* . Paper presented at the Fourth International Conference on Structural Stability and Dynamics (ICSSD 2012), 4–6 January, 2012.

Hadi, M. N., and Tran, T. M. (2016). Seismic rehabilitation of reinforced concrete beam–column joints by bonding with concrete covers and wrapping with FRP composites. *Materials and Structures, 49*(1-2), 467-485.

Hakuto, S., Park, R., and Tanaka, H. (2000). Seismic load tests on interior and exterior beam-column joints with substandard reinforcing details. *ACI Structural Journal, 97*(1), 11-25.

Hanson, N. W., and Conner, H. W. (1967). Seismic resistance of reinforced concrete beam-column joints. *Journal of the Structural Division, 93*(5), 533-560.

Hasaballa, M., Mady, M., El-Ragaby, A., and El-Salakawy, E. (2009). *GFRP-REINFORCED CONCRETE BEAM-COLUMN JOINTS.* Paper presented at the The Second Official International Conference of International Institute for FRP in Construction for Asia-Pacific Region.

He, A., Cai, J., Chen, Q.-J., Liu, X., Huang, P., and Tang, X.-L. (2018). Seismic behaviour of steel-jacket retrofitted reinforced concrete columns with recycled aggregate concrete. *Construction and Building Materials, 158*, 624-639.

Hegger, J., Sherif, A., and Roeser, W. (2004). Nonlinear finite element analysis of reinforced concrete beam-column connections. *ACI Structural Journal, 101*(5), 604-614.

Hwang, S.-J., and Lee, H.-J. (1999). Analytical model for predicting shear strengths of exterior reinforced concrete beam-column joints for seismic resistance. *ACI Structural Journal, 96*(5), 846-857.

Hwang, S.-J., and Lee, H.-J. (2002). Strength prediction for discontinuity regions by softened strut-and-tie model. *Journal of Structural Engineering, 128*(12), 1519-1526.

Javanmardi, M., and Maheri, M. R. (2017). *Anisotropic Damage Plasticity Model for Concrete and Its Use in Plastic Hinge Relocation in RC Frames with FRP.* Paper presented at the Structures.

Jirsa, S. M. A. a. J. O. (1993). *Strength of reinforced concrete frame connections rehabilitated by jacketing.* Paper presented at the ACI Structural Journal.

Kadhim, M. M. A., Mohammed, M. J., and Chabuk, A. J. (2012). Effect of prestressed CFRP plate location on behavior of RC beam strengthened with prestressed CFRP plate. *Journal of University of Babylon, 20*(1), 105-113.

Kaku, T., and Asakusa, H. (1991). Bond and anchorage of bars in reinforced concrete beam-column joints. *ACI Special Publication, 123*, 401-424.

Karayannis, C., Chalioris, C., and Sideris, K. (1998). Effectiveness of RC beam-column connection repair using epoxy resin injections. *Journal of Earthquake Engineering, 2*(02), 217-240.

Kim, J., and LaFave, J. M. (2007). Key influence parameters for the joint shear behaviour of reinforced concrete (RC) beam–column connections. *Engineering Structures, 29*(10), 2523-2539.

Kurihashi, Y., Kishi, N., Ali, A., and Mikami, H. (2011). Load-carrying capacity of flexural reinforced PC beams with pretensioned AFRP sheet *Advances in FRP Composites in Civil Engineering* (pp. 695-698): Springer.

Kurose, Y. (1988). *Study of reinforced concrete beam-column joints under uniaxial and biaxial loading*: Phil M. Ferguson Structural Engineering Laboratory, University of Texas at Austin.

Lakshmi, G., Dutta, A., and Deb, S. (2008). Numerical studies of strengthening of beam column joint under cyclic excitation using FRP composites. *Journals of structural Engineering, 35*(1), 59-65.

Le-Trung, K., Lee, K., Lee, J., Lee, D. H., and Woo, S. (2010). Experimental study of RC beam–column joints strengthened using CFRP composites. *Composites Part B: Engineering, 41*(1), 76-85.

Le-Trung, K., Lee, K., Shin, M., and Lee, J. (2011). Analytical assessment and modeling of RC beam-column connections strengthened with CFRP composites. *Composites Part B: Engineering, 42*(7), 1786-1798.

Li, B., and Chua, H. G. (2009). Seismic performance of strengthened reinforced concrete beam-column joints using FRP composites. *Journal of structural engineering*, 1177-1190.

Li, B., Lam, E. S.-s., Cheng, Y.-k., Wu, B., and Wang, Y.-y. (2015). Strengthening of non-seismically designed beam-column joints by ferrocement jackets with chamfers. *Earthquakes and Structures, 8*(5), 1017-1038.

Liu, J., Driver, R. G., and Lubell, A. S. (2008). *Rehabilitation and repair of reinforced concrete short columns with external steel collars* (Vol. 70).

Lowes, L. N., Altoontash, A., and Mitra, N. (2005). Closure to "Modeling Reinforced-Concrete Beam-Column Joints Subjected to Cyclic Loading" by Laura N. Lowes and Arash Altoontash. *Journal of Structural Engineering, 131*(6), 993-994.

Mahini, S., Ronagh, H., and Dalalbashi, A. (2008). *Numerical modeling of CFRP-retrofitted RC exterior beam-column joints under cyclic loads.* Paper presented at the the 4th International Conference on FRP Composites in Civil Engineering (CICE2008).

Mahini, S., Ronagh, H., and Smith, S. T. (2005). *CFRP-retrofitted RC exterior beam-column connections under cyclic loads.* Paper presented at the International Conference on FRP Composites in Civil Engineering.

Mahmoud, M. H., Afefy, H. M., Kassem, N. M., and Fawzy, T. M. (2014). Strengthening of defected beam–column joints using CFRP. *Journal of advanced research, 5*(1), 67-77.

McCormac, J. C., and Brown, R. H. (2015). *Design of reinforced concrete*: John Wiley & Sons.

Migliacci, A., Antonucci, R., Maio, N., Napoli, P., Ferretti, A., and Via, G. (1983). *Repair techniques of reinforced concrete beam-column joints.* Paper presented at the Final Report of the IABSE Symposium on Strengthening of Building Structures-Diagnosis and Therapy.

Mitra, N., and Lowes, L. N. (2007). Evaluation, calibration, and verification of a reinforced concrete beam–column joint model. *Journal of Structural Engineering, 133*(1), 105-120.

Mosallam, A. (2000). Strength and ductility of reinforced concrete moment frame connections strengthened with quasi-isotropic laminates. *Composites Part B: Engineering, 31*(6), 481-497.

Mosallam, A. S. (2008). Structural Upgrade of Reinforced Concrete Column-Tie Beam Assembly using FRP Composites. *Seismic Strengthening of Concrete Buildings Using FRP Composites*, 63-74.

Mostofinejad, D., and Talaeitaba, S. (2006). Finite element modeling of RC connections strengthened with FRP laminates. *Iranian Journal of Science & Technology, Transaction B, Engineering, 30*(B1), 21-30.

Mukherjee, A., and Joshi, M. (2005). FRPC reinforced concrete beam-column joints under cyclic excitation. *Composite structures, 70*(2), 185-199.

Mukherjee, A., and Rai, G. L. (2009). Performance of reinforced concrete beams externally prestressed with fiber composites. *Construction and Building Materials, 23*(2), 822-828.

Nehdi, M., and Said, A. (2005). Performance of RC frames with hybrid reinforcement under reversed cyclic loading. *Materials and structures, 38*(6), 627-637.

Nordin, H. (2005). *Strengthening structures with externally prestressed tendons: literature review*.

Nordin, H., and Täljsten, B. (2006). Concrete beams strengthened with prestressed near surface mounted CFRP. *Journal of Composites for Construction, 10*(1), 60-68.

Ozbakkaloglu, T., and Fanggi, B. A. L. (2015). FRP–HSC–steel composite columns: behavior under monotonic and cyclic axial compression. *Materials and Structures, 48*(4), 1075-1093.

Pampanin, S., Calvi, G. M., and Moratti, M. (2002). Seismic behavior of RC beam-column joints designed for gravity only.

Pannirselvam, N., Raghunath, P., and Suguna, K. (2008). Strength Modeling of Reinforced Concrete Beam with Externally Bonded Fibre Reinforcement Polymer Reinforcement. *American Journal of Engineering and Applied Sciences, 1*(3).

Pantazopoulou, S., and Bonacci, J. (1993). Consideration of questions about beam-column joints. *ACI structural Journal, 89*(1), 27-36.

Pantelides, C., Clyde, C., Lau, C., and Reaveley, L. (2001). *Seismic rehabilitation of reinforced concrete building corner joints.* Paper presented at the Proceedings of the Fifth International Symposium on Non-Metallic Reinforcement for Concrete Structures.

Pantelides, C. P., Okahashi, Y., and Reaveley, L. (2008). Seismic rehabilitation of reinforced concrete frame interior beam-column joints with FRP composites. *Journal of Composites for Construction, 12*(4), 435-445.

PARME, A. L. (1976). Recommendations for Design of Beam-Column Joints in Monolithic Reinforced Concrete Structures. *ACI JOURNAL*, 375.

Parvin, A., and Granata, P. (2000). Investigation on the effects of fiber composites at concrete joints. *Composites Part B: Engineering, 31*(6), 499-509.

Patil, S. M. S., and Manekari, S. (2013). Analysis of Reinforced Beam-Column Joint Subjected to Monotonic Loading. *International Journal of Engineering and Innovative Technology (IJEIT), vol, 2*.

Paulay, T., Park, R., and Preistley, M. (1978). *Reinforced concrete beam-column joints under seismic actions.* Paper presented at the ACI Journal Proceedings.

Perumal, P., and Thanukumari, B. (2010). Use of fibre cocktails to Increase the seismic Performence of beam-column Joints. *International journal of engineering science and technology, 2*(9), 3997-4006.

Pessiki, S. P., Conley, C., Gergely, P., and White, R. (1990). Seismic behavior of lightly-reinforced concrete column and beam-column joint details.

Pohoryles, D., Melo, J., Rossetto, T., Varum, H., and D'ayala, D. (2015). Experimental investigation on the seismic FRP retrofit of realistic full-scale RC beam-column joints *Improving the Seismic Performance of Existing Buildings and Other Structures 2015* (pp. 619-631).

Priestley, M., Seible, F., and Calvi, G. (1996). Seismic design and retrofit of bridgesWiley. *New York*.

Prota, A., Manfredi, G., Nanni, A., and Cosenza, E. (2002). *Capacity assessment of GLD RC Frames Strengthened with FRP.* Paper presented at the Proceedings of the Twelfth European Conference on Earthquake Engineering.

Prota, A., Nanni, A., Manfredi, G., and Cosenza, E. (2000). Seismic upgrade of beam-column joints with FRP reinforcement. *L'Industria Italiana del Cemento, 70*(11), 868-877.

Prota, A., Nanni, A., Manfredi, G., and Cosenza, E. (2001). *Selective upgrade of beam-column joints with composites.* Paper presented at the Proceedings of the International conference on FRP Composites in Civil Engineering, Hong kong.

Rajaram, P., Murugesan, A., and Thirugnanam, G. (2010). Experimental Study on behavior of Interior RC Beam Column Joints Subjected to Cyclic Loading. *International Journal of Applied Engineering Research, 1*(1), 49-58.

Rao, G. A., Mahajan, M., Gangaram, M., and Eligehausen, R. (2008). Performance of non seismically designed RC beam column joints strengthened by various schemes subjected to seismic loads. *Journal of structural engineering, 35*(1), 52-58.

Ravi, S. R., and Arulraj, G. P. (2010). Experimental investigation on behavior of reinforced Concrete Beam Column Joints Retrofitted with GFRP-AFRP Hybrid wrapping. *International Journal of Civil & Structural Engineering, 1*(2), 245-253.

Said, A., and Nehdi, M. (2004). Use of FRP for RC frames in seismic zones: Part I. Evaluation of FRP beam-column joint rehabilitation techniques. *Applied Composite Materials, 11*(4), 205-226.

Shannag, M. J., Abu-Dyya, N., and Abu-Farsakh, G. (2005). Lateral load response of high performance fiber reinforced concrete beam–column joints. *Construction and Building Materials, 19*(7), 500-508.

Silva, P. F. (2008). *Hysteretic Rotation Model HRM4 for CFRP-Strengthened Joints*.

Standard, I. (1893). Criteria for earthquake resistant design of structures. *IS. Reproduced with permission of the copyright owner. Further reproduction prohibited without permission*.

Standard, I. (1993). Ductile detailing of reinforced concrete structures subjected to seismic forces–code of practice. *New Delhi: Bureau of Indian Standards*.

Standard, I. (2000). Plain and reinforced concrete–code of practice. *New Delhi: Bureau of Indian Standards*.

Standards, B. o. I. (1993). *Ductile Detailing of Reinforced Concrete Structures Subjected to Seismic Forces: Code of Practice*: The Bureau.

Subramanian, N., and Rao, D. P. (2003). Seismic design of joints in RC structures- A review. *Indian Concrete Journal, 77*(2), 883-892.

Subramanian, N., Rao, D.S.P; . (2003). Seismic Design of Joints in RC Strucutres,. *The Indian Concrete Journal, , Vol. 77, No.2,*, pp. 883- 892.

Supaviriyakit, T., and Pimanmas, A. (2008). Comparative performance of sub-standard interior reinforced concrete beam–column connection with various joint reinforcing details. *Materials and Structures, 41*(3), 543-557.

Tan, K.-H., and Tjandra, R. A. (2003). Shear deficiency in reinforced concrete continuous beams strengthened with external tendons. *ACI Structural Journal, 100*(5), 565-572.

Tang, W., Balendran, R., Nadeem, A., and Leung, H. (2006). Flexural strengthening of reinforced lightweight polystyrene aggregate concrete beams with near-surface mounted GFRP bars. *Building and environment, 41*(10), 1381-1393.

Thomas, P., and Priestley, M. (1992). Seismic design of reinforced concrete and masonry buildings: New York Wiley-Interscience, America.

Triantafillou, T. C., Deskovic, N., and Deuring, M. (1992). Strengthening of concrete structures with prestressed fiber reinforced plastic sheets. *ACI structural Journal, 89*(3), 235-244.

Tsai, S. W., and Wu, E. M. (1971). A general theory of strength for anisotropic materials. *Journal of composite materials, 5*(1), 58-80.

Tsonos, A. G. (2002). Seismic repair of reinforced concrete beam-column subassemblages of modern structures by epoxy injection technique. *Structural Engineering and Mechanics, 14*(5), 543-563.

Tsonos, A. G. (2008). Effectiveness of CFRP-jackets and RC-jackets in post-earthquake and pre-earthquake retrofitting of beam–column subassemblages. *Engineering Structures, 30*(3), 777-793.

Uma, S. R. P., A.M;. (2003). *Department of Civil Engineering Indian Institute of technology Madras",* . Chennai.

Vecchio, F. J., and Collins, M. P. (1993). Compression response of cracked reinforced concrete. *Journal of Structural Engineering, 119*(12), 3590-3610.

Walker, S. G. (2001). *Seismic performance of existing reinforced concrete beam-column joints*.

White, R. N., and Mosalam, K. M. (1997). Seismic evaluation and rehabilitation of concrete buildings *Technical Report NCEER* (pp. 177-196): US National Center for Earthquake Engineering Research.

Woo, S.-K., Kim, J.-H. J., Byun, K.-J., and Song, Y.-C. (2013). Bond-slip parameter determination procedure of RC flexure member strengthened with prestressed CFRP plates. *KSCE Journal of Civil Engineering, 17*(1), 179-191.

Woo, S.-K., Nam, J.-W., Kim, J.-H. J., Han, S.-H., and Byun, K. J. (2008). Suggestion of flexural capacity evaluation and prediction of prestressed CFRP strengthened design. *Engineering Structures, 30*(12), 3751-3763.

Xue, W., Tan, Y., and Zeng, L. (2010). Flexural response predictions of reinforced concrete beams strengthened with prestressed CFRP plates. *Composite Structures, 92*(3), 612-622.

Yu, P., Silva, P. F., and Nanni, A. (2003). Flexural performance of RC beams strengthened with prestressed CFRP sheets. *Center for Infrastructure and Engineering Studies Department of Civil, Architectural, and Environmental Engineering University of Missouri-Rolla Rolla, MO*, 65409-60030.

Zureick, A., and Kahn, L. (2001). Rehabilitation of reinforced concrete structures using fiber-reinforced polymer composites. *ASM handbook, 21*, 906-913.

LIST OF PUBLICATIONS AND PAPERS PRESENTED

Sinaei, H., Jumaat, M.Z., and Shariati, M. (2011). Numerical investigation on exterior reinforced concrete Beam-Column joint strengthened by composite fiber reinforced polymer (CFRP). *International Journal of Physical Sciences, 6*(28), 6572-6579. (**Published**).

Sinaei, H., Shariati, M., Abna, A.H., Aghaei, M., and Shariati, A. (2012). Evaluation of reinforced concrete beam behaviour using finite element analysis by ABAQUS. Scientific Research and Essays, 7(21), 2002-2009. **(Published**).

Sinaei, H., Ibrahim, Z., and Jumaat, M.Z. (2018). Analysis of joints reinforced with CFRP plates on the beam flanges. *Steel and Composite Structures*. (**1st revision submitted**).

Sinaei, H., Ibrahim, Z., and Jumaat, M.Z. (2018).The effect of carbon fiber reinforced polymer on behavior of reinforce concrete beam column connections- An experimental study. Steel and Composite Structures. **(submitted).**

Sinaei, H., Jumaat, M.Z., and Abna, A.H. (2011). Finite element modelling on behaviour of exterior reinforced concrete beam-column Joint strengthened using CFRP composites. Proceeding of the 2011 Word Congress on Advances in Structural Engineering and Mechanics (ASEM11+), Seoul, South Korea. (**Published**).